

**The role of Tight Junction Protein 1a and Leukocyte Tyrosine Kinase in
the development and organisation of pigment cells in the Zebrafish**

Dissertation

der Mathematisch-Naturwissenschaftlichen Fakultät
der Eberhard Karls Universität Tübingen
zur Erlangung des Grades eines Doktors
der Naturwissenschaften
(Dr. rer. nat.)

vorgelegt von
Andrey Fadeev
aus Almetyevsk
(Russland)

Tübingen
2015

Tag der mündlichen Qualifikation: 27.01.2016

Dekan: Prof. Dr. Wolfgang Rosenstiel

1. Berichterstatter: Prof. Dr. Christiane Nüsslein-Volhard

2. Berichterstatter: Prof. Dr. Rolf Reuter

Contents

Abstract	1
Zusammenfassung	3
List of publications presented	5
Abbreviations	6
Introduction	7
1.1 Pigment patterns in vertebrates	7
1.2 Zebrafish colour pattern	8
1.3 Zebrafish pigment pattern mutants	11
1.4 Colour patterns in other teleost species	14
Results and discussion	16
2.1 Publication 1	16
2.1.1 Lesions in zebrafish <i>tight junction protein 1a</i> result in a spotted pattern	16
2.1.2 The spotted pattern in <i>schachbrett</i> is not caused by a reduced number of melanophores	16
2.1.3 Iridophores display an abnormal behaviour at mid-metamorphic stages in <i>schachbrett</i>	17
2.1.4 The pale appearance of metamorphic mutant fish is caused by the persistent migratory shape of melanophores	18
2.1.5 <i>schachbrett</i> is cell-autonomous to iridophores, with regard to pigment pattern formation	18
2.1.6 <i>schachbrett</i> is expressed in dense, but not in loose iridophores	18
2.1.7 Possible functional redundancy of <i>tjps</i>	19
2.1.8 Potential mechanisms of Tjp1a control over cell shape	19
2.2 Publication 2	39
2.2.1 The ALK/LTK subfamily of tyrosine kinases	39
2.2.2 <i>moonstone</i> is a gain-of-function allele of <i>leukocyte tyrosine kinase</i>	39
2.2.3 The novel role of <i>ltk</i>	40
2.2.4 <i>ltk</i> specifically regulates iridophores	40
2.2.5 <i>ltk^{mne}</i> displays a normal stripe pattern despite the presence of ectopic iridophores in the skin of metamorphic fish	41
2.2.6 Ectopic iridophores on the scales are accompanied by melanophores	41
2.2.7 <i>Ltk</i> and <i>Ednrba</i> regulate distinct aspects of iridophore behaviour	42
2.2.8 <i>ltk^{mne}</i> iridophores form overgrowths in the wild type environment	42
2.3 Publication 3	57

Concluding remarks	75
Bibliography	76
Contributions	88
Curriculum Vitae	89
Full publications list	90
Acknowledgements	91

Abstract

Vertebrates possess a unique structure, the neural crest, which contributes cells to a wide spectrum of tissues and organs, amongst them are pigment cells or chromatophores. In mammals and birds only one type of chromatophore is present – the melanocytes. However, more basal animals – reptilians, amphibians and fish – display an array of specialized chromatophores. Different arrangements of these cells produce an astonishing multitude of colouration patterns, especially in teleost fish.

Zebrafish show a highly regular pattern of alternating dark and light stripes composed of three pigment cell types: black melanophores, yellow xanthophores and silvery iridophores. The formation of this pattern requires coordinated cell movements and cell shape changes of pigment cells during metamorphosis. Iridophores play a crucial part in this process by switching between the dense shape of the light stripes and the loose shape of the dark stripes. It has been suggested that homotypic interactions regulate iridophore proliferation and dispersal. Communication with xanthophores and melanophores, on the other hand, regulates a stereotypical sequence of aggregation and loosening, which establishes the stripes along dorso-ventral axis. However, not much is known about the molecular mechanisms that mediate the formation of the adult striped pattern.

Analysing mutants obtained in several screens, we describe two novel regulators of iridophore behaviour. In the *schachbrett* (*sbr*) mutants the dark stripes are undulating or broken into spots. Using confocal microscopy and transgenic lines, we demonstrate that *sbr* iridophores are not able to switch from the dense shape to the loose shape in an appropriate spatio-temporal manner. As a result, dense iridophores invade the dark stripe areas, drive away melanophores, which leads to interruptions. We demonstrate that the phenotype is due to truncations of Tight Junction Protein 1a (Tjp1a, ZO-1a). Antibody labelling and chimeric analysis indicate that Tjp1a is expressed in the dense iridophores, but is down-regulated in the loose iridophores.

The *moonstone* mutants display ectopic iridophores inside the trunk throughout development. In the adult fish, ectopic iridophores are present on the scales, in the fins and occasionally on the eyes. We demonstrate, using pharmacological and genetic approaches, that *moonstone* is a dominant allele of *leukocyte tyrosine kinase*, which carries a missense mutation in a conserved position of the kinase domain. Loss-of-function zebrafish mutants in *ltk* lack iridophores. Therefore, it has been suggested that

ltk is required for iridophore specification. Using gain- and loss-of-function *ltk* alleles and inhibitor treatments, we show that mutant Ltk is hyperactive and that Ltk does not only specifically regulate iridophore establishment, but also proliferation and survival. Using chimeric analysis and confocal microscopy, we propose that Ltk facilitates the homotypic competition-based control of iridophore proliferation, but does not affect communication with xanthophores and melanophores.

The question of the conservation of functions of the genes controlling pigment pattern formation is of prime importance in other model organisms, such as guppy. With the example of two guppy mutants, *golden* and *blue*, we demonstrate the conserved functions of two tyrosine kinases – Kita and Csf1ra.

Zusammenfassung

Wirbeltiere zeichnen sich durch die Neuralleiste aus; dabei handelt es sich um eine vorübergehende embryonale Struktur, deren Zellen zu einer Vielzahl von Geweben und Organen im adulten Tier beitragen. So stammen unter anderem die Pigmentzellen, die Chromatophoren, aus der Neuralleiste.

Säugetiere und Vögel haben nur eine Art von Chromatophoren, die Melanozyten.

Basale Wirbeltiere wie Reptilien, Amphibien und Fische, besitzen eine größere Bandbreite von spezialisierten Chromatophoren. Unterschiedliche Zusammenstellungen dieser Zellen sind für die Vielfalt der Farbmuster dieser Tiere verantwortlich, besonders beeindruckend bei den *Teleostei*.

Zebrabärblinge, *Dani rerio*, zeigen ein sehr regelmäßiges Muster aus alternierenden dunklen und hellen Streifen, das aus 3 Pigmentzelltypen gebildet wird: Schwarzen Melanophoren, gelben Xanthophoren und silbernen Iridophoren. Die Bildung dieser Muster erfordert koordinierte Zellbewegungen und Zellformveränderung während der Metamorphose. Die Iridophoren spielen dabei eine besondere Rolle. Sie wechseln von einer dichten Form in den hellen Streifen zu einer losen Form in den dunklen Streifen. Es wurde vorgeschlagen, dass homotypische Interaktionen zwischen den Iridophoren die Zellteilung und Ausbreitung regulieren, während die Kommunikation mit Xanthophoren und Melanophoren die Aggregation bzw. Verteilung der Zellen entlang der dorso-ventralen Achse bestimmt, und somit das spätere Streifenmuster festlegt. Die molekularen Mechanismen, die diese Prozesse der Musterbildung kontrollieren, sind bislang noch wenig verstanden.

In der vorliegenden Arbeit werden zwei neue Regulatoren des Zellverhaltens der Iridophoren beschrieben. In *schachbrett* (*sbr*) Mutanten sind die dunklen Streifen unregelmäßig und unterbrochen. Durch konfokale Mikroskopie und mit transgenen Linien konnten wir zeigen, dass in *sbr* Mutanten die Iridophoren nicht in der Lage sind, am richtigen Ort und zur richtigen Zeit von der dichten in die lose Form zu wechseln. Dadurch dringen dichte Iridophoren in die dunklen Streifen ein, sie vertreiben die Melanophoren, und verursachen Unterbrechungen. Wir haben gezeigt, dass der Phänotyp durch verkürztes Tight Junction Protein 1a (*Tjp1a*, *ZO-1a*) verursacht wird. Antikörperfärbungen und die Analyse von chimären Fischen deuten darauf hin, dass *Tjp1a* in dichten aber nicht losen Iridophoren exprimiert ist. *moonstone* Mutanten zeigen

ektopische Iridophoren im Rumpf; bei den erwachsenen Fischen treten diese zusätzlich auch auf den Schuppen, Flossen und gelegentlich auf den Augen auf. Durch pharmakologische und genetische Ansätze konnten wir zeigen, dass *moonstone* ein dominantes Allel der *leukocyte tyrosin kinase (ltk)* ist, das eine Mutation trägt, die zum Austausch eines Aminosäurerestes in einer hochkonservierten Position der Kinasedomäne führt. Der Funktionsverlust von *ltk* in *shady* Mutanten, führt zur Abwesenheit von Iridophoren; das zeigt, dass *ltk* für die Spezifizierung der Iridophoren notwendig ist. Durch die Analyse der unterschiedlichen Allele, sowie durch den Einsatz eines pharmakologischen Inhibitors, konnten wir zeigen, dass *Ltk* in *moonstone* hyperaktiv ist. Unsere Ergebnisse deuten darauf hin, dass *Ltk* nicht nur für die Iridophorbildung wichtig ist, sondern später auch für ihre Proliferation und das Überleben. Unsere Untersuchungen von chimären Fischen weisen darauf hin, dass *Ltk* an der Kontrolle der Zellteilung der Iridophoren beteiligt ist, aber nicht die Kommunikation mit Xanthophoren und Melanophoren beeinflusst.

Die aus *Danio rerio* bekannten Gene der Pigmentmusterbildung sind von Bedeutung für die Untersuchung von anderen Fischen, u.a. Guppys, *Poecilia reticulata*. Am Beispiel der beiden *P. reticulata* Mutanten *golden* und *blue* haben wir die konservierten Funktionen von zwei Tyrosin-Kinasen, *Kita* und *Csfla*, aufgezeigt.

List of publications presented

1. **Fadeev, A.**, Krauss, J., Frohnhöfer, H.G., Irion, U., Nüsslein-Volhard, C.* (2015) Tight Junction Protein 1a regulates pigment cell organisation during zebrafish colour patterning. *eLife*. doi: /10.7554/eLife.06545
2. **Fadeev, A.**, Krauss, J., Singh, A.P., Nüsslein-Volhard, C.* (2016) Zebrafish Leucocyte tyrosine kinase controls iridophore establishment, proliferation and survival. *Pigment Cell and Melanoma Research*. doi: /10.1111/pcmr.12454
3. Kottler, V.A.*, **Fadeev, A.**, Weigel, D., and Dreyer, C. (2013) Pigment pattern formation in the guppy, *Poecilia reticulata*, involves the Kita and Csf1ra receptor tyrosine kinases. *Genetics* 194.3 (2013): 631-646

* Corresponding author

Abbreviations

alb – albino/*slc45a2*
dpf – days post fertilisation
DRG – dorsal-root ganglion
kar – karneol/*ece2b*
leo – leopard/*cx41.8*
luc – luchs/*cx39.4*
nac – nacre/*mitfa*
NC – neural crest
obe – obelix/jaguar/*kir7.1*
pfe – pfeffer/*csf1r*
rse – rose/*ednrba*
sbr – schachbrett/*tjp1a*
seu – seurat/*igsf11*
shd – shady/*ltk*
SL – standard length
slk – sparse-like/*kitla*
spa – sparse/*kita*
tra – transparent/*mpv17*

Introduction

1.1 Pigment patterns in vertebrates.

The diversity of colour patterns in the animal kingdom has attracted the attention of researchers for over a century (Darwin, 1871; Rawles, 1948). Colour patterns serve a multitude of roles, such as the protection of organs from harmful radiation, which is achieved with dark or reflective pigments (Mosse *et al*, 2000; Hairston, 1976). The most widely known functions of colour patterns are camouflage, which allows the protection from predators, and sexual selection, which allows an animal to attract a potential mate. The former function leads, at times, to astounding similarities between the patterns of animals from distant evolutionary groups, whereas the latter forces selection of strikingly different colouration in closely related species (Endler, 1984; Stevens & Merilaita, 2009; Galeotti *et al*, 2003). Moreover, colour patterns might play an important role in kin recognition for animals belonging to the same group (Spence & Smith, 2007). This results in a rapid adaptive evolution of colour patterns as compared to other systems of the body. The importance of these functions is underscored by the fact that animals that have evolved in light-deficient conditions are often colourless.

Animals have developed a wide array of strategies for generating colour. Most mammals are clad in different shades of grey or brown owing to the pigment melanin, which is produced by specialized cells – melanocytes – and released into the skin or hairs. Birds employ a similar strategy, using in addition pigments consumed with food to colour their feathers. More basal vertebrates – amphibians, reptiles and fish – possess several types of chromatophores, such as yellow xanthophores, white leucophores, and silvery iridophores. Located in the hypodermis, on the scales and in the fins, ensembles of these cells are not only able to produce different patterns between individuals, but even different patterns in the same individual, accommodating for the animal's environment or mating status (Denefle & Lechaire, 1990; Kobelt & Linsenmair, 1986; Cooper & Greenberg, 1992; Hawkes, 1974; Rawles, 1948). In vertebrates, all chromatophores (with the exception of the pigmented retina) originate from a single source – the neural crest (NC). The NC is a transient structure composed of multipotent cells, located on the neuroectodermal ridge, and it produces a large number of structures, including parts of

jaws and skull, glia, neurons, and gills (Le Douarin & Kalcheim, 1999; Mongera *et al*, 2013).

There are still many gaps in the knowledge of the mechanisms governing the generation of colour patterns. In some cases, the pattern may be a consequence of body organisation, but in most of the cases there is no obvious pre-pattern for pigment cells to fill-in: for example, the stripes of tigers and zebras or the labyrinthine patterns of some eels, which do not follow any clear anatomical structures. In these examples, colour patterns are likely to be the result of pigment cells organizing themselves in the skin (Bard, 1981; Murray, 1981; Godfrey *et al*, 1987). There are several theoretical models that propose mechanisms of pattern formation, and a number of genes affecting the various aspects of pigment cell biology have been described. However, in most organisms, pigment pattern formation is all but impossible to study due to long development times and increasingly large body sizes. Furthermore, the pattern formation in mammals and birds occurs while the individuals are protected in the mother's womb or enclosed within an egg. Indeed it is hard to conceive of direct experiments to study mammalian or avian pattern formation.

As a result, fish became a prime focus of pigment pattern formation studies, in particular the zebrafish, *Danio rerio*. A short generation time (2.5-3.5 months), small size, external fertilisation, and ease of observing and manipulating a developing embryo have made the zebrafish a model of choice for many developmental processes, including pigment pattern formation. It is also an excellent model for studying the fundamental genetics and molecular mechanisms of pattern formation, owing to its highly regular pattern of longitudinal dark and light stripes. Another model fish, the guppy, *Poecilia reticulata*, on the other hand, displays an astounding variation of male patterns between ecotypes, which provides insights into the mechanisms of the rapid evolution of a pigment patterns.

1.2 Zebrafish colour pattern

Zebrafish display two pigment patterns: a relatively simple larval pattern and an adult one, developing during metamorphosis from 3 to 6 weeks past fertilisation. The larval pattern in the trunk is formed by the pigment cells that are derived directly from early neural crest cells that migrate in early embryogenesis (Singh & Nüsslein-Volhard, 2015; Kelsh *et al*, 1996). It is comprised of dorsal, ventral and lateral stripes of dark

melanophores containing melanin, and scattered yellow xanthophores. Iridophores are organized in the dorsal and ventral stripes, with about one iridophore per segment. In addition, a layer of iridophores covers the developing swimming bladder (Kelsh *et al*, 2009).

The adult pigment pattern presents 4-5 alternating dark and light longitudinal stripes in the trunk, anal and caudal fins of the fish. The stripes in the body are multi-layered arrangements of pigment cells in the hypodermis. Melanophores are present only in the dark stripes. They have a compact arrangement, with almost no space between them. At least three different classes of silvery iridophores are distinguishable: silvery-white dense S-iridophores, blue loose S-iridophores, and L-iridophores. All iridophores contain small densely packed guanine platelets, which diffract light and generate iridescent colours. Dense iridophores are tightly packed cells in the light stripes. Loose iridophores are located on top of melanophores in the dark stripes as a loose net. L-iridophores are long spindle-like cells, underlying melanophores. Yellow xanthophores, containing pteridines, cover the whole body of the fish and develop a compact bright-orange or yellow appearance on top of the dense iridophores in the light stripes. In the dark stripes, xanthophores are present on top of melanophores, forming a net of stellate, pale yellow cells (Hirata *et al*, 2003, 2005; Frohnhöfer *et al*, 2013; Mahalwar *et al*, 2014; Singh *et al*, 2014). Interestingly, all three cell types are mixed together (do not form stripes) in a dark longitudinal band on the dorsum of zebrafish (Singh & Nüsslein-Volhard, 2015).

In addition to the trunk, chromatophores are also present in the fins, scales, eyes and viscera of zebrafish. In most of these locations no stripes are formed, however the caudal and anal fins display horizontal stripes, consistent with the trunk stripes. In these fins, the organisation of chromatophores is different from the one in the trunk. The fin pattern is composed of a continuous sheet of xanthophores, sandwiched between two layers of melanophores in the dark stripe regions. Iridophores are thinly distributed along the fin rays in the light stripe regions of the fins. On the scales, all three pigment cell types are present and intermingle to form a belt along the distal edge of a scale (Hirata *et al*, 2005).

Larval chromatophores directly differentiate from migrating neural crest cells. The pigment cells that form the adult pattern, while also neural crest-derived, arise during

metamorphosis, when the neural crest has already disappeared. Adult xanthophores have been shown to be a product of proliferation of larval xanthophores (Mahalwar *et al*, 2014). Melanophores have been shown to come from a small population of stem cells (scarcely more than one per hemisegment) of dorsal-root ganglia (DRGs), which are dependent on Kita-signalling. Melanophore progenitors migrate along the spinal nerves and emerge in the skin mostly over the dorsal and ventral myotomes. Once in the skin they rarely divide and do not migrate far (Singh *et al*, 2014; Budi *et al*, 2008; Dooley *et al*, 2013). Similarly, iridophores are shown to come from segmentally organised multipotent precursors, which reside in DRGs. Iridophores migrate through the horizontal myoseptum and, unlike melanophores, are capable of extensive proliferation and migration (Singh *et al*, 2014).

Once in the skin, at the onset of metamorphosis, pigment cells begin the process that ultimately leads to stripe formation. Iridophores appear as small clusters below the horizontal myoseptum and begin to proliferate, keeping tight contacts with each other. Eventually clusters merge, forming a rough stripe, composed of dense iridophores, with cells from different segments mixed together. Experiments performed in our laboratory suggest that the expansion of iridophores, originating from the same segment, along the anterior-posterior axis is regulated by homotypic competition with iridophores of neighbouring segments (Walderich *et al.*, in review). Subsequently the borders of the forming stripe are sharpened and the first light stripe (X0) forms. Dense iridophores continue to proliferate and start to loosen their contacts with each other on the borders of the light stripe and acquire the loose shape. They migrate toward the ventral and dorsal aspects of the fish, over regions where melanophores are beginning to arise and form the first two dark stripes (1D and 1V). In the dark stripes, iridophores form a loose net. When they reach the borders of the dark stripes, they aggregate again into a dense sheet to form the next two light stripes (X1D and X1V). This sequence of repeated dispersal and aggregation prefigures the formation of the dark stripes in the trunk of the fish (Singh *et al*, 2014; Frohnhöfer *et al*, 2013). The origin and function of L-iridophores have not been investigated, but it is thought that they do not play a pivotal role in stripe formation, as they appear only after the pattern is laid out (Frohnhöfer *et al.*, 2013). Xanthophores, which cover the whole flank of the fish, acquire either a pale stellate or a

bright round shape depending on whether they are located on top of a dark or a light stripe (Mahalwar *et al*, 2014).

1.3 Zebrafish pigment pattern mutants

One of the decisive advantages of the zebrafish as a model organism for pattern formation is the availability of mutants. In recent years, following the establishment of a reliable genome assembly, multiple reverse genetics techniques have been established, including morpholinos (Nasevicius & Ekker, 2000), TALENs (Huang *et al*, 2011; Sander *et al*, 2011) and, most recently, the CRISPR-Cas system (Hwang *et al*, 2013). However, the majority of our knowledge of zebrafish biology comes from mutants that have been acquired using forward genetics techniques such as random insertions, radiation-treatment or chemicals, most notably *N*-Ethyl-*N*-Nitrosourea (ENU) (Haffter & Nüsslein-Volhard, 1996; Haffter *et al*, 1996; Amsterdam *et al*, 1999; Mullins *et al*, 1994; Driever *et al*, 1996). Although most of the mutants acquired are systemic, this approach has proven indispensable for the identification of many specific phenotypes, for example *no tail*, deficient in the formation of the notochord (Stemple *et al*, 1996), *acerebellar*, affecting the formation of the midbrain/hindbrain boundary and the cerebellum (Brand *et al*, 1996), *another long fin*, affecting the size of the fins (van Eeden *et al*, 1996). In a similar way, a large collection of mutants that are affected in pigment pattern formation have been assembled (Haffter *et al*, 1996; Odenthal *et al*, 1996; Kelsh *et al*, 1996; Johnson *et al*, 1995). Several of these mutants correspond to genes which were confirmed (or already known) to be important for the colouration of other vertebrates as well, such as Sox10, Mitfa (Microphthalmia-associated transcription factor a), members of Kit and endothelin pathways (Kelsh *et al*, 2009; Miwa *et al*, 2007; Liu *et al*, 2015; Gunnarsson *et al*, 2011; Geissler *et al*, 1988; Parichy *et al*, 2000a). Zebrafish provides a unique opportunity to study the function of these and other genes, as the teleost genome was duplicated and many genes exist in two copies with functions frequently diverging (Amores *et al*, 1998). As a result, many mutations, which are lethal in other vertebrates, are tolerable in fish. It was also suggested that the genome-wide duplication is what, in fact, allowed for the emergence of the diverse colour patterns in teleost (Braasch *et al*, 2009).

Mutants affected in pigment pattern formation can be separated into two large groups. The first group of mutants is affected in the establishment of one or more pigment cell types. The second produces aberrant patterns while all three pigment cell types are present.

One of the best examples of the first group of mutants is *colourless*, encoding Sox10, which is required for the development of most of the neural-crest derived tissues. In this mutant no pigment cells are present (Dutton *et al*, 2001). Of particular interest are mutants that lack a single type of pigment cell completely. These mutants facilitated the genetic analysis of the contribution of a particular cell type to pigment pattern formation. *nacre/mitfa* mutants display a complete lack of melanophores (beside those in the eye) and result in a loss of stripes, although iridophores still show a dense/loose dimorphism, albeit in a seemingly random fashion (Lister *et al*, 1999). *sparse/kita* and *sparse-like/kitla* mutants established Kita signalling as a requirement for the development of larval melanophores as well as a subpopulation of metamorphic melanophores. There is also a population of metamorphic Kita-independent melanophores, as *sparse* and *sparse-like* do not have any melanophores before metamorphosis, when they subsequently appear in reduced numbers, ultimately leading to an adult phenotype with less than half of the wild type melanophore number. It is important to note that these mutants still produce stripes (Johnson *et al*, 1995; Parichy *et al*, 1999; Dooley *et al*, 2013). *pfeffer/colony stimulating factor receptor a* (*Csflra*) regulates the migration and survival of xanthophores. The mutant exhibits a reduction in the number of melanophores and an expansion of dense iridophore areas (Parichy *et al*, 2000b; Maderspacher & Nüsslein-Volhard, 2003; Parichy & Turner, 2003). Leukocyte Tyrosine Kinase (*Ltk*) has been suggested to regulate the establishment of iridophores as indicated by the *shady/ltk* mutant which lacks all iridophores, except small clonal patches (Lopes *et al*, 2008). Endothelin signalling is required for the proper expansion and possibly aggregation of iridophores in the skin as evidenced by the mutants with perturbed Endothelin receptor b1 (*rose*) and Endothelin converting enzyme 2 (*karneol*) (Parichy *et al*, 2000a; Krauss *et al*, 2014). *transparent/mpv17* encodes a mitochondrial protein required for iridophore survival (Krauss *et al*, 2013). All iridophore mutants form only the first two dark stripes with reduced melanophore numbers, frequently breaking up into spots. In mild cases rudiments of additional dark stripes can be observed. These phenotypes have been shown

to be a result of the absence of dense iridophores necessary for melanophore survival. Consequently, the number of melanophores is reduced. (Frohnhofer *et al*, 2013; Patterson & Parichy, 2013; Singh *et al*, 2014).

The second class of pigment pattern mutants is comprised of mutants that present all three cell types, but do not form normal stripes. The first described mutant of this type is *leopard/connexin41.8*, which forms spots of varying size (depending on the allele) instead of stripes. It facilitates communication between and within melanophores and xanthophores (Maderspacher & Nüsslein-Volhard, 2003; Watanabe *et al*, 2006; Irion *et al*, 2014). Recently, *luchs/connexin39.4* was identified as an enhancer of the *leopard* phenotype. The analysis suggests that these two connexins form heteromeric gap junctions required for cell-cell interaction and communication (Irion *et al*, 2014). A similar phenotype is displayed by *seurat/immunoglobulin superfamily member 11* mutants. These mutants are proposed to be affected in melanophore migration, survival, and cell adhesion (Eom *et al*, 2012). Other mutants of this group include *obelix/jaguar/kir7.1* and *dali/tetraspanin 3c* mutants, which display broader and fewer stripes (Inoue *et al*, 2014; Iwashita *et al*, 2006). *obelix/jaguar* encodes an inwardly-rectifying potassium channel (Kir7.1), which is required in melanophores for their communication with xanthophores (Maderspacher & Nüsslein-Volhard, 2003; Iwashita *et al*, 2006; Inaba *et al*, 2012). It was suggested by *in vitro* experiments that both mutants demonstrate abnormal xanthophore-melanophore contact response, however implications of these findings are unclear (Inaba *et al*, 2012).

The analysis of the phenotypes of mutants, double mutants, and chimeras, obtained by blastomere transplantations, establish several important points. Iridophores attract xanthophores and locally inhibit melanophore survival, while promoting melanophore survival at a distance. Xanthophores and melanophores exhibit short-range repulsion; however, melanophores require xanthophores at a distance. Most importantly, in the absence of the other two pigment cell types, the remaining cell type tends to spread uniformly over the fish flank in double mutants. Furthermore, in the absence of even one single pigment cell type, only a rudimentary pattern is formed. Taken together, these findings suggest that all three cell types are required for the normal striped pattern to

form (Frohnhofer *et al*, 2013; Maderspacher & Nüsslein-Volhard, 2003; Patterson & Parichy, 2013; Nakamasu *et al*, 2009).

Interestingly, the mutant *choker* displays an abnormal initial positioning of pigment cells in the skin due to the absence of the horizontal myoseptum. As a result, pigment cells form a pattern of meandering stripes, though they are normal in width and organisation (Frohnhofer *et al*, 2013). With the fact, that many known pigment pattern mutations of the second class affect cell-cell interaction molecules, a strong case can be made that the zebrafish pattern is a result of cell-cell communication and the subsequent reorganisation or migration of pigment cells. This notion is further supported by the fact that the active migration and cell shape changes of iridophores are necessary for pattern formation (Singh *et al*, 2014). This mechanism of colour pattern formation in zebrafish is different from the one in the butterfly wings, which is a response of stationary cells to signalling molecules, which provide positional information (Monteiro *et al*, 2006; Otaki, 2011; Serfas & Carroll, 2005).

Intriguingly, the same approaches that facilitate the investigation of trunk pigment cell interactions, suggest that patterning in the fins is governed by a different set of mechanisms. Most notably, iridophore-deficient mutants display normal stripe patterns in the anal and caudal fins, while exhibiting degraded patterns in the trunk. This suggests that iridophores are not involved in fin patterning (Krauss *et al*, 2014; Lopes *et al*, 2008; Frohnhofer *et al*, 2013; Parichy *et al*, 2000a; Krauss *et al*, 2013; Singh *et al*, 2014). The same holds true for the *choker* mutant with its meandering trunk pattern and double mutant *shady; sparse-like* which has almost no melanophores in the trunk (Singh & Nüsslein-Volhard, 2015). Moreover, *luchs* displays intact stripes in the fins but spots in the trunk (Irion *et al*, 2014). Taken together these data suggest that there is an independent patterning mechanism for trunk and fin stripe formation.

1.4 Colour patterns in other teleost species

Multiple *Danio* species present a colour pattern that is remarkably different from that of zebrafish. The fin patterns are also strikingly diverse and do not necessarily follow the trunk pattern. For example, *Danio albolineatus* does not form stripes, except for one light and one dark stripe at the posterior end of the trunk, and one dark stripe in the anal fin.

Danio choprae and *Danio erythromicron* display vertical bars, *Danio nigrofasciatus* has only two dark stripes in the body and caudal fin and spots in the anal fin. *Danio margaritatus* has a striking pattern of light spots on the dark background. However, all of these species develop larval patterns very similar to the one of *Danio rerio*. Observations of these fish, taken together with the knowledge of molecular mechanisms of stripe formation in zebrafish, open exciting possibilities for studying the evolution of pattern formation among *Danio* species (Kelsh *et al*, 2009; Parichy & Johnson, 2001; McClure, 1999). For example, it has been hypothesized that the pattern of *Danio nigrofasciatus*, which is similar to that of zebrafish iridophore mutants, is due to an aberrant patterned aggregation of iridophores (Singh & Nüsslein-Volhard, 2015). *Danio albolineatus* might owe its pattern to an increased expression of CSF-1 leading to early xanthophore differentiation, which in turn suppresses dark stripe formation (Patterson & Parichy, 2013; McMenamin *et al*, 2014).

Many teleost fish display a fast evolution of pigment patterns, for example guppies and cichlids. The insights, obtained in zebrafish, are valuable for studying pigment pattern formation in these fish as well. For example, the formation of egg-spots in cichlids is suggested to require the attraction of xanthophores by iridophores, similar to zebrafish (Santos *et al*, 2014; Frohnhofer *et al*, 2013; Patterson & Parichy, 2013). Guppies, *Poecilia reticulata*, are thought to be among the most colour-polymorphic vertebrates, with striking differences even between geographically close ecotypes (Endler, 1984). However both forward and reverse genetics studies are challenging in guppies due to internal fertilisation, live-bearing, relatively small brood size and the ability of females to store sperm (Houde, 1997). The knowledge of molecules involved in pigment pattern formation is invaluable for a candidate gene-driven approach in studying guppy pattern formation.

Results and discussion

2.1 Publication 1

Fadeev, A., Krauss, J., Frohnhöfer, H.G., Irion, U., Nüsslein-Volhard, C.* (2015)
Tight Junction Protein 1a regulates pigment cell organisation during zebrafish colour
patterning.

eLife. doi: /10.7554/eLife.06545

*Corresponding author

2.1.1 Lesions in zebrafish *tight junction protein 1a* result in a spotted pattern

Colour pattern formation in zebrafish relies on the precise spatio-temporal control of cell behaviour that is provided by a flexible and dynamic network of pigment cell interactions with each other and their surroundings (Patterson & Parichy, 2013; Singh *et al*, 2014; Mahalwar *et al*, 2014; Frohnhöfer *et al*, 2013; Nakamasu *et al*, 2009; Yamanaka & Kondo, 2014; Maderspacher & Nüsslein-Volhard, 2003). The mutants that display all three pigment cell types, but form an aberrant pattern, are particularly useful in elucidating the molecular nature of these interactions. In this study, we focus on the cell behaviour responsible for the formation of the adult pattern of the *schachbrett* (*sbr*) mutant. These fish display an unchanged arrangement and width of the stripes, but the dark stripes undulate or form interruptions (Figure 1A). The first allele, *sbr^{mh009b}* was identified as a recessive, homozygous viable mutant. Meiotic mapping and allele screens allowed us to identify 4 more alleles, all of which contained nonsense mutations in *tight junction protein 1a* (the product of this gene is named ZO-1 in mammals) (Kiener *et al*, 2007), demonstrating it as a gene, lesions in which lead to the spotted appearance of the fish (Figure 1A-D).

2.1.2 The spotted pattern in *schachbrett* is not caused by a reduced number of melanophores

As the pattern is unaffected in mutant larvae, we investigated the metamorphic stages of the mutant development. In multiple series of repeated daily imaging, we assessed that the phenotype becomes apparent at about 10 mm SL. It manifests as melanophore spots with dense iridophores and xanthophores arranged between them in a manner very

similar to that of the light stripes. However, as early as 7 mm SL, melanophores in the *sbr* fish appear as dots, whereas wild type melanophores are expanded (Figure 2A). There is no difference in melanophore numbers between wild type and mutant fish from 4 to 10 mm SL; however melanophore numbers diverge at 10 mm SL, when the spotted phenotype has already been established (Figure 2A, B). An additional indication that a reduced melanophore number does not explain the spotted phenotype, comes from the observation showing that *sparse* mutants have significantly reduced melanophore numbers (Johnson *et al*, 1995), yet still form uninterrupted stripes. In addition, double mutants for *spa;sbr* display both phenotypes: a reduced number of melanophores and spots (Figure 2C). Taken together, these findings suggest that the dark stripe interruptions in *sbr* are not caused by a reduction in melanophore number, and that the pale phenotype is a result of an abnormal size or pigment arrangement, rather than a reduced number of melanophores.

2.1.3 Iridophores display an abnormal behaviour at mid-metamorphic stages in *schachbrett*

The presence of iridophores in the dark stripe areas, called for an investigation of iridophore behaviour. To this end, repeated confocal imaging of wild-type and *sbr* individuals was performed. The fish that we used carried the *Tg(TDL358:GFP)* transgene alone or together with *Tg(sox10:mRFP)*. *Tg(TDL358:GFP)* labels iridophores and glia with GFP (Levesque *et al*, 2013) and *Tg(sox10:mRFP)* labels all neural crest derivatives with membrane-bound mRFP (Figures 3 and 4). The results of our time-series demonstrate that iridophores do not delaminate from the dense iridophore sheet after forming the first light stripe, but instead continue to expand into the presumptive dark stripes at the 7 mm SL stage. Subsequently, most of these iridophores become loose and normally pattern, but some remain dense and form interruptions in the dark stripes. This suggests that the *sbr* mutations perturb the processes that allow for the spatio-temporally appropriate transition of iridophores from the dense shape to the loose shape and subsequent iridophore dispersal. Occasionally, extensions of dense iridophores into the dark stripes can be observed in the wild type fish, but this appears to be corrected for later. Interruptions in adult wild type stripes are very rare, but do occur. In *sbr*, iridophore invasions occur along the entire length of the dark stripes, which results in random interruptions of the dark stripes. Interestingly, L-iridophores, which are restricted

to the dark stripe areas in wild-type, are present in and even traverse the light stripes in the adult *sbr* fish.

2.1.4 The pale appearance of metamorphic mutant fish is caused by the persistent migratory shape of melanophores

The fish, carrying the transgene *Tg(kita:mCherry)*, which labels melanophores (Anelli *et al.*, 2009), was used to investigate melanophore behaviour. In mutants, individual metamorphic melanophores move away from invading dense iridophores, or disappear, if they become surrounded by dense iridophores, at the stages 7-10 mm SL (Figure 5). This observation offers an explanation for the dot-like appearance of mutant melanophores at these stages (Figure 2A), since migratory melanophores have their pigment concentrated in the centre of a cell.

2.1.5 *schachbrett* is cell-autonomous to iridophores, with regard to pigment pattern formation

Analysis of chimeras, which were obtained by blastomere transplantations with *sbr* embryos as donors and *nacre* or *pfeffer* as recipients, allowed us to conclude that melanophores and xanthophores are not affected in the mutant and can participate in normal pattern formation (Figure 6). However when *sbr;shd* hosts, lacking iridophores, were supplied with iridophore progenitors from *nacre;pfeffer* donors, which have only this type of pigment cell, the chimeric animals exhibited regions with a normal stripe pattern. This confirmed that *sbr* is required cell-autonomously in iridophores and does not directly affect xanthophores or melanophores. Further support for this notion comes from the fact that in the double mutants *sbr;nacre* and *sbr;pfeffer* dense iridophores expand farther than they do in single mutants *nacre* and *pfeffer*. In contrast, *shd* and *sbr;shd*, which both lack iridophores, display indistinguishable phenotypes (Figure 6).

2.1.6 *schachbrett* is expressed in dense, but not in loose iridophores

Two polyclonal antibodies were generated against the parts of Tjp1a flanking the nonsense mutation in the *sbr^{mh009b}*. Subsequent antibody staining allowed us to demonstrate the presence of Tjp1a in epithelial cells in both wild type and mutant fish larvae. This indicates that the Tjp1a protein is retained in the *sbr^{mh009b}* mutants, and is able to normally localise, which suggests that the missing domains (ZU-5 and possibly

parts of afadin and actin binding regions (Bauer et al, 2010) are crucial for the function of Tjp1a in iridophores. Staining series, performed on the metamorphic fish carrying the iridophore marker *Tg(TDL358:GFP)*, demonstrated the presence of Tjp1a in dense iridophores, but not in loose or L-iridophores (Figure 7).

We stained the skin of *nac;pfe→sbr;shd* chimeras that showed a wild type pattern with the antibody recognizing only wild type Tjp1a. The signal was detected in the donor-derived iridophores but not in the epithelium. This result confirms supplying wild-type iridophores is sufficient for the formation of a wild-type pattern.

2.1.7 Possible functional redundancy of *tjps*

Antibody staining demonstrated the presence of Tjp1a in multiple tissues throughout development, such as blood vessels and epithelium, which is in agreement with earlier reports on zebrafish and mice (Blum *et al*, 2008; Anderson & Itallie, 1995). Unlike the *sbr* mutants, mice deficient in Tjp1 (ZO-1) are embryonic lethal (Katsuno *et al*, 2008). This can be explained by the fact that there are three Tjps (1-3) in mammals, but five in zebrafish (1a and b, 2a and b, 3), which is due to the whole genome duplication event that occurred in teleost evolution (Amores *et al*, 1998). The lack of a functional Tjp1a is likely compensated by its paralogue, Tjp1b, as indicated by the angiogenesis block, which was produced by morpholino-mediated knockdown of *tjp1b* in a *sbr* background. The mildness of the *sbr* pigment pattern phenotype suggests that Tjp1a and Tjp1b might have redundant functions in colour patterning. Depletion of ZO-1/TJP1 in mammalian cell cultures leads to the recruitment of ZO-2/TJP2 to cell membranes, which compensates for the absence of ZO-1 function (Umeda *et al*, 2004). Iridophore-specific depletion of both Tjp1a and 1b might inhibit the transition from the dense to the loose shape completely.

2.1.8 Potential mechanisms of Tjp1a control over cell shape

Several zebrafish mutants, such as *leopard/connexin 41.8* (Haffter *et al.*, 1996; Watanabe *et al.*, 2006), *luchs/connexin 39.4* (Irion *et al*, 2014) and *seurat/immunoglobulin superfamily member 11* (Eom *et al.*, 2012) exhibit spotted patterns where iridophores seem to invade the dark stripe areas. *luchs* and *leo* are required in melanophores and xanthophores (Maderspacher & Nüsslein-Volhard, 2003; Irion *et al*, 2014). This lead

Irion *et al.* to suggest that Cx39.4 and Cx41.8 form heteromeric gap junctions, which fail to properly function in the mutants, leading to abnormalities in melanophore and xanthophore communication. As a result, these cells might fail in giving appropriate guidance cues to iridophores. Interestingly, Cx41.8 and Igsf11 could be the possible interacting partners of Tjps, as they have putative PDZ domain-binding motifs on their extreme C-termini (Hung & Sheng, 2002; Suzu *et al.*, 2002). Indeed, yeast two-hybrid assays confirmed the possibility of Tjp1a interaction with both Cx39.4 and Cx41.8. However, both connexins are specific to melanophores and xanthophores. It is possible that there are iridophore-specific connexins that facilitate iridophore communication with melanophores and xanthophores.

In the absence of any of the other pigment cell type, dense iridophores expand (Frohnhofer *et al.*, 2013), and because of this, it is plausible that iridophores remain in their dense shape in the absence of signals directing them to transition. Tjp1a in iridophores may be involved in communicating transition signals, from membrane proteins to unknown downstream partners, either directly, or by establishing an interaction platform. This idea is corroborated by the increased strength of the spotted phenotypes in the double mutants *leo;sbr* and *luc;sbr* (Figure 8). It is well established that as scaffold proteins, Tjps utilize their multiple protein-protein interacting domains (for example, connexins mostly interact with PDZ domains) to form extensive complexes, in the proximity of cell membranes, that are associated with tight, adherens and gap junctions (Bauer *et al.*, 2010; Willott *et al.*, 1992; Kausalya *et al.*, 2001; Fanning *et al.*, 1998; Ikenouchi *et al.*, 2007; Umeda *et al.*, 2006). Because the *sbr^{mh009b}* allele yields a protein that is normally localised, it is plausible that the phenotype is caused by the absence of the ZU-5 domain, which is truncated in all of the alleles. This makes the potential interacting partners of this poorly investigated domain particularly interesting. A possible candidate for such a partner is Cdc42 effector kinase MRCK β (myotonic dystrophy kinase-related), which ZO-1 specifically directs to the leading edge of migrating cells, regulating actin-myosin mediated cell migration (Huo *et al.*, 2011; Unbekandt & Olson, 2014). It was shown that knockdowns of endogenous ZO-1 in COS-7 cells coupled with the expression of the ZO-1 version lacking the ZU5 domain, reduce the wound healing response in scratch assays (Huo *et al.*, 2011). However, knockouts of ZO-1 in Eph4 cells do not affect motility, which suggests that there is differential

regulation of cells by ZO-1 (Umeda *et al*, 2004). In SV40 cell cultures, long-term expression of truncated ZO-1 changes cell shape from a confluent hexagonal-like shape to a loose fibroblast-like shape (Ryeom *et al*, 2000). This shape change is reminiscent of the transition of iridophores from the dense shape to the loose shape during stripe formation. Together these reports support a possibility that the ZU5 domain, which is absent in the *sbr* mutants, is mediating the function of Tjp1a in iridophores.

However, one cannot exclude other mechanisms in the delay in the cell shape transition, since Tjps are known to control many aspects of cell biology, such as junction assembly, cell proliferation and gene expression (Xu *et al*, 2012; Ryeom *et al*, 2000; Balda & Matter, 2009).

In summary, we have demonstrated a crucial role of cell shape and organisation changes in the striped pigment pattern formation of zebrafish and identified Tjp1a as a novel regulator of this process. The regulation of iridophore shape transitions by Tjp1a might contribute to the variety of patterns observed in teleosts. For example, *Danio kyathit* displays a spotted or undulating pattern, quite similar to *sbr* in appearance and variability. The viability of the *sbr* mutants presents exciting opportunities for studying the behaviour of Tjp1-deficient cells *in vivo*.

Tight Junction Protein 1a regulates pigment cell organisation during zebrafish colour patterning

Andrey Fadeev, Jana Krauss[†], Hans Georg Frohnhöfer, Uwe Irion, Christiane Nüsslein-Volhard*

Max Planck Institute for Developmental Biology, Tübingen, Germany

Abstract Zebrafish display a prominent pattern of alternating dark and light stripes generated by the precise positioning of pigment cells in the skin. This arrangement is the result of coordinated cell movements, cell shape changes, and the organisation of pigment cells during metamorphosis. Iridophores play a crucial part in this process by switching between the dense form of the light stripes and the loose form of the dark stripes. Adult *schachbrett* (*sbr*) mutants exhibit delayed changes in iridophore shape and organisation caused by truncations in Tight Junction Protein 1a (ZO-1a). In *sbr* mutants, the dark stripes are interrupted by dense iridophores invading as coherent sheets. Immuno-labelling and chimeric analyses indicate that Tjp1a is expressed in dense iridophores but down-regulated in the loose form. Tjp1a is a novel regulator of cell shape changes during colour pattern formation and the first cytoplasmic protein implicated in this process.

DOI: [10.7554/eLife.06545.001](https://doi.org/10.7554/eLife.06545.001)

*For correspondence: christiane.nuesslein-volhard@tuebingen.mpg.de

Present address: [†]Auengrund 7, Schönau-Berzdorf, Germany

Competing interests: The authors declare that no competing interests exist.


Funding: See page 14

Received: 18 January 2015

Accepted: 24 April 2015

Published: 27 April 2015

Reviewing editor: Marianne E Bronner, California Institute of Technology, United States

 Copyright Fadeev et al. This article is distributed under the terms of the [Creative Commons Attribution License](https://creativecommons.org/licenses/by/4.0/), which permits unrestricted use and redistribution provided that the original author and source are credited.

Introduction

One of the most fascinating features of vertebrates is their display of remarkable colour patterns in skin, fur, or plumage, frequently varying strikingly between closely related species. Teleost fish exhibit a particularly high diversity of patterns formed by several types of pigment cells distributed in a multilayered arrangement in the hypodermis (Singh and Nüsslein-Volhard, 2015). Adult zebrafish display a conspicuous pattern of alternating dark and light stripes; remarkably different from a relatively simple larval pattern, which is generated directly from neural crest cells migrating during embryogenesis (Kelsh et al., 1996). The adult pattern is formed from neural crest-derived progenitors during metamorphosis (3–6 weeks of development). Metamorphic iridophores (silvery cells containing reflective guanine platelets) and melanophores (dark cells containing the black pigment melanin) arise from neural crest-derived stem cells associated with the peripheral nervous system, whereas metamorphic xanthophores (yellow–orange cells containing pteridine based pigments) originate from proliferating larval xanthophores (Budi et al., 2011; Dooley et al., 2013; Mahalwar et al., 2014; McMenamin et al., 2014; Singh et al., 2014). Several adult viable zebrafish mutants displaying abnormal adult pigment patterns have been described (Haffter et al., 1996; Kelsh et al., 1996; Lister et al., 1999). One class of genes primarily affects the formation of one of the three cell types. For example *nacre/mitfa* mutants lack melanophores, *pfeffer/csf1ra/fms* mutants lack xanthophores, and in *shady/ltk* iridophores are compromised (Lister et al., 1999; Parichy et al., 2000; Lopes et al., 2008). Genetic analyses and regeneration studies revealed that interactions between all three cell types are necessary for proper stripe formation in the trunk of the fish (Maderspacher and Nüsslein-Volhard, 2003; Nakamasu et al., 2009; Frohnhöfer et al., 2013; Patterson and Parichy, 2013).

Long-term in vivo imaging has shown that stripe formation involves intricate cell shape and density changes of metamorphic pigment cells (Mahalwar et al., 2014; Singh et al., 2014). Iridophores take a lead in stripe formation: they appear along the horizontal myoseptum, proliferate and spread as

eLife digest The striking horizontal striped pattern of the zebrafish makes it a decorative addition to many home aquariums. The stripes are a result of three different pigment cells interacting with each other, and first begin to emerge when the animal is two to three weeks old. At that time, iridescent cells called iridophores begin to multiply and spread in the skin. In the light-coloured stripes, the iridophores are compact and 'dense'; in the dark stripes the cells change into a 'loose' shape and organisation. Black-pigmented cells fill in the dark stripes, and a third cell type with a yellow hue condenses over the light stripes. How the three types of cell work together to make the striped pattern is not fully understood.

Fadeev et al. examined a zebrafish variant with a genetic mutation that disrupts the function of a protein called Tight Junction Protein 1a (or Tjp1a)—a fish variant of a mammalian protein called ZO-1. This protein helps cells to interact with each other. The mutant fish appear spotted rather than striped, because light regions containing sheets of the dense iridophores interrupt the dark stripes.

Experiments using fluorescent markers showed that Tjp1a is produced in much lower amounts in the loose iridophores in the dark stripes than in the dense iridophores of the light stripes. This led Fadeev et al. to suggest that the transition from the dense to the loose shape is dependent on the presence of Tjp1a in the cell.

Tjp1a is likely to regulate how colour patterns form by controlling how iridophores interact with other types of pigment cell. The Tjp1a mutant fish provides the first glimpse into the machinery inside cells that underlies colour pattern formation, and will help to identify other components and cues responsible for cell interactions.

DOI: [10.7554/eLife.06545.002](https://doi.org/10.7554/eLife.06545.002)

a dense sheet in the skin to form the first light stripe. At the margins of this first light stripe, the dense iridophores undergo a transition into a loose form and spread over the dark stripe region. Past the presumptive dark stripe, they change into the dense form again and aggregate into sheets forming new light stripes (Singh et al., 2014). The first two dark stripes form dorsally and ventrally of the first light stripe by melanoblasts migrating along spinal nerves into the skin in the presumptive dark stripe region. They initially appear as stellate cells with the pigment located in the centre of the cells but later expand into the stationary rounded form (Dooley et al., 2013; Singh et al., 2014). Metamorphic xanthophores originate from larval xanthophores, they compact over the dense iridophores of the light stripe and change into a pale stellate shape above the loose iridophores and melanophores of the dark stripe (Mahalwar et al., 2014). A different type of iridophores—L-iridophores—underlie the melanophores of the dark stripe. L-iridophores appear only after the first two dark stripes are formed and do not participate in laying out the pattern (Frohnhofer et al., 2013; Hirata et al., 2003, 2005). Interestingly, iridophore-deficient mutants are not affected in the stripe pattern of the fins, suggesting differences in the mechanisms involved in patterning of the trunk and fins (Frohnhofer et al., 2013).

Mutants in which all three chromatophore types develop, but stripe formation is impaired, are of particular interest, as they can provide insights in the molecular mechanisms of cell–cell interactions underlying stripe formation. Several mutants have been described in which dark stripes are broken into spots. *leopard/Cx 41.9*, *luchs/Cx39.4* encode components of gap junctions involved in cell–cell communications (Maderspacher and Nüsslein-Volhard, 2003; Watanabe et al., 2006; Irion et al., 2014). In the absence of *leo* or *luc*, iridophores fail to change to the loose form and suppress melanophores. *leo* and *luc* presumably form heteromeric gap junctions among and between melanophores and xanthophores, instructing iridophores to change shape in a spatially controlled manner (Irion et al., 2014).

In this study, we present the mutant *schachbrett (sbr)* (German for checkerboard) that exhibits interruptions in dark stripes by light stripe regions. *sbr* encodes Tight Junction Protein 1a (Tjp1a/ZO-1). Immunostaining revealed that Tjp1a is expressed in dense iridophores but neither in loose iridophores nor any other pigment cell type. Analysis of double mutants and chimeras shows that *sbr* is cell-autonomously required in iridophores. During metamorphosis, dense iridophores invade the dark stripe regions and temporarily suppress the expansion of melanophores, suggesting that Tjp1a is required to regulate the transition of dense iridophores into the loose shape and their organisation.

Results

schachbrett encodes Tight Junction Protein 1a

Adult *sbr* fish display an unchanged arrangement and approximately normal width of stripes, however, the dark stripes are interrupted and undulating (**Figure 1A**). The allele *sbr^{tnh009b}* was isolated during a screen for ENU-induced recessive, homozygous viable mutants affecting adult pattern formation. The mutation was mapped to the region 29.6–32.5 Mb of chromosome 7 (Ensembl Zebrafish release 72) (**Figure 1B**). Using a candidate approach, we sequenced *tjp1a* cDNA of *sbr^{tnh009b}* and detected a nonsense mutation leading to Y1143Stop change in the C-terminal part of the protein (**Figure 1C**). To confirm the suggestion that this mutation is causative for the *sbr* phenotype, we performed a screen for additional alleles. ENU-mutagenized Tü males were crossed to *sbr^{tnh009b}* females; the progeny was raised to the adulthood and screened for the *sbr* phenotype. Four new

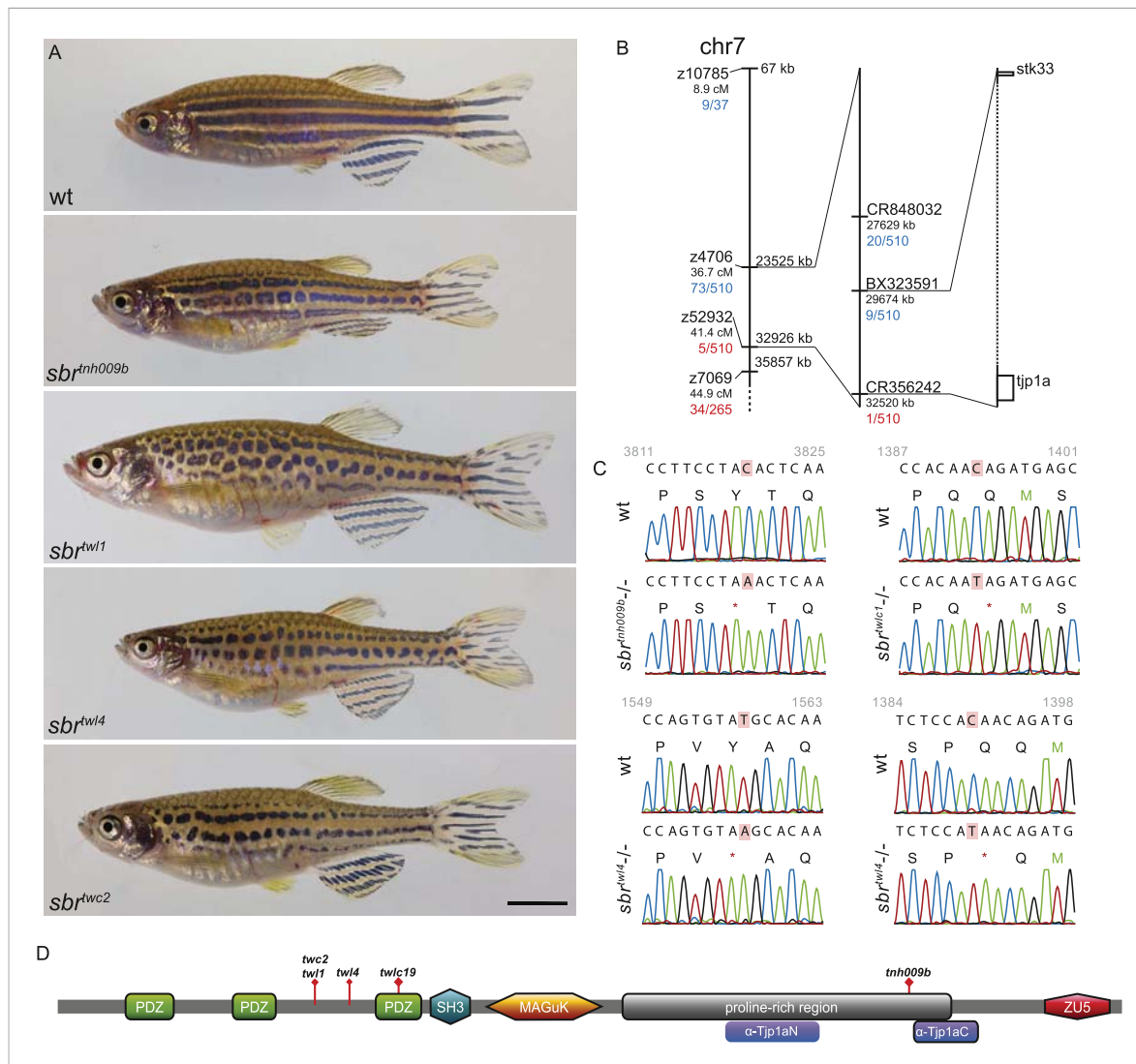


Figure 1. *schachbrett* encodes Tjp1a. **(A)** All alleles of *sbr* exhibit interrupted, undulating dark stripes of normal arrangement and width when compared to wild type, but no other obvious defects. Scale bar: 5 mm. **(B)** Scheme of meiotic mapping of *sbr*. Marked are z-markers and contigs on which SNPs were found with their genomic and genetic (where applicable) coordinates. The numbers of recombinants among all fish tested are given in red and blue. The right-most bar shows genes on the ends of the final mapped region. The dotted region is not to scale and contains multiple genes. **(C)** DNA sequence traces for four alleles of *sbr*. Red rectangles mark the mutated residues. Red asterisks stand for stop codons. **(D)** Scheme of Tjp1a protein. Purple rounded squares indicate regions corresponding to polypeptides used for antibody generation. Red diamonds show the positions of stop codons in the mutants. DOI: 10.7554/eLife.06545.003

alleles not complementing the original allele were isolated. We identified novel stop codons in positions of the *tjp1a* gene corresponding to the N-terminal part of the protein in all four new alleles. The phenotype is variable, and no qualitative differences between the alleles could be recognized. Individual fish of the *sbr^{tnh009b}* allele with the C-terminal truncation may show a weaker phenotype not seen in the other alleles, therefore, we cannot exclude that it may have residual function. In subsequent crosses, we never observed a segregation of the *sbr* phenotype and the *tjp1a* mutant alleles. These results show that the loss of Tjp1a function causes the *sbr* phenotype.

The *sbr* phenotype is not caused by a decrease in melanophore number

The larval pigment pattern is unaffected in *sbr* mutants (**Figure 2A**, 6.5 mm). Repeated photography of individual fish revealed that mutants can be distinguished from wild-type siblings at stage 7.5 mm SL (Standard Length [Parichy et al., 2009]) (about 4 weeks post fertilisation) shortly after the first metamorphic melanophores appear (**Figure 2A**). At this and following stages, melanophores in the mutants appear as small dots when compared to melanophores of wild type, giving the metamorphic fish a pale appearance (**Figures 2A**, 9.0–10.2 mm). Later (11 mm SL), the melanophores acquire

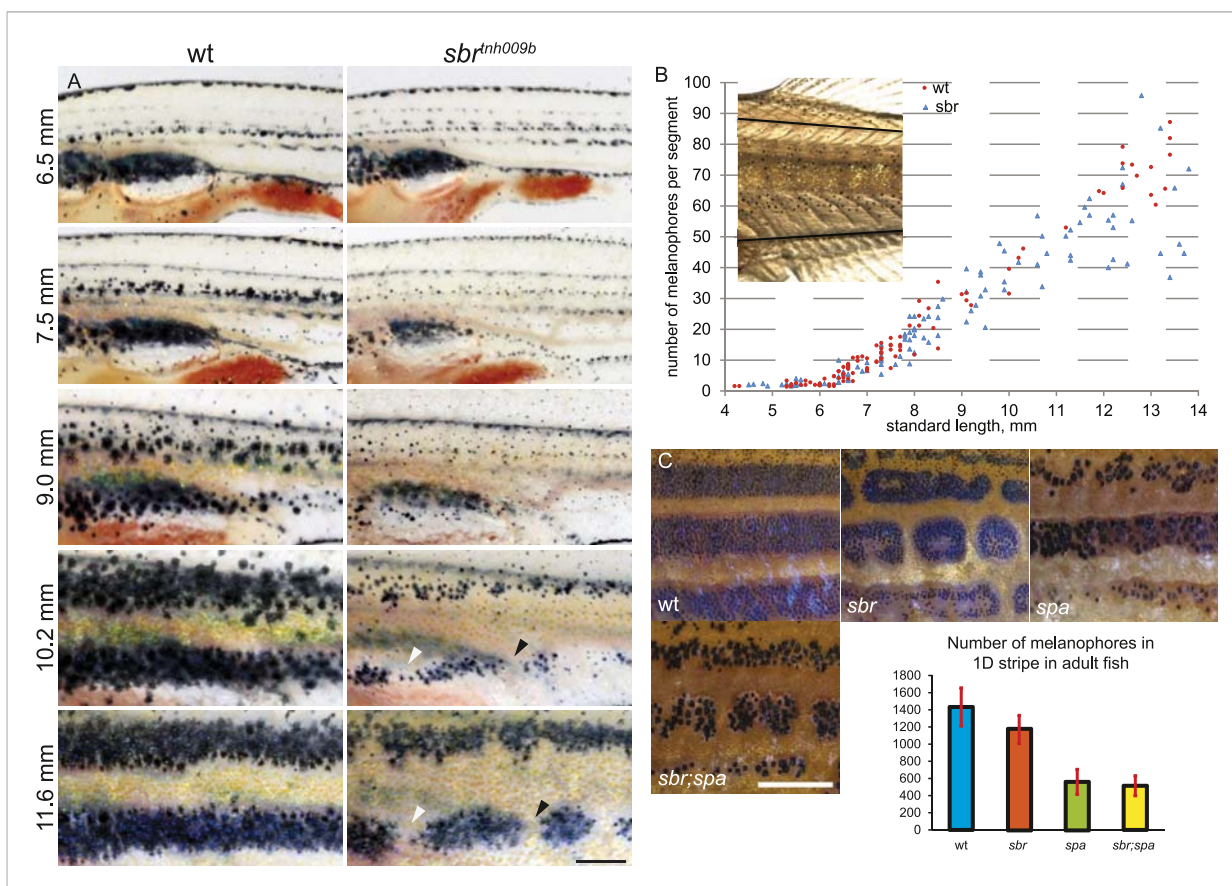


Figure 2. Abnormal behaviour of *sbr* mutant melanophores. **(A)** Pigment pattern during metamorphosis in the mid-trunk of individual wild type and *sbr* mutant fish. Arrowheads: forming interruptions. White arrowheads: disappearing melanophores (N = 6). Scale bar: 1 mm. **(B)** Average number of melanophores per segment in the first two dark stripes in wild type and mutant fish plotted against standard length. Red circles—individual wild type fish; blue squares—individual *sbr* fish. Inset shows the area where melanophores were counted. Distributions of melanophore numbers in mutants and wild type fish do not differ significantly until the 10 mm stage as shown by Kolmogorov–Smirnov statistics. At 10–14 mm stages the distributions are different with p-values < 0.05. **(C)** Close-ups of mid-trunk regions of adult wild type, *sbr*, *spa* and *sbr;spa* and melanophore numbers in a dark stripe dorsal to the first light stripe of adult fish. Red lines—standard deviation. Scale bar: 2 mm.

DOI: 10.7554/eLife.06545.004

The following figure supplement is available for figure 2:

Figure supplement 1. Width of the first light stripe in *sbr* and wild type fish.

DOI: 10.7554/eLife.06545.005

a shape similar to wild-type cells (**Figure 2A**, 11.6 mm). The melanophore numbers in mutant and wild-type fish do not differ significantly until 10 mm SL (**Figure 2B**), when the pale phenotype is already established. In older mutant fish, there is a slight decrease in the average number of melanophores, likely due to the interruptions of the stripe areas (**Figure 2C**, wt, *sbr*). To assess the impact of melanophore number on stripe integrity, we compared *sbr* to *sparse* (*spa*) mutants, which have decreased numbers of melanophores (**Johnson et al., 1995**). *spa* mutants have only about a third as many melanophores as wild-type fish (**Figure 2C**, plot); however, these cells form uninterrupted stripes (**Figure 2C**, *spa*). Double mutants *sbr;spa* display a combination of both phenotypes (**Figure 2C**, *sbr;spa*). This indicates that the pale appearance of the mutant metamorphic fish is caused by an abnormal size, shape, or pigment arrangement rather than a reduced number of melanophores.

***sbr* iridophores fail to undergo shape change during early stripe formation**

In early metamorphic mutant fish, but not in adults, the width of the first light stripe, composed of dense iridophores covered by compact yellow xanthophores, is increased compared to wild type (**Figure 2A**, 11.6 mm; **Figure 2—figure supplement 1**).

After 10 mm SL, dense S-iridophores and xanthophores can be observed in the dark stripe region in *sbr* mutants (**Figure 2A**, arrowheads) and melanophores disappear from these areas (**Figure 2A**, white arrowheads), ultimately leading to the interruptions. To investigate iridophore behaviour, we performed repeated imaging of wild-type and *sbr* individuals over a period of 2 weeks. To allow a more detailed visualisation of the cell shapes, we imaged fish carrying the *Tg(TDL358:GFP)* transgene (labelling iridophores and glia with cytosolic GFP [**Levesque et al., 2013**]) alone (**Figure 3**) or together with a second transgene, *Tg(sox10:mRFP)* (**Figure 4**), which labels neural crest derivatives with membrane-bound mRFP. In both, wild type and mutants, iridophores appeared in segmental clusters during early metamorphosis (about 7 mm SL), they increased in number and merged to form the first light stripe (**Figure 3A**, **Figure 4A**). In wild type, iridophores proceeded to define the edge of the light stripe, there they delaminated and formed loose iridophores, which spread dorsally and ventrally over the dark stripe regions (**Figure 3A**, 8.9 mm; **Figure 4**; **Singh et al., 2014**). Dense iridophores occasionally spread too far from the horizontal myoseptum (**Figure 3B**, wt), but later formed sharp light stripe borders. However, in the mutants the dense iridophores did not delaminate but continued to spread over the metamorphic melanophores as a coherent sheet (**Figure 3A**, *sbr* 8.9 mm; **Figure 4**, *sbr*, 8.3 mm). At later stages, eventually some of them switched to the loose form (arrowheads in **Figure 3B**; **Figure 4A**) and occasionally seemed to disappear from the dark stripe regions at a time point, which coincided with expansion of melanophores (10.5 mm SL, **Figure 3—figure supplement 1**). When this retreat did not happen, the iridophores persisted in interruptions of the dark stripes (**Figure 2A**, 11.6 mm). The failure to precisely form the boundary between light and dark stripes might be a cause for another anomaly observed in *sbr* mutants: L-iridophores, which are restricted to dark stripe areas in wild type, were observed in light stripes of adult *sbr* mutants (**Figure 3—figure supplement 2**).

Analysing fish carrying the transgene *Tg(kita:GalTA4:UAS:mCherry)*, which labels melanophores (**Anelli et al., 2009**), we observed that in *sbr* mutants individual melanophores moved away from invading dense iridophores, while maintaining a migratory stellate shape, or they disappeared after being trapped (**Figure 5**, **Figure 5—figure supplement 1**). This is in agreement with the observed reduction in the number of melanophores in *sbr* during later stages of development (**Figure 2B**).

Tjp1a is required in iridophores for pattern formation

To investigate in which cell type *sbr* function is required, we analysed *sbr* in combination with mutants lacking one of the three pigment cell types. Both *shady* mutants, lacking iridophores (*shd*, **Figure 6C**, **Figure 6—figure supplement 1A**) and *shd;sbr* double mutants (**Figure 6D**, **Figure 6—figure supplement 1B**), display the *shd* phenotype with no detectable differences, suggesting that *sbr* function is only required in iridophores. In contrast, the phenotypes of double mutants with *nacre* (*nac*, no melanophores, **Figure 6E**) or *pfeffer* (*pfe*, no xanthophores, **Figure 6G**) differ from the single mutants. Both *pfe* and *nac* alone exhibit expanded areas of dense iridophores. In combination with *sbr*, both double mutants show a further expansion of these dense iridophore regions (**Figure 6F,H**), covering most of the body. This phenotypic enhancement suggests that the cell type affected in *sbr* is

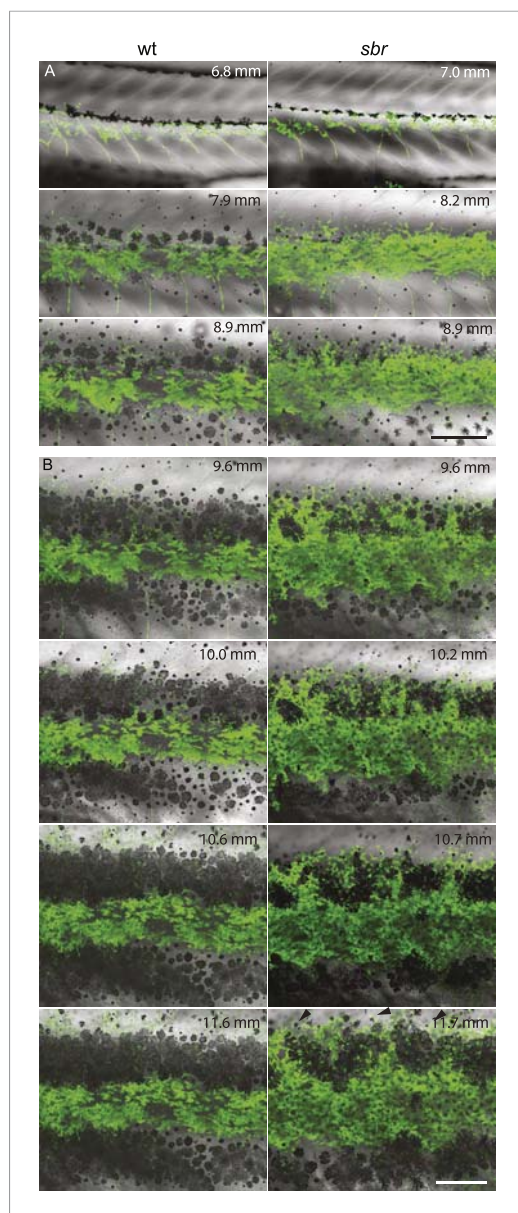


Figure 3. Behaviour of *sbr* mutant iridophores during metamorphosis. **(A)** Repeated imaging of *Tg(TDL358:GFP)* wild type and mutant metamorphic individual (N = 5 each, one shown). Scale bar: 300 μ m. **(B)** Same individuals with another magnification. Empty patches in the light stripe of wild type fish are caused by variegation of the transgene expression. Arrowheads: loose iridophores. Scale bar: 300 μ m.

DOI: [10.7554/eLife.06545.006](https://doi.org/10.7554/eLife.06545.006)

The following figure supplements are available for figure 3:

Figure supplement 1. Invading *sbr* iridophores occasionally retreat.

DOI: [10.7554/eLife.06545.007](https://doi.org/10.7554/eLife.06545.007)

Figure supplement 2. L-iridophores in wt and *sbr*.

DOI: [10.7554/eLife.06545.008](https://doi.org/10.7554/eLife.06545.008)

still present in *nac* and *pfe* mutants, again pointing to iridophores. To confirm these findings, we created chimeric animals by blastomere transplantations. Experiments with *sbr* donors and *nac* or *pfe* recipients revealed that *sbr* melanophores and xanthophores can participate in normal pattern formation (**Figure 6I,J**). When we used *shd;sbr* double mutants as recipients (**Figure 6D**) and *nac;pfe* (**Figure 6K**) as donors, which can provide only iridophores, we observed regional restoration of the striped pattern in the chimeric fish (**Figure 6L**). This indicates that *sbr* is required cell autonomously in iridophores and confirms that mutant *sbr* melanophores and xanthophores can contribute to the normal pattern when confronted with wild-type iridophores.

The fins of *sbr* mutants are striped, although we detect branching and supernumerary stripes to various extents in the caudal fins of some *sbr* mutant fish but not in their anal fins suggesting that there is no systematic defect in fin patterning. This is in agreement with the finding that iridophores are not required for striping the fins (**Hirata et al., 2005; Frohnhöfer et al., 2013; Krauss et al., 2013**).

Tjp1a is expressed in dense iridophores but not in loose iridophores nor other pigment cells

We raised two polyclonal antibodies in rabbits specific to zebrafish Tjp1a (**Figure 1D**). α -Tjp1aN was designed to recognize both, truncated *sbr^{tnh009b}* and wild-type Tjp1a protein, whereas α -Tjp1aC would only bind to the wild-type protein. Both antibodies allow the detection of Tjp1a in epithelial cells of larval and adult zebrafish skin (**Figure 7—figure supplements 1, 2**). This staining is absent in mutants with stop codons in the N-terminal part of *tjp1a* but present in *sbr^{tnh009b}* mutants stained with α -Tjp1aN (**Figure 7—figure supplement 1**). We also detected expression of Tjp1a in blood vessels during larval and adult stages (**Figure 7—figure supplement 2**), corroborating earlier reports on the expression of Tjps in zebrafish and mice (**Anderson and Itallie, 1995; Blum et al., 2008**). Immunostaining of skin in metamorphic fish carrying the *Tg(TDL358:GFP)* transgene (**Figure 7A**) shows that Tjp1a is expressed in dense iridophores of the light stripe. Intriguingly, delaminated loose iridophores still express GFP, but no Tjp1a is detectable (**Figure 7B**). This indicates that Tjp1a is down-regulated during delamination of loose iridophores from the dense

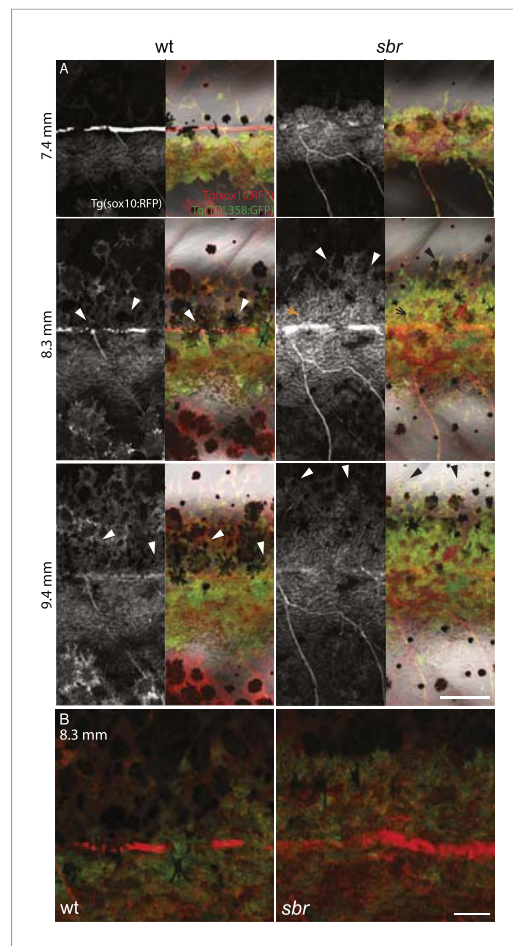


Figure 4. Behaviour of *sbr* mutant iridophores during establishment of the first dark stripes. **(A)** *Tg(TDL358:GFP)*; *Tg(sox10:mRFP)* wild type and *sbr* metamorphic fish ($N = 4$ each, one shown). Arrowheads point to delaminating loose iridophores. Arrow shows dense iridophores failing to delaminate. Scale bar: 150 μm . **(B)** Close-ups of *Tg(TDL358:GFP)*; *Tg(sox10:mRFP)* wild type and *sbr* metamorphic fish 8.3 SL. Note difference in iridophore shapes in wild-type. Scale bar: 50 μm . DOI: 10.7554/eLife.06545.009

complete loss of melanophore clustering is observed; the upper part of the body is covered with a layer of dense iridophores. In the case of *sbr;leo*, the melanophore spots are even smaller and the dense iridophore-free areas around them are narrower. These results suggest that connexins and *tjp1a* do not act in a linear pathway affecting pigmentation. To investigate whether zebrafish *Tjp1a* can interact directly with connexins, we performed yeast two-hybrid assays (**Figure 8—figure supplement 1**). We observed interactions between Cx41.8 and all three PDZ domains of *Tjp1a* and between Cx39.4 and PDZ-2 and 3 in this assay.

Discussion

We show that *Tjp1a*-deficient fish develop multiple interruptions of the dark stripes in the trunk by light stripe structures composed of dense iridophores covered by compact xanthophores. In *sbr* mutants, dense iridophores of the light stripe spread during metamorphosis as a coherent sheet invading dark stripes rather than loosening up and dispersing. Melanophore expansion into the stationary rounded form is temporarily suppressed. However, clustered melanophores later expand and seem to repulse iridophores in a process, which is similar to the one involved in smoothening of stripe boundaries

sheet in the light stripe. In adult skin preparations, the signal can be observed in dense iridophores of the light stripes but not in xanthophores, melanophores, L-, or loose iridophores (**Figure 7C**). Together with our observation that the loss of *tjp1a* function in *sbr* mutants compromises the transition of iridophores from dense to loose state, these results suggest that *Tjp1a* is a component of the molecular switch that regulates iridophore shape changes during their dispersal.

Additionally, we analysed chimeras obtained by transplanting blastomeres from *sbr^{tw/d}* embryos, where transplanted cells were labelled with expression of the ubiquitous *Tg(H2A:GFP)* transgene, into blastula stage wild-type embryos. Double stainings with α -*Tjp1a*N and α -GFP antibodies show that the donor-derived *sbr* dense iridophores integrate with the wild-type recipient iridophores but do not express *Tjp1a* (**Figure 7D**). This suggests that the *sbr* phenotype is not caused by over-proliferation of iridophores, since they do not produce large clusters. We stained skin of *nac;pfe/shd;sbr* chimeras with α -*Tjp1a*C and detected *Tjp1a* in donor-derived iridophores but not in the epithelium, suggesting that loss of *Tjp1a* function in the epithelium does not affect pattern formation (**Figure 7—figure supplement 3**).

sbr enhances connexin mutant phenotypes

To investigate the genetic interactions between *tjp1a* and potential partners, *cx39.4* and *cx41.8*, we evaluated the phenotypes of double mutants with *luc^{t32241}* and *leo^{t1}* (**Figure 8**). *luc* mutant fish display meandering and broken stripes, whereas in *leo^{t1}* the stripes are broken into spots. In the double mutants with *sbr*, we observe considerably stronger patterning defects than in the single mutants. In the case of *sbr;luc*, an almost

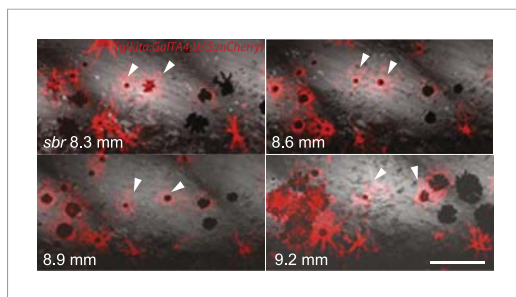


Figure 5. Two closely positioned melanophores in *sbr* (arrowheads), are migrating away from the iridophores in posterior and anterior directions. Scale bar: 100 μ m.

DOI: [10.7554/eLife.06545.010](https://doi.org/10.7554/eLife.06545.010)

The following figure supplement is available for figure 5:

Figure supplement 1. Melanophores trapped in the mass of iridophores are disappearing in *sbr*.

DOI: [10.7554/eLife.06545.011](https://doi.org/10.7554/eLife.06545.011)

(Frohnhofer et al., 2013; Singh et al., 2014). The location of the interruptions seems to be random. Genetic mosaics, double mutant analysis, as well as immunostaining indicate that Tjp1a is expressed and required in dense iridophores but not in melanophores or xanthophores. We show that, surprisingly, Tjp1a-deficient iridophores do display a dense shape and organisation, however, intriguingly, they fail to undergo the transition to the loose shape. This suggests that the cell shape of loose iridophores is not determined by the absence of Tjp1a per se. In contrast, a reduction in the levels of Tjp1a may be read by iridophores as a trigger for the transition or the cell shape change might result in a down-regulation of Tjp1a. In the absence of Tjp1a, other Tjps might take over the role in cell compaction but may not be able to properly respond to cues guiding the transition to the loose shape.

Gene duplication and redundancy of Tjps functions in zebrafish

One surprising finding of this study is that Tjp1a-deficient zebrafish are viable unlike embryonic lethal Tjp1^{-/-} mice (Katsuno et al., 2008). There are three *tjp* genes (1–3) in mammals and five in zebrafish (1a–b, 2a–b, 3), due to the whole genome duplication in teleosts (Amores et al., 1998). The lack of Tjp1a function in epithelial cells in *sbr* mutants might be compensated for by other Tjps, for example, Tjp1b, which does not exist in mammals. This is supported by the observation that morpholino-mediated knockdown of *tjp1b* in *sbr* mutants, but not wild-type embryos, results in impaired blood flow and death at 5 dpf (Videos 1–3). This suggests that Tjp1b and Tjp1a have redundant functions at least in the vasculature epithelial cells. This notion is supported by experiments with mammalian cell cultures showing that absence of ZO-1 leads to increased recruitment of ZO-2 to cell membranes, which is suggested to compensate for the absence of ZO-1 (Umeda et al., 2004).

Tjp1a-induced cell shape transition during colour pattern formation

Our data show that in *sbr* dense iridophores fail to switch to the loose form in dark stripe regions. In wild type, dense iridophores normally stay restricted to developing light stripes, but occasionally spread into the prospective dark stripe areas. This irregularity is usually corrected and sharp stripe boundaries are formed. However, in *sbr*, the invasion of dense iridophores occurs along the whole length of stripes. Not all dense iridophores persist in dark stripe regions in *sbr* mutants. In summary, we hypothesize that the loss of Tjp1a impairs the ability of iridophores to recognise the (as yet unknown) cues defining the dark stripe areas or their ability to react to them efficiently. So far, only a rather small number of molecules have been identified, which are involved in the various interactions between chromatophores. Tjp1a is the first for which a molecular distribution and cell type specific expression has been shown.

Tjp1a might interact with connexins/gap junctions

Several zebrafish mutants including *leopard* (Haffter et al., 1996; Watanabe et al., 2006), *luchs* (Irion et al., 2014), and *seurat* (Eom et al., 2012) exhibit a spotted pattern formed by ingressions of iridophores into the dark stripe area. *luc* and *leo* encode Connexin41.8 (Cx41.8) and Connexin39.4 (Cx39.4), respectively, which are, in contrast to *sbr*, required in melanophores and xanthophores (Maderspacher and Nüsslein-Volhard, 2003; Irion et al., 2014). Irion et al. suggest that Cx39.4 and Cx41.8 form heteromeric gap junctions, promoting interactions of melanophores and xanthophores that result in the appropriate patterning of iridophores. In the absence of xanthophores or melanophores, dense iridophore regions are expanded (Frohnhofer et al., 2013), suggesting that Tjp1a in iridophores may be involved in cell communication with xanthophores and/or melanophores. However, the downstream cytoplasmic partners of the transmembrane proteins shown to be involved in patterning in melanophores and xanthophores are unknown as well as transmembrane molecules in

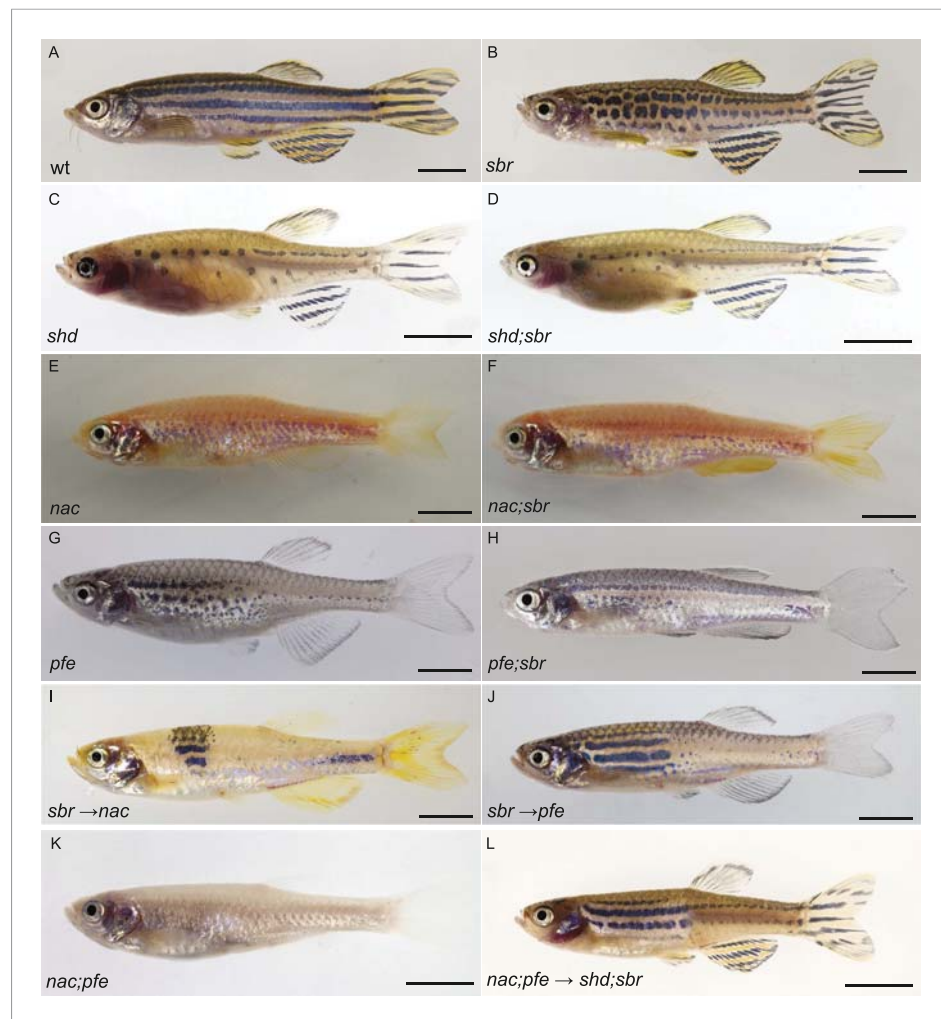


Figure 6. *tjp1a* is required in iridophores, but not melanophores or xanthophores. (A) Wild type fish. (B) *sbr* fish. (C) *shady* (*shd*) mutant, which lacks iridophores. (D) *shd;sbr* mutant is indistinguishable from *shd*. (E) *nacre* (*nac*) mutant, which lacks melanophores. (F) *nac;sbr* double mutant exhibiting expanded dense iridophore areas in comparison to *nac* alone. (G) *pfeffer* (*pfe*) mutant, which has no xanthophores. (H) *pfe;sbr* double mutant exhibiting expanded dense iridophore areas in comparison to *pfe* alone. (I) Chimeras, obtained from transplantation of *sbr* blastomeres into *nac* recipient blastulas, show clonal rescue. (J) Chimeras obtained from transplantation of *sbr* blastomeres into *pfe* recipient blastulas, show clonal rescue. (K) *nac;pfe* fish have only one type of pigment cells—iridophores. (L) Chimeras obtained from transplantation of *nac;pfe* blastomeres into *shd;sbr* recipient blastulas, show clonal rescue. Scale bars: 5 mm.

DOI: [10.7554/eLife.06545.012](https://doi.org/10.7554/eLife.06545.012)

The following figure supplement is available for figure 6:

Figure supplement 1. Phenotypes of *shd* and *shd;sbr* mutants.

DOI: [10.7554/eLife.06545.013](https://doi.org/10.7554/eLife.06545.013)

iridophores that are responsible for the interactions. Another mutant displaying a spotted pattern is *seurat*, encoding the transmembrane protein immunoglobulin superfamily member 11 (Igsf11) (Eom et al., 2012). Interestingly, Cx41.8 and Igsf11 are possible interacting partners of Tjps since they have putative PDZ-binding motifs on their extreme C-termini (Hung and Sheng, 2002; Suzu et al., 2002). The multiple protein–protein interacting domains in Tjps allow for many interacting partners and facilitate formation of large complexes in proximity of cell membranes that are associated with tight, adherens, and gap junctions. These provide a link between transmembrane proteins and the cytoskeleton and were shown to participate in regulation of many cellular processes such as junction assembly, cell proliferation, and differentiation (Balda and Matter, 2000; Bauer et al., 2010;

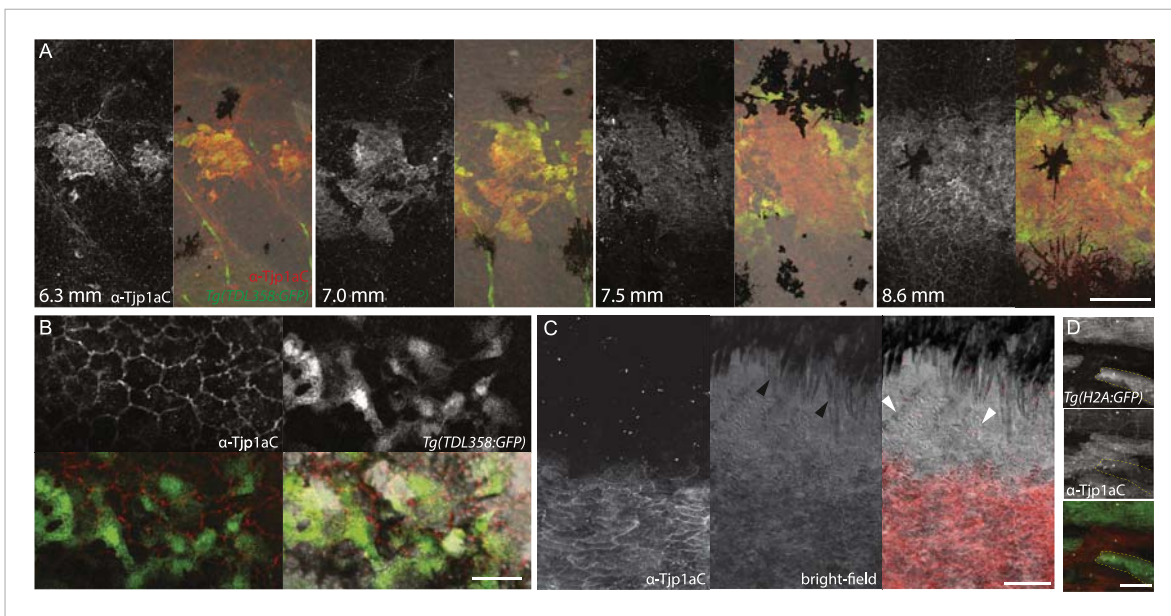


Figure 7. Tjp1a is expressed in dense iridophores. **(A)** Double antibody staining of metamorphic *Tg(TDL358:GFP)* fish with α -Tjp1aC and α -GFP antibodies. Note: not all iridophores are expressing GFP due to transgenic line variegation. Scale bar: 100 μ m. **(B)** Loose iridophores migrating over the dark stripe in 8.3 mm metamorphic *Tg(TDL358:GFP)* fish express GFP, but not Tjp1a, although the epithelial staining is still visible. Scale bar: 30 μ m. **(C)** α -Tjp1aC staining in skin of adult wild type fish. The protein is detected in the sheet of dense S-iridophores of the light stripe, but not in L-iridophores (black arrowheads), loose iridophores (white arrowheads), melanophores or xanthophores. Scale bar: 100 μ m. **(D)** Double antibody staining with α -Tjp1aC and α -GFP of skin of adult chimera, obtained by transplanting *sbr;Tg(H2A:GFP)* blastomeres into wild type blastula. Either GFP or Tjp1a was detected in cells, never both. Some *sbr* cells express no GFP due to variegation of the transgene expression. Scale bar: 30 μ m.

DOI: [10.7554/eLife.06545.014](https://doi.org/10.7554/eLife.06545.014)

The following figure supplements are available for figure 7:

Figure supplement 1. Tjp1a stainings in wild type and *sbr*.

DOI: [10.7554/eLife.06545.015](https://doi.org/10.7554/eLife.06545.015)

Figure supplement 2. Characterization of the Tjp1a expression domain.

DOI: [10.7554/eLife.06545.016](https://doi.org/10.7554/eLife.06545.016)

Figure supplement 3. Correlation between clonal rescue of *sbr* phenotype and Tjp1a expression.

DOI: [10.7554/eLife.06545.017](https://doi.org/10.7554/eLife.06545.017)

Xu et al., 2012; González-Mariscal et al., 2014). Our results show that *sbr* enhances the phenotypes of both *luc* and *leo* mutants. This suggests that Tjp1a and connexins do not act in a linear pathway to regulate pattern formation, but most likely work through different mechanisms. One possible explanation is that Tjp1a is required for spatially and temporally controlled reaction of iridophores in response to melanophores (directly or through xanthophores). Absence or truncation of Tjp1a results in a delayed switch to the loose form, which in turn forces melanophores to reorganize according to the presence of dense iridophores in normally iridophore-free regions. In *luchs* and *leopard*, the melanophore and xanthophore autonomous mutations also affect patterning of iridophores, likely due to the failure to properly guide iridophores (*Irion et al., 2014*). The combined effect of failure of melanophores and xanthophores to provide cues to iridophores, and the delayed reaction of iridophores might be responsible for the enhanced phenotypes in the double mutants.

Interestingly, Tjp1a and Cx39.4 and Cx41.8 can interact in a yeast 2-hybrid assay. As in the fish they are required in different pigment cell types, this may point to the existence of other, as yet unknown, connexins, similar to the Cx41.8 and Cx39.4, that are expressed in iridophores and interact with Tjp1a. ZO-1 was shown to regulate gap junction assembly, localization, and regulate plaque size in mammalian cell cultures (*Hunter et al., 2005; Laing et al., 2005; Rhett et al., 2011*). Defective Tjp1a in *sbr* might affect proper interaction of iridophore connexins with their counterparts in melanophores and xanthophores, compromising cell–cell communication and recognition.

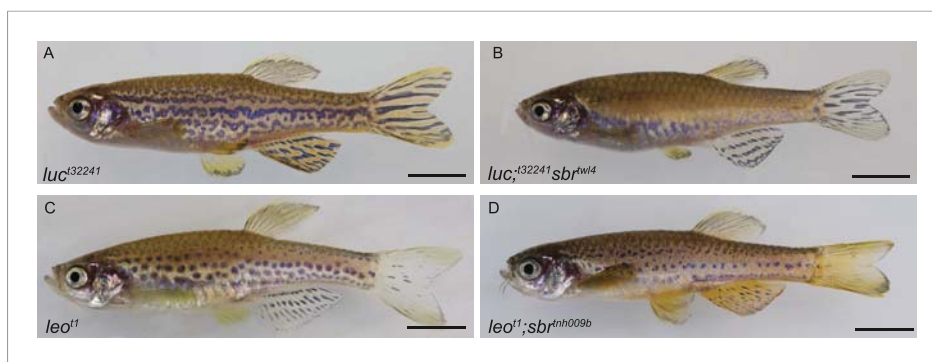


Figure 8. Genetic interactions between *luc*, *leo* and *sbr*. (A) *luc*^{t32241} (*luc*) mutant affects Cx39.4 and results in meandering and broken stripes. (B) *luc*^{t32241};*sbr*^{twl4} mutant exhibits complete loss of stripes and expansion of dense iridophore area. (C) leopard^{t1} (*leo*, *cx41.8*) stripes are broken into spots. (D) *leo*^{t1};*sbr*^{tnh009b} double mutant displays decrease in the size of the spots. Scale bars: 5 mm.

DOI: [10.7554/eLife.06545.018](https://doi.org/10.7554/eLife.06545.018)

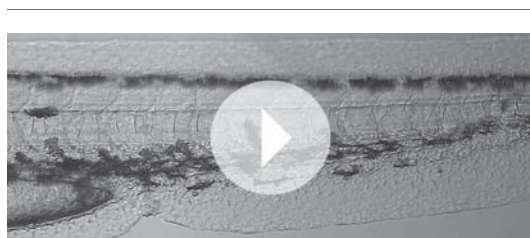
The following figure supplement is available for figure 8:

Figure supplement 1. Interaction of PDZ domains of Tjp1a with connexins.

DOI: [10.7554/eLife.06545.019](https://doi.org/10.7554/eLife.06545.019)

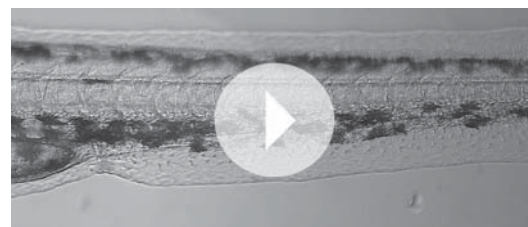
Tjp1a as a regulator of cell shape

Iridophore-specific connexins or other molecules, responsible for communication between pigment cells, might also transmit signals via Tjp1a, controlling iridophore migration or shape change in a spatiotemporally appropriate manner. Immunostainings show that Tjp1a is expressed in dense iridophores, but not in loose iridophores. Intriguingly, the absence of Tjp1a does not obviously affect the morphology of dense iridophores, which display normal shape and organisation. In vitro studies of the past decade have demonstrated a function of ZO-1 in organisation of confluent cell layers. Counterintuitively, ZO-1 $-/-$ Eph4 cells polarize and form tight junctions morphologically indistinguishable from those of ZO-1 $+/+$ cells, but the formation is delayed. These cells do not exhibit abnormal growth or motility in scratch assays (Umeda et al., 2004). However, knockdown of endogenous ZO-1 in COS-7 cells hampers delamination and migration of cells to fill the wound area in scratch assays (Huo et al., 2011). These data suggest that epithelial cells of different origin may react differently to the absence of ZO-1. Our Tjp1aN antibody shows that the non-functional truncated protein is at least partially retained and normally localized in *sbr*^{tnh009n} mutants, suggesting that the missing domains (ZU-5 and possibly parts of afadin- and actin-binding regions [Bauer et al., 2010]) are crucial for the function of Tjp1a in iridophores. It was shown that absence of the ZU5 domain of ZO-1 causes defective delamination and migration of COS-7 cells (Huo et al., 2011). Furthermore, mis-expression of truncated ZO-1 in the presence of the wild-type protein in CE culture leads to the expression of mesenchymal markers and to an epithelial–mesenchymal transition (EMT) (Ryeom et al., 2000). Taken together with our findings, these data suggest a role of ZO-1 in regulating and fine-tuning of cell shape and state.



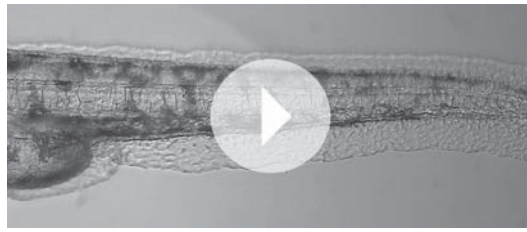
Video 1. 50 hpf wild type embryo. Note normal blood flow.

DOI: [10.7554/eLife.06545.020](https://doi.org/10.7554/eLife.06545.020)



Video 2. 50 hpf wild type embryo injected with morpholino against Tjp1b. Note normal blood flow (N = 53/53). The result shows non-toxicity of morpholino. No defects are observed in the injected fish (observed until adulthood).

DOI: [10.7554/eLife.06545.021](https://doi.org/10.7554/eLife.06545.021)



Video 3. 50 hpf *sbr* embryo injected with morpholino against Tjp1b. No blood flow is observed, possibly due to disrupted angiogenesis (N = 30/38). None of the 30 individuals without blood flow survived past 5 dpf.

DOI: [10.7554/eLife.06545.022](https://doi.org/10.7554/eLife.06545.022)

over, the viability of *sbr* mutants presents exciting opportunities for studying the behaviour of Tjp1 deficient cells in vivo.

Materials and methods

Zebrafish maintenance

Fish were bred and maintained as described (Nüsslein-Volhard and Dahm, 2002). Fish of the following genotypes were used: Tü, WIK, TE wild-type strains (Tübingen zebrafish stock centre), *luchs*^{t32241} (Irion et al., 2014), *leo*^{t1} (Watanabe et al., 2006), *nacre*^{w2} (Lister et al., 1999), *pfeffer*^{tm236b} (Odenthal et al., 1996), *shady*^{js1} (Lopes et al., 2008), *sparse*^{b134} (Kelsh et al., 1996), *Tg(TDL358:GFP)* (Levesque et al., 2013), *Tg(kdrl:GFP)* (Jin et al., 2005), *Tg(kita:GalTA4:UAS:mCherry)* (Anelli et al., 2009), *Tg(sox10:mRFP)* (M Levesque; CN-V laboratory), *Tg(H2A:GFP)* (A Mongera; CN-V laboratory). Fish were staged according to the normal table of zebrafish development (Parichy et al., 2009).

Mutagenesis

The original allele *sbr*^{tnh009b} was identified in a screen for mutants induced with N-ethyl-N-nitrosourea (N5809, Sigma-Aldrich, St. Louis, Missouri) in Tü wild-type background. Mutagenesis was carried out as described previously (Rohner et al., 2011). Subsequently, fish were crossed to TE and later maintained in homozygosity by regular outcrossing. Four new alleles were isolated by crossing mutagenized Tü males to *sbr*^{tnh009b} females and screening the adult progeny for the *sbr* phenotype.

Mapping and alleles testing

sbr^{tnh009b}/WIK fish were incrossed and used for meiotic mapping as described previously (Nüsslein-Volhard and Dahm, 2002). The mutation was mapped to the region between microsatellite markers z4706 (36.7 cM) and z52932 (41.4 cM) on chromosome 7. Further, the interval was narrowed to the region 29.6–32.5 Mb of chromosome 7, between contigs CR356242 and BX3235912 (Ensembl Zebrafish release 72). The following primers were used:

CR356242_F GTAGTATATGGATATGGATG
 CR356242_R CCACCGCTGCATACCCTGC
 BX3235912_F CTTGCACAGGGAATGTGT
 BX3235912_R CTGCAGTGTCTCACGCT

To check for presence of lesions in *tjp1a*, RNA was extracted from blastema of adult wild-type and *sbr* fish using TRIzol reagent (15596, Thermo Fisher Scientific, Waltham, Massachusetts). cDNA was obtained using Omniscript RT kit (205111, Qiagen, Netherlands). Four overlapping regions of the coding region of *tjp1a* (ENS DART00000148347) were amplified using Taq polymerase S (M3001.0250, Genaxxon, Germany) and the following primers:

*tjp1a*_1F 5'-GACTGCGGGATTTCAAGTTGT-3'
*tjp1a*_1R 5'-CACTATTCGCCGGTACACATC-3'
*tjp1a*_2F 5'-GCAGAAGAAGAAAGATGTGTAC-3'

tjp1a_2R 5'-ATGTGAACCGTCCGCCTTG-3'
tjp1a_3F 5'-CAACCATCATCTCTTCACAGCCACT-3'
tjp1a_3R 5'-GATTTTCTCCACTGACTCTGCTCTGG-3'
tjp1a_4F 5'-CTGGATCAAGAGAAGACCTTTAGAACTC-3'
tjp1a_4R 5'-TCCCTGCAGTCTCAGAGGTT-3'.

PCR products were cloned into pGEM-T Easy (A360, Promega, Fitchburg, Wisconsin) and sequenced using Big Dye Terminator v3.1 kit (4337455, Thermo Fisher Scientific).

Generation of polyclonal antisera

Two parts of the *tjp1a* cDNA corresponding to 992–1143 a.a. (α -Tjp1aN) and 1293–1397a.a. (α -Tjp1aC) of Tjp1a (ENS DART00000148347) were cloned both into pET28-nusA (Novagen) and pOPT-GST-Kan (gift from U Irion and O Perisic) plasmids to produce 6xHis-nusA and GST-tagged fusions. The following primers were used to amplify these regions:

tjp1aN_F 5'-CATATGTACAAGAAGGATATCTACCGACCC-3'
tjp1aN_R 5'-GGATCCTTAGGAAGGCCTTTGGG-3'
tjp1aC_F 5'-CATATGAAACCCTCCACACAGCTGACAC-3'
tjp1aC_R 5'-GGATCCTTAGCTGGACGTGGCAG-3'.

Obtained constructs were used to transform BL21-CodonPlus DE3-RIPL (230280, Agilent Technologies, Santa Clara, California) cells. The cells were grown in 1 ml of 2xTY medium containing 20 mM glucose and 15 μ g/ml kanamycin for 3 hr on 37°C, 220 rpm. This culture was used to inoculate 50 ml of the same medium and was grown overnight on 20°C, 220 rpm. His-tagged polypeptides were purified using HiTrap IMAC FF 1 ml (17-0921, GE Healthcare, UK) charged with Ni²⁺ and 250 mM imidazole in the elution buffer. GST-tagged polypeptides were purified using GSTrap FF 1 ml (17-5130, GE Healthcare). In all cases, the samples of eluted proteins were loaded on NuPage Novex 4–12% Bis-Tris gel (NP0322BOX, Thermo Fisher Scientific) and stained with Coomassie Brilliant Blue G-250 to assess the purity. The polypeptides were dialyzed in PBS using Slide-A-Lyzer Dialysis Cassettes 10K MWCO (66383, Thermo Fisher Scientific). The protein concentrations were assessed using Bradford method. His-tagged polypeptides were used to immunize rabbits with Freund's complete adjuvant (F5881, Sigma-Aldrich) as immunopotentiator. GST-tagged polypeptides were bound to HiTrap NHS-activated HP columns (17-0716, GE Healthcare) and used to purify the corresponding antibodies from rabbit serum, using PBS as binding buffer and 100 mM glycine pH 2.3 as elution buffer. The purified antibodies were neutralized with Tris-HCl pH 9.5 and mixed 1:1 with glycerol.

Immunohistochemistry

Antibody staining was performed as described previously (Singh *et al.*, 2014) omitting methanol hydration/rehydration and HCl steps. Antibodies used were mouse α -E-cadherin (610181, BD Biosciences, Franklin Lakes, New Jersey), mouse α -GFP (11814460001, Roche, Germany), goat α -rabbit coupled with Cy3 (111-165-003, Dianova, Germany), goat α -mouse AlexaFluor 488 (A21131, Molecular Probes, Eugene, Oregon). All antibodies were used in 1:400 dilution, except α -Tjp1aN and α -Tjp1aC, which were used in 1:100 dilution.

Transplantations

Chimeras were produced as described (Nüsslein-Volhard and Dahm, 2002) using mid-blastula stage (1000 cell stage) embryos, transplanting 30–60 cells.

Image acquisition

We used Zeiss LSM 780 NLO confocal microscope and Canon 5D Mk II camera to obtain images. Fiji (Schindelin *et al.*, 2012), Adobe Photoshop, and Adobe Illustrator CS6 were used for image processing and analysis. Maximum intensity projection was made for fluorescent channels of confocal scans. For bright-field images, we used 'stack focuser' plugin or a single slice on an appropriate depth. For adult fish photos, multiple RAW camera images were taken in different focal planes and auto-align and auto-blend functions of Photoshop were used. Repeated imaging of metamorphic fish and anaesthesia were performed as described previously (Singh *et al.*, 2014).

Melanophore counts

Melanophores in metamorphic fish were counted in five segments in the middle 70% of myotome starting with the one above the first ray of the anal fin and proceeding posteriorly.

A Kolmogorov–Smirnov test was conducted in SciPy (*Jones et al., 2001*) to compare the distributions of melanophore counts in mutant vs wild-type fish. An initial comparison was conducted on fish of 4–6 mm SL. Sample sizes were then increased to include the melanophore counts of fish of 6–7 mm SL, and each subsequent data set was formed in a similar fashion by 1 mm increment. The null hypothesis of the samples being drawn from the same distribution was rejected with a p-value of 0.011 when a data set composed of 4–10 mm SL fish was used.

Light stripe width quantification

For measuring the first light stripe width, the light stripe was defined as an area taken by dense iridophores. The width of the stripe was measured along five lines, perpendicular to the lateral line and drawn from the bases of each second fin ray in the anal fin starting with the first. The body height was measured along the first line.

Morpholino injections

The knockdown was performed as described before (*Nüsslein-Volhard and Dahm, 2002*) using 3 ng of *tjp1b*-MO (CGAGTATGTGATCAGTCTTACTGCA), obtained from Gene Tools, LLC, Philomath, Oregon.

Yeast two-hybrid assay

The PDZ domains of ZO-1 were amplified by RT-PCR from wild-type zebrafish RNA with the following primer pairs:

T878: 5'-CATATGGTGACTCTTCACAGGGCACC-3'

T879: 5'-GGATCCTTCCGCTTCTCTGCGGATAG-3'

T880: 5'-CATATGGTCACACTCGTCAAGTCCCGC-3'

T881: 5'-GGATCCTTCATCTCTCTGCACCACCAT-3'

T882: 5'-CATATGAAGTTTAAGAAAGGGGAAAGTG-3'

T883: 5'-GGATCCTTCTTCTTCTGCGCAAGGATGG-3'

and cloned in the vector pGBKT7 (Takara, Japan) via NdeI and BamHI.

Similarly, the C-termini of Cx39.4, Cx41.8, and Cx43 were amplified by RT-PCR with the following primer pairs:

T886: 5'-CATATGCTTCAGTTGGTGATAAC-3'

T887: 5'-GGATCCTCAAACATAATGTCTCGGTTTG-3'

T884: 5'-CATATGGCATGGAAGCAGTTGAGG-3'

T885: 5'-GGATCCTATACCGCAAGGTCGTCCGG-3'

T888: 5'-CATATGCTCTTCAAACGAATCAAGGACC-3'

T889: 5'-GGATCCTAGACGTCCAGGTCATCAGG-3'

and cloned into the vector pGADT7 (Clontech) via NdeI and BamHI.

The plasmids were transformed into the yeast strain Y2HGold (Clontech) by standard procedures, and we screened for positive interactions using X- α -Gal and His as markers.

Acknowledgements

We thank A Mongera and M Levesque for providing transgenic lines; A Singh for discussions, expertise, and valuable comments on the manuscript; M Sonawane and D Gilmour for discussions and comments on the manuscript; O Perisic for providing plasmids; R Neher for help in melanophore count statistics. We thank H-M Maischein for help with blastomere transplantations, C Liebig for support in light microscopy, B Walderich and the fish facility, W Antonin and the rabbit facility for great support. This work was financially supported by the Max-Planck Society for the Advancement of Science and by ZF-HEALTH grant (Project number 242048).

Additional information

Funding

Funder	Grant reference	Author
Max-Planck-Gesellschaft (Max Planck Society)		Christiane Nüsslein-Volhard

Funder	Grant reference	Author
European Commission (EC)	ZF-HEALTH grant (Project number 242048)	Christiane Nüsslein-Volhard

The funders had no role in study design, data collection and interpretation, or the decision to submit the work for publication.

Author contributions

AF, Conception and design, Acquisition of data, Analysis and interpretation of data, Drafting or revising the article; JK, Identification of *twl4*, *twl1*, *twc2* alleles, Conception and design, Analysis and interpretation of data; HGF, Isolated *tnh009b* allele; UI, Acquisition of data, Analysis and interpretation of data, Drafting or revising the article; CN-V, Conception and design, Analysis and interpretation of data, Drafting or revising the article

Ethics

Animal experimentation: All animal experiments were performed in accordance with the rules of the State of Baden-Württemberg, Germany. The protocol for ENU mutagenesis was approved by the Regierungspräsidium Tübingen (Aktenzeichen: 35/9185.81-5/Tierversuch-Nr. E 1/09).

References

- Amores A, Force A, Yan YL, Joly L, Amemiya C, Fritz A, Ho RK, Langeland J, Prince V, Wang YL, Westerfield M, Ekker M, Postlethwait JH. 1998. Zebrafish hox clusters and vertebrate genome evolution. *Science* **282**: 1711–1714. doi: [10.1126/science.282.5394.1711](https://doi.org/10.1126/science.282.5394.1711).
- Anderson JM, Itallie CM. 1995. Tight junctions and the molecular basis for regulation of paracellular permeability. *The American Journal of Physiology* **32**:467–475.
- Anelli V, Santoriello C, Distel M, Köster RW, Ciccarelli FD, Mione M. 2009. Global repression of cancer gene expression in a zebrafish model of melanoma is linked to epigenetic regulation. *Zebrafish* **6**:417–424. doi: [10.1089/zeb.2009.0612](https://doi.org/10.1089/zeb.2009.0612).
- Balda MS, Matter K. 2000. The tight junction protein ZO-1 and an interacting transcription factor regulate ErbB-2 expression. *The EMBO Journal* **19**:2024–2033. doi: [10.1093/emboj/19.9.2024](https://doi.org/10.1093/emboj/19.9.2024).
- Bauer H, Zweimueller-Mayer J, Steinbacher P, Lametschwandtner A, Bauer HC. 2010. The dual role of zonula occludens (ZO) proteins. *Journal of Biomedicine & Biotechnology* **2010**:402593. doi: [10.1155/2010/402593](https://doi.org/10.1155/2010/402593).
- Blum Y, Belting HG, Ellertsdottir E, Herwig L, Lüders F, Affolter M. 2008. Complex cell rearrangements during intersegmental vessel sprouting and vessel fusion in the zebrafish embryo. *Developmental Biology* **316**:312–322. doi: [10.1016/j.ydbio.2008.01.038](https://doi.org/10.1016/j.ydbio.2008.01.038).
- Budi EH, Patterson LB, Parichy DM. 2011. Post-embryonic nerve-associated precursors to adult pigment cells: genetic requirements and dynamics of morphogenesis and differentiation. *PLOS Genetics* **7**:e1002044. doi: [10.1371/journal.pgen.1002044](https://doi.org/10.1371/journal.pgen.1002044).
- Dooley CM, Mongera A, Walderich B, Nüsslein-Volhard C. 2013. On the embryonic origin of adult melanophores: the role of ErbB and Kit signalling in establishing melanophore stem cells in zebrafish. *Development* **140**: 1003–1013. doi: [10.1242/dev.087007](https://doi.org/10.1242/dev.087007).
- Eom DS, Inoue S, Patterson LB, Gordon TN, Slingwine R, Kondo S, Watanabe M, Parichy DM. 2012. Melanophore migration and survival during zebrafish adult pigment stripe development require the immunoglobulin superfamily adhesion molecule Igsf11. *PLOS Genetics* **8**:e1002899. doi: [10.1371/journal.pgen.1002899](https://doi.org/10.1371/journal.pgen.1002899).
- Frohnhofer HG, Krauss J, Maischein HM, Nüsslein-Volhard C. 2013. Iridophores and their interactions with other chromatophores are required for stripe formation in zebrafish. *Development* **140**:2997–3007. doi: [10.1242/dev.096719](https://doi.org/10.1242/dev.096719).
- González-Mariscal L, Domínguez-Calderón A, Raya-Sandino A, Ortega-Olvera JM, Vargas-Sierra O, Martínez-Revollar G. 2014. Tight junctions and the regulation of gene expression. *Seminars in Cell & Developmental Biology* **36**:213–223. doi: [10.1016/j.semcdb.2014.08.009](https://doi.org/10.1016/j.semcdb.2014.08.009).
- Haffter J, Odenthal J, Mullins MC, Lin S, Farrell MJ, Vogelsang E, Haas F, Brand M, van Eeden FJ, Furutani-Seiki M, Granato M, Hammerschmidt M, Heisenberg CP, Jiang YJ, Kane DA, Kelsh RN, Hopkins N, Nüsslein-Volhard C. 1996. Mutations affecting pigmentation and shape of the adult zebrafish. *Development Genes and Evolution* **206**:260–276. doi: [10.1007/s004270050051](https://doi.org/10.1007/s004270050051).
- Hirata M, Nakamura K, Kanemaru T, Shibata Y, Kondo S. 2003. Pigment cell organization in the hypodermis of zebrafish. *Developmental Dynamics* **227**:497–503. doi: [10.1002/dvdy.10334](https://doi.org/10.1002/dvdy.10334).
- Hirata M, Nakamura KI, Kondo S. 2005. Pigment cell distributions in different tissues of the zebrafish, with special reference to the striped pigment pattern. *Developmental Dynamics* **234**:293–300. doi: [10.1002/dvdy.20513](https://doi.org/10.1002/dvdy.20513).
- Hung AY, Sheng M. 2002. PDZ domains: structural modules for protein complex assembly. *The Journal of Biological Chemistry* **277**:5699–5702. doi: [10.1074/jbc.R100065200](https://doi.org/10.1074/jbc.R100065200).
- Hunter AW, Barker RJ, Zhu C, Gourdie RG. 2005. Zonula occludens-1 alters connexin43 gap junction size and organization by influencing channel accretion. *Molecular Biology of the Cell* **16**:5686–5698. doi: [10.1091/mbc.E05-08-0737](https://doi.org/10.1091/mbc.E05-08-0737).
- Huo L, Wen W, Wang R, Kam C, Xia J, Feng W, Zhang M. 2011. Cdc42-dependent formation of the ZO-1/MRCKβ complex at the leading edge controls cell migration. *The EMBO Journal* **30**:665–678. doi: [10.1038/emboj.2010.353](https://doi.org/10.1038/emboj.2010.353).

- Irion U**, Frohnhöfer HG, Krauss J, Çolak Champollion T, Maischein HM, Geiger-Rudolph S, Weiler C, Nüsslein-Volhard C, Bronner ME. 2014. Gap junctions composed of connexions 41.8 and 39.4 are essential for colour pattern formation in zebrafish. *eLife* **3**:e05125. doi: [10.7554/eLife.05125](https://doi.org/10.7554/eLife.05125).
- Jin SW**, Beis D, Mitchell T, Chen JN, Stainier DY. 2005. Cellular and molecular analyses of vascular tube and lumen formation in zebrafish. *Development* **132**:5199–5209. doi: [10.1242/dev.02087](https://doi.org/10.1242/dev.02087).
- Johnson SL**, Africa D, Walker C, Weston JA. 1995. Genetic control of adult pigment stripe development in zebrafish. *Developmental Biology* **167**:27–33. doi: [10.1006/dbio.1995.1004](https://doi.org/10.1006/dbio.1995.1004).
- Jones E**, Oliphant T, Peterson P. 2001. SciPy: open source scientific tools for Python. <http://www.scipy.org/> Available at: citeulike-article-id:2644428.
- Katsuno T**, Umeda K, Matsui T, Hata M, Tamura A, Itoh M, Takeuchi K, Fujimori T, Nabeshima Y, Noda T, Tsukita S, Tsukita S. 2008. Deficiency of zonula occludens-1 causes embryonic lethal phenotype associated with defected yolk sac angiogenesis and apoptosis of embryonic cells. *Molecular Biology of the Cell* **19**:2465–2475. doi: [10.1091/mbc.E07-12-1215](https://doi.org/10.1091/mbc.E07-12-1215).
- Kelsh RN**, Brand M, Jiang YJ, Heisenberg CP, Lin S, Haffter P, Odenthal J, Mullins MC, van Eeden FJ, Furutani-Seiki M, Granato M, Hammerschmidt M, Kane DA, Warga RM, Beuchle D, Vogelsang L, Nüsslein-Volhard C. 1996. Zebrafish pigmentation mutations and the processes of neural crest development. *Development* **123**:369–389.
- Krauss J**, Astrinidis P, Astrinides P, Frohnhöfer HG, Walderich B, Nüsslein-Volhard C. 2013. Transparent, a gene affecting stripe formation in zebrafish, encodes the mitochondrial protein Mpv17 that is required for iridophore survival. *Biology Open* **2**:703–710. doi: [10.1242/bio.20135132](https://doi.org/10.1242/bio.20135132).
- Laing JG**, Chou BC, Steinberg TH. 2005. ZO-1 alters the plasma membrane localization and function of Cx43 in osteoblastic cells. *Journal of Cell Science* **118**:2167–2176. doi: [10.1242/jcs.02329](https://doi.org/10.1242/jcs.02329).
- Levesque MP**, Krauss J, Koehler C, Boden C, Harris MP. 2013. New tools for the identification of developmentally regulated enhancer regions in embryonic and adult zebrafish. *Zebrafish* **10**:21–29. doi: [10.1089/zeb.2012.0775](https://doi.org/10.1089/zeb.2012.0775).
- Lister JA**, Robertson CP, Lepage T, Johnson SL, Raible DW. 1999. Nacre encodes a zebrafish Microphthalmia-related protein that regulates neural-crest-derived pigment cell fate. *Development* **126**:3757–3767.
- Lopes SS**, Yang X, Müller J, Carney TJ, McAdow AR, Rauch GJ, Jacoby AS, Hurst LD, Delfino-Machin M, Haffter P. 2008. Leukocyte tyrosine kinase functions in pigment cell development. *PLoS Genetics* **4**:e1000026. doi: [10.1371/journal.pgen.1000026](https://doi.org/10.1371/journal.pgen.1000026).
- Maderspacher F**, Nüsslein-Volhard C. 2003. Formation of the adult pigment pattern in zebrafish requires leopard and obelix dependent cell interactions. *Development* **130**:3447–3457. doi: [10.1242/dev.00519](https://doi.org/10.1242/dev.00519).
- Mahalwar P**, Walderich B, Singh AP, Nüsslein-Volhard C. 2014. Local reorganization of xanthophores fine-tunes and colors the striped pattern of zebrafish. *Science* **345**:1362–1364. doi: [10.1126/science.1254837](https://doi.org/10.1126/science.1254837).
- McMenamin SK**, Bain EJ, McCann AE, Patterson LB, Eom DS, Waller ZP, Hamill JC, Kuhlman JA, Eisen JS, Parichy DM. 2014. Thyroid hormone-dependent adult pigment cell lineage and pattern in zebrafish. *Science* **358**:1358–1361. doi: [10.1126/science.1256251](https://doi.org/10.1126/science.1256251).
- Nakamasu A**, Takahashi G, Kanbe A, Kondo S. 2009. Interactions between zebrafish pigment cells. *Proceedings of the National Academy of Sciences of USA* **106**:8429–8434. doi: [10.1073/pnas.0808622106](https://doi.org/10.1073/pnas.0808622106).
- Nüsslein-Volhard C**, Dahm R. 2002. *Zebrafish: a practical approach*. Oxford University Press.
- Odenthal J**, Rossnagel K, Haffter P, Kelsh RN, Vogelsang E, Brand M, van Eeden FJ, Furutani-Seiki M, Granato M, Hammerschmidt M, Heisenberg CP, Jiang YJ, Kane DA, Mullins MC, Nüsslein-Volhard C. 1996. Mutations affecting xanthophore pigmentation in the zebrafish, *Danio rerio*. *Development* **123**:391–398.
- Parichy DM**, Elizondo MR, Mills MG, Gordon TN, Engeszer RE. 2009. Normal table of postembryonic zebrafish development: staging by externally visible anatomy of the living fish. *Developmental Dynamics* **238**:2975–3015. doi: [10.1002/dvdy.22113](https://doi.org/10.1002/dvdy.22113).
- Parichy DM**, Ransom DG, Paw B, Zon LI, Johnson SL. 2000. An orthologue of the kit-related gene *fms* is required for development of neural crest-derived xanthophores and a subpopulation of adult melanocytes in the zebrafish, *Danio rerio*. *Development* **127**:3031–3044.
- Patterson LB**, Parichy DM. 2013. Interactions with iridophores and the tissue environment required for patterning melanophores and xanthophores during zebrafish adult pigment stripe formation. *PLoS Genetics* **9**:e1003561. doi: [10.1371/journal.pgen.1003561](https://doi.org/10.1371/journal.pgen.1003561).
- Rhett JM**, Jourdan J, Gourdie RG. 2011. Connexin 43 connexon to gap junction transition is regulated by zonula occludens-1. *Molecular Biology of the Cell* **22**:1516–1528. doi: [10.1091/mbc.E10-06-0548](https://doi.org/10.1091/mbc.E10-06-0548).
- Rohner N**, Perathoner S, Frohnhöfer HG, Harris MP. 2011. Enhancing the efficiency of N-ethyl-N-nitrosourea-induced mutagenesis in the zebrafish. *Zebrafish* **8**:119–123. doi: [10.1089/zeb.2011.0703](https://doi.org/10.1089/zeb.2011.0703).
- Ryeom SW**, Paul D, Goodenough DA. 2000. Truncation mutants of the tight junction protein ZO-1 disrupt corneal epithelial cell morphology. *Molecular Biology of the Cell* **11**:1687–1696. doi: [10.1091/mbc.11.5.1687](https://doi.org/10.1091/mbc.11.5.1687).
- Schindelin J**, Arganda-Carreras I, Frise E, Kaynig V, Longair M, Pietzsch T, Preibisch S, Rueden C, Saalfeld S, Schmid B, Tinevez JY, White DJ, Hartenstein V, Eliceiri K, Tomancak P, Cardona A. 2012. Fiji: an open-source platform for biological-image analysis. *Nature Methods* **9**:676–682. doi: [10.1038/nmeth2019](https://doi.org/10.1038/nmeth2019).
- Singh AP**, Nüsslein-Volhard C. 2015. Zebrafish stripes as a model for vertebrate colour pattern formation. *Current Biology* **25**:R81–R92. doi: [10.1016/j.cub.2014.11.013](https://doi.org/10.1016/j.cub.2014.11.013).
- Singh AP**, Schach U, Nüsslein-Volhard C. 2014. Proliferation, dispersal and patterned aggregation of iridophores in the skin prefigure striped colouration of zebrafish. *Nature Cell Biology* **16**:607–614. doi: [10.1038/ncb2955](https://doi.org/10.1038/ncb2955).
- Suzu S**, Hayashi Y, Harumi T, Nomaguchi K, Yamada M, Hayasawa H, Motoyoshi K. 2002. Molecular cloning of a novel immunoglobulin superfamily gene preferentially expressed by brain and testis. *Biochemical and Biophysical Research Communications* **296**:1215–1221. doi: [10.1016/S0006-291X\(02\)02025-9](https://doi.org/10.1016/S0006-291X(02)02025-9).

- Umeda K**, Matsui T, Nakayama M, Furuse K, Sasaki H, Furuse M, Tsukita S. 2004. Establishment and characterization of cultured epithelial cells lacking expression of ZO-1. *The Journal of Biological Chemistry* **279**:44785–44794. doi: [10.1074/jbc.M406563200](https://doi.org/10.1074/jbc.M406563200).
- Watanabe M**, Iwashita M, Ishii M, Kurachi Y, Kawakami A, Kondo S, Okada N. 2006. Spot pattern of leopard Danio is caused by mutation in the zebrafish connexin41.8 gene. *The EMBO Reports* **7**:893–897. doi: [10.1038/sj.embor.7400757](https://doi.org/10.1038/sj.embor.7400757).
- Xu J**, Lim SB, Ng MY, Ali SM, Kausalya JP, Limvipuvadh V, Maurer-Stroh S, Hunziker W, Rippon H, Bishop A. 2012. ZO-1 regulates Erk, Smad1/5/8, Smad2, and RhoA Activities to Modulate Self-Renewal and differentiation of mouse embryonic stem cells. *Stem Cells* **30**:1885–1900. doi: [10.1002/stem.1172](https://doi.org/10.1002/stem.1172).

2.2 Publication 2

Fadeev, A., Krauss, J., Singh, A.P., Nüsslein-Volhard, C.* (2016) Zebrafish Leucocyte tyrosine kinase controls iridophore establishment, proliferation and survival.

Pigment Cell and Melanoma Research. doi: /10.1111/pcmr.12454

*Corresponding author

2.2.1 The ALK/LTK subfamily of tyrosine kinases

Many aspects of the specification, proliferation and survival of chromatophores are regulated by specific receptor-ligand pairs (with the receptor being expressed in the pigment cell). One such receptor is *shady/leukocyte tyrosine kinase (ltk)*, which is suggested to regulate the establishment of iridophores. Loss-of-function mutants of *ltk* lack of iridophores throughout all stages of development (Lopes *et al*, 2008).

Due to the similarities of their kinase domains, Ltk and Alk (anaplastic lymphoma kinase) comprise a subgroup of the insulin receptor superfamily. Zebrafish Ltk and Alk possess a domain structure similar to that of mammalian Alk, but not Ltk (Figure 2C) (Lopes *et al*, 2008; Palmer & Hallberg, 2015; Toyoshima *et al*, 1993; Cismasiu *et al*, 2004; Fass *et al*, 1997). Mammalian Ltk and Alk are major factors in tumorigenesis, and a number of activating mutations in ALK have been reported in human cancers (Carén *et al*, 2008; Mossé *et al*, 2008; Martinsson *et al*, 2011; Chen *et al*, 2008; George *et al*, 2008). The mutations F1174I/S/L in the kinase domain are frequent in neuroblastoma tissues, especially in relapsed tumours (De Brouwer *et al*, 2010; Martinsson *et al*, 2011). LTK mutations have been found in various human cancers (Catalogue of Somatic Mutations in Cancer, <http://cancer.sanger.ac.uk/>, Forbes *et al*. 2015). F1174 mutations in human ALK and the corresponding mutation in LTK (F568L) were shown to cause ligand-independent activation of these kinases (Chand *et al*, 2013; Janoueix-Lerosey *et al*, 2008; Roll & Reuther, 2012; Chen *et al*, 2008; George *et al*, 2008; Martinsson *et al*, 2011). However, despite the importance of the Alk/Ltk family for cancer research, their endogenous physiological functions under normal conditions are poorly understood.

2.2.2 moonstone is a gain-of-function allele of leukocyte tyrosine kinase

The dominant zebrafish mutant *moonstone* (*mne*) was identified during an ENU-induced mutagenesis screen for adult pigment pattern phenotypes (Figure 1A-C). The mutant larvae exhibit the normal number of iridophores (Figure 1L), which are arranged in ventral and dorsal stripes. In addition they display ectopic iridophores located inside the body. Adults display a normal striped pattern but an increased number of iridophores on the scales and in the fins, which gives the fish a green-blue sheen (Figure 1A-C, F, G). Ectopic iridophore sheets are also observed in the viscera and occasionally in the eye (Figure 1H, I). Meiotic mapping demonstrated the lesion to be located in a region including *ltk*. *shady/ltk* loss-of-function mutants lack iridophores, and therefore, a candidate gene approach was used. Sequencing of *ltk* cDNA revealed a missense mutation that leads to the substitute F993I in a highly conserved position of the Ltk kinase domain (Figure 2). The F993 position corresponds to F1174 in human ALK and F586 in human LTK.

Series of treatments with TAE684 (TAE, an ALK inhibitor that has been shown to inhibit zebrafish Ltk as well (Rodrigues *et al*, 2012), alleviated *mne* phenotype (Figure 3A). Double heterozygous *ltk^{mne}/+;ltk^{shd}/+* animals demonstrated a weaker phenotype than *mne/+* animals, suggesting that the strength of the phenotype is a function of Ltk activity (Figure 1E). Taken together, these data confirm that *ltk* is *moonstone*. The mutant will be referred to as *ltk^{mne}* from now on.

2.2.3 The novel role of *ltk*

ltk^{mne} leads to an increased number of iridophores – a phenotype opposite to that of the loss-of-function mutant *shd*, which is suggested to lack iridophore precursors (Lopes *et al*, 2008). The role of Ltk in iridophore establishment was confirmed by experiments in which fish were treated with TAE684 from 9 to 72 hpf. Doing this resulted in a complete loss of iridophores in both mutant and wild type (Figure 3B). Interestingly, when 14 dpf fish were treated with the inhibitor, the number of iridophores was reduced (Figure 3H,I) in both wild type and mutant fish. This result strongly suggests that Ltk is required not only for specification, but also for survival of iridophores. Importantly, untreated fish did not display significant differences in the iridophore proliferation rate between wild type and mutant animals.

2.2.4 *ltk* specifically regulates iridophores

No effect on xanthophores or melanophores was observed in the mutant, as confirmed by counts of xanthophores in early larvae (data not shown) and melanophores at 5-9 mm SL stages (Figure 4C). Additionally, double mutants for *spa;ltk^{mne}* display superpositions of both mutant phenotypes: the number of melanophores that is typical for *spa* (less than half of the wild type number) and an increased number of iridophores on the scales, which is typical for *ltk^{mne}*. These results indicate that supernumerary iridophores in *ltk^{mne}* are not produced at the expense of melanophores (Figure 6). Taken together, these data show that Ltk function is specific to iridophores.

2.2.5 *ltk^{mne}* displays a normal stripe pattern despite the presence of ectopic iridophores in the skin of metamorphic fish

Repeated imaging of the skin of metamorphic fish using confocal microscopy was performed (Figure 4A). The fish carried the *Tg(TDL358:GFP)* and *Tg(sox10:RFP)* transgenes, which label iridophores and neural crest derivatives respectively. Imaging allowed us to detect ectopic iridophores that appeared in the dorsal and ventral regions of the body. These iridophores divide and form clusters. In addition, iridophores in *ltk^{mne}* transiently form clusters of dense iridophores in the presumptive dark stripe area. In the *schachbrett* mutant (see Publication 1), the presence of dense iridophores in the developing dark stripes leads to interruptions in the dark stripes, which is likely due to an aberrant communication between iridophores and other pigment cell types. In *ltk^{mne}*, however, the normal arrangement of the two first dark stripes is established by 12 mm SL, and the stripes of adult *ltk^{mne}* fish display a normal width and apparently normal iridophore numbers (Figure 1K). These results suggest that *ltk^{mne}* iridophores are able to react to cues provided to them by xanthophores and melanophores and ultimately establish a normal pattern.

2.2.6 Ectopic iridophores on the scales are accompanied by melanophores.

An increased number of melanophores was observed on the scales, but not in the body of the *ltk^{mne}* fish. Melanophores are present on the scales located centrally along the dorso-ventral axis, which are normally devoid of melanophores (Figure 5). There is a larger number of ectopic iridophores in the homozygous mutants. It can be speculated that since

the Ltk function is specific to iridophores, the effect on scale melanophores is secondary and they merely follow cues provided by the supernumerary iridophores.

2.2.7 Ltk and Ednrba regulate distinct aspects of iridophore behaviour

The *rose* (*rse/ednrba*) mutants display a strong reduction in the overall iridophore number and lack dense iridophores, which results in the formation of only two dark stripes with reduced melanophore numbers (Frohnhofer *et al*, 2013; Singh *et al*, 2014; Parichy *et al*, 2000a). Double mutants for *ltk^{mne};rse* display a combination of *ltk^{mne}* and *rse* phenotypes –increased numbers of iridophores and melanophores on the scales and reduced numbers of trunk melanophores and iridophores (Figure 6). These results indicate that these two genes are affecting separate aspects of iridophore behaviour. It is reasonable to suggest that Ltk regulates iridophore proliferation, while Ednrba has a primary role in establishing dense iridophores.

2.2.8 *ltk^{mne}* iridophores form overgrowths in the wild type environment

In order to assess the behaviour of *ltk^{mne}* cells in the wild type environment, transplantations of *ltk^{mne}* blastomeres into *albino* hosts were performed. In the majority of the cases, the resulting donor-derived clusters displayed a sheen on the scales, which is characteristic of *ltk^{mne}*, and the wild type pattern spanning antero-posteriorly along 2-5 segments in the trunk, as is typical for such transplantations (Walderich *et al*, in review). However, in some cases an abnormal spread of iridophores was observed, which can be described as iridophore overgrowth – a phenotype that is not observed in mutants (Figure 7). In addition, the eyes of the chimeras were frequently overgrown with iridophores; this phenotype is also observed in the mutants, albeit not as frequently. It has been suggested that iridophore proliferation is controlled by homotypic competition. In chimeric animals, wild type-derived iridophores in *shd* hosts spread farther along anterior-posterior axis in the absence of competing iridophores, compared to experiments with wild type hosts (Walderich *et al*, in review). In the *ltk^{mne}* mutants, all iridophores behave similarly, whereas in the wild type environment, the *ltk^{mne}* mutant iridophores outcompete *ltk⁺* iridophores, and their behaviour resembles uncontrolled tumour outgrowth. These results suggest that Ltk participates in the homotypic inhibition of iridophore growth.

In summary, we show that the gain-of-function, possibly constitutively active, allele of *ltk*, *moonstone*, causes emergence of ectopic iridophores. These ectopic iridophores are

still able to participate in normal stripe pattern formation in the skin; however they divide and spread in abnormal locations, if those are free of competing iridophores. When surrounded by wild type pigment cells, mutant iridophores produce large overgrowths. Therefore, we suggest that Ltk plays a role not only in establishment, but also maintenance and cell-cell interactions of iridophores. Mammalian *ltk* and *alk*, that carry similar mutations in the same conserved position display tumorigenic properties. The *ltk^{mme}* phenotype is readily visible in larval fish and is suppressed by the treatment with drugs that specifically inhibit tyrosine kinase receptors.

Zebrafish Leucocyte tyrosine kinase controls iridophore establishment, proliferation and survival

Andrey Fadeev, Jana Krauss*, Ajeet Pratap Singh and Christiane Nüsslein-Volhard

Max-Planck-Institut für Entwicklungsbiologie, Tübingen, Germany *Current address: Auengrund 7, 02899, Schönau-Berzdorf, Germany

CORRESPONDENCE Christiane Nüsslein-Volhard, e-mail: cnv@tuebingen.mpg.de

KEYWORDS iridophores/pigment cells/zebrafish/homotypic competition/leucocyte tyrosine kinase/tumorigenesis

PUBLICATION DATA Received 18 November 2015, revised and accepted for publication 19 January 2016, published online 23 January 2016

doi: 10.1111/pcmr.12454

Summary

The zebrafish striped pattern results from the interplay among three pigment cell types; black melanophores, yellow xanthophores and silvery iridophores, making it a valuable model to study pattern formation *in vivo*. It has been suggested that iridophore proliferation, dispersal and cell shape transitions play an important role during stripe formation; however, the underlying molecular mechanisms remain poorly understood. Using gain- and loss-of-function alleles of *leucocyte tyrosine kinase (Itk)* and a pharmacological inhibitor approach, we show that Ltk specifically regulates iridophore establishment, proliferation and survival. Mutants in *shady/Itk* lack iridophores and display an abnormal body stripe pattern. *Moonstone* mutants, *Itk^{mne}*, display ectopic iridophores, suggesting hyperactivity of the mutant Ltk. The dominant *Itk^{mne}* allele carries a missense mutation in a conserved position of the kinase domain that highly correlates with neuroblastomas in mammals. Chimeric analysis suggests a novel physiological role of Ltk in the regulation of iridophore proliferation by homotypic competition.

Introduction

Vertebrates display an astounding variety of colour patterns in their skin, fur or feathers that often strikingly differ even between closely related species. Teleost fish show a particularly high diversity of patterns, which are formed by pigment cells distributed in superimposed layers in the skin (Singh and Nüsslein-Volhard, 2015; Irion et al., 2016). In the zebrafish *Danio rerio*, a characteristic pattern of alternating dark and light stripes is produced by

three pigment cell types: melanophores (dark cells containing the black pigment melanin), xanthophores (yellow-orange cells containing pteridine-based pigments) and iridophores (silvery cells containing reflective guanine platelets) in the flank of the body (Kirschbaum, 1975; Kelsh et al., 2009; Hirata et al., 2005; Hirata et al., 2003). Cell-cell interactions between all the three pigment cell types are essential for appropriate stripe pattern formation (Maderspacher and Nüsslein-Volhard, 2003; Frohnhöfer et al., 2013; Patterson and Parichy, 2013;

Significance

Development of the striped pattern in zebrafish is a complex process involving three pigment cell types. It has been shown that light-reflecting pigment cells – iridophores – are crucial for the repetition of stripe pattern. We describe a mutant in *leucocyte tyrosine kinase (Itk)* containing a lesion highly similar to those implicated in human cancers, especially neuroblastoma, and confirm the role of Ltk in establishing the iridophore population in zebrafish. We describe a new role of Ltk in the control of iridophore survival and maintenance. Aggressive behaviour of mutant cells with hyperactive Ltk in chimeric animals suggests that Ltk is involved in homotypic competition-dependent iridophore proliferation.

Nakamasu et al., 2009). It has been suggested that homotypic competition regulates pigment cell proliferation and dispersal, whereas heterotypic interactions regulate cell shape transition (Irion et al., 2016; Walderich et al., 2016; Fadееv et al., 2015; Irion et al., 2014).

Zebrafish develops two patterns. It has a relatively simple larval pattern comprised of a dorsal, ventral and lateral stripe of melanophores and scattered xanthophores (Kelsh et al., 2009). Iridophores are organized in a dorsal and ventral stripe, comprising about one iridophore cell per segment. These pigment cells are derived directly from neural crest cells migrating during early embryogenesis (Singh and Nüsslein-Volhard, 2015; Kelsh et al., 1996). The adult zebrafish pattern arises during metamorphosis (3–6 weeks post-fertilization).

Recent studies underscored a key role of iridophores in stripe formation (Fadееv et al., 2015; Singh et al., 2014; Frohnhöfer et al., 2013; Patterson and Parichy, 2013). However, despite recent advances not much is known about the establishment and regulation of iridophores. Clonal analysis revealed that adult iridophores are derived from multipotent stem cells located at the dorsal root ganglia of the peripheral nervous system. At the onset of metamorphosis, they appear along the horizontal myoseptum, proliferate and spread as a dense sheet in the skin to form the first light stripe. At its borders iridophores start to spread as a loose sheet over the dark stripe region. Past the presumptive dark stripe they aggregate to form new light stripes (Singh et al., 2014). Melanoblasts migrate along spinal nerves into the skin to form dark stripes (Singh et al., 2014; Dooley et al., 2013a; Budi et al., 2011), whereas metamorphic xanthophores are a product of proliferation of larval xanthophores (Mahalwar et al., 2014; McMenamin et al., 2014). Interestingly, iridophores do not participate in the stripe pattern of the fins, but are lined along the fin rays, suggesting differences in the mechanisms involved in patterning of the trunk and fins (Frohnhöfer et al., 2013). The mid-dorsum is covered by a longitudinal band of melanophores.

On the scales, all three cell types form a belt of intermingled pigment cells along the posterior edge of the scale, with pigment cell numbers decreasing along the dorso-ventral axis (Kirschbaum, 1975). Scale iridophores share a lineage with stripe iridophores (Singh et al., 2014), but otherwise still virtually nothing is known about the establishment and interactions of this pigment cell population.

Several genes have been described that affect the development and/or maintenance of iridophores. In *shady* (*shd*) mutants, which are deficient in the gene encoding Leucocyte tyrosine kinase (Ltk), both larval and adult iridophores are missing (Lopes et al., 2008). Other iridophore mutants, such as are *rose* (*rse*, *endothelin receptor ba*) and *karneol* (*endothelin-converting enzyme 2*), lead to a severe reduction of the number of dense

iridophores in adult fish (Parichy et al., 2000; Krauss et al., 2014). *transparent* (*MpV17 mitochondrial inner membrane protein*) mutants display loss of iridophores throughout larval and adult stages (Krauss et al., 2013). It has been suggested that *shd/ltk* is required for the establishment of iridophores and affects fate specification of iridoblasts from multipotent neural crest cells. *shd/ltk* mutants are devoid of all types of iridophores, although sometimes they develop clonal patches of iridophores in the adult pattern that are several segments wide and are likely due to a single escaping progenitor that proliferates in the absence of competing iridophores (Singh et al., 2014; Lopes et al., 2008; Frohnhöfer et al., 2013). The creation of chimeras by blastomere transplantation has revealed that *shd/ltk* is autonomously required in iridophores (Lopes et al., 2008; Frohnhöfer et al., 2013). Clusters of donor-derived iridophores in a wild-type environment are confined along the antero-posterior axis to two to four segments, whereas in *shd/ltk* mutant recipients they have a tendency to spread laterally over several segments (Walderich et al., 2016). This indicates that the rate of iridophore proliferation in wild-type fish is controlled by homotypic cell competition between iridophores.

Based upon similarities of their kinase domains, Ltk and Alk (Anaplastic lymphoma kinase) form a subgroup of the insulin receptor superfamily of receptor tyrosine kinases. There is only one protein of this class in *Drosophila* (dALK) and *C. elegans* (SCD-2) (Liao et al., 2004; Lorén et al., 2001), but both proteins are present in zebrafish and mammals (Ben-Neriah and Bauskin, 1988; Bernards and de la Monte, 1990; Shiota et al., 1994). This suggests that the divergence is unique to vertebrates. Mammalian LTK and ALK display highly similar kinase domains, but only a few similarities in their extracellular domains, beside glycine-rich regions (Toyoshima et al., 1993; Cismasiu et al., 2004; Fass et al., 1997). In contrast, both zebrafish Alk and Ltk possess domain structures similar to mammalian ALK, for example MAM domains (mephrin/A5-protein/PTPu), thought to mediate homophilic cell adhesion function (Lopes et al., 2008; Palmer and Hallberg, 2015; Cismasiu et al., 2004). In addition, unlike mammalian LTK, which was shown to be expressed in pre-B and B lymphocytes and in the adult brain (Ben-Neriah and Bauskin, 1988; Bernards and de la Monte, 1990), zebrafish Ltk is expressed in neural crest (Lopes et al., 2008), sharing this characteristic with mammalian ALK (Dirks et al., 2002), and making it an attractive model for studying physiological functions of human ALK (Challa and Chatti, 2013).

Both ALK and LTK in humans were shown to be major factors in tumorigenesis. A number of activating mutations in ALK were reported in human cancers (Carén et al., 2008; Mossé et al., 2008; Chen et al., 2008; George et al., 2008). Specifically, mutations F1174I/S/L were shown to be frequent in neuroblastoma samples, especially in relapsed post-treatment tumours (De Brouwer et al., 2010; Mar-

tinsson et al., 2011). It was shown that expression of F1174L ALK in mice leads to tumour formation (Heukamp et al., 2012; Chen et al., 2008). LTK mutations were found in various human cancers (Catalogue of Somatic Mutations in Cancer, <http://cancer.sanger.ac.uk/>, Forbes et al., 2015), and high expression levels of LTK have been demonstrated to correlate with an increased risk of metastasis in non-small cell lung cancer (Müller-Tidow et al., 2005). F1174 mutations in hALK and a corresponding mutation in hLTK (F568L) were shown to cause ligand-independent activation of these kinases (Chand et al., 2013; Janoueix-Lerosey et al., 2008; Roll and Reuther, 2012; Chen et al., 2008; George et al., 2008; Martinsson et al., 2011).

In this study, we describe *moonstone*, *ltk^{mne}*, a dominant allele of *shd/ltk* in zebrafish. It contains a F993I mutation in the kinase domain, which corresponds to human ALK residue F1174. Homozygous and heterozygous zebrafish *ltk^{mne}* mutants display ectopic iridophores inside the trunk at larval stages, and an increased number of iridophores on scales and fins, giving the fish a strong green-blue sheen. Treatment with ALK inhibitors causes a decrease in the number of iridophores in both wild-type

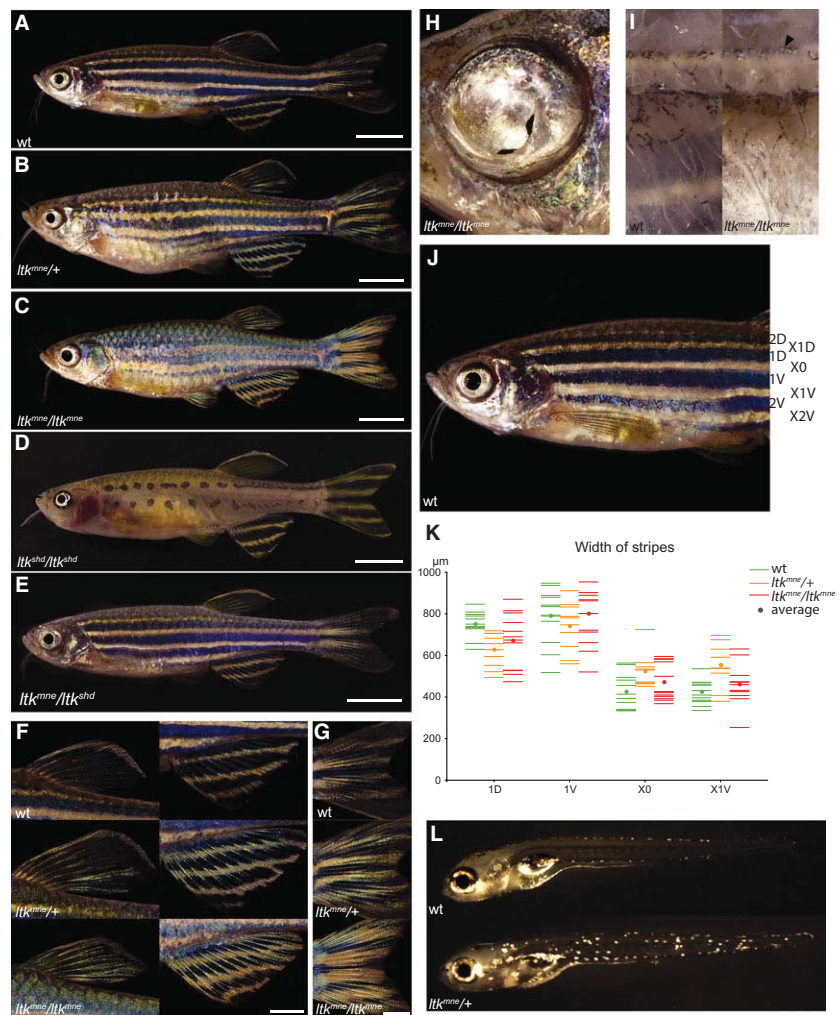
and mutant fish during larval stages as well as metamorphosis. This suggests that *Ltk* is continually required during iridophore development and maintenance. When presented with an *ltk⁺* wild-type environment in chimeric animals, *ltk^{mne}* iridophores can massively overgrow in the surrounding skin. Our data indicate that the phenotype is a result of an increase in *Ltk* activity. Our gain-of-function and loss-of-function analysis allows us to conclude that *Ltk* plays an instructive role in the establishment of iridophores and to propose a role for *Ltk* in regulating proliferation in post-embryonic fish through homotypic competition.

Results

moonstone encodes Leucocyte tyrosine kinase

The dominant mutant *moonstone* (*mne*) was isolated during a screen for ENU-induced mutants affecting adult pigment pattern formation (Fadeev et al., 2015) due to the striking glow of the adult fish. Adult mutants display a strong green-blue sheen on the body owing to an increased number of iridophores on the scales (Fig-

Figure 1. *moonstone* mutants exhibit an increase in iridophore numbers. (A–C) *moonstone*, *ltk^{mne}*, adults show a strong green-blue sheen, owing to supernumerary iridophores on the scales, especially dorsally. Scale bars: 5 mm. (D) Phenotype of *ltk^{shd}* (*shady*), a loss-of-function mutant for *Ltk*. Scale bar: 5 mm. (E) Transheterozygous *ltk^{mne}/ltk^{shd}* fish exhibit *ltk^{mne}* phenotype comparable to or weaker than *ltk^{mne}/+*. Scale bar: 5 mm. (F, G) *ltk^{mne}* mutant fish exhibit increased iridophore numbers in dorsal, anal and caudal fins. Scale bars: 2 mm. (H) Overgrowth of eye iridophores onto pupils in *ltk^{mne}* fish. (I) Ectopic iridophore clusters can be observed in *ltk^{mne}* adults next to spinal column on sagittal sections (arrowhead). The inner side of abdominal cavity is also covered by iridophores in *ltk^{mne}*. (J) The nomenclature of adult stripes. All light stripes start with X (for xanthophore), with X0 being the first interstripe, and 1D and 1V are the first dark stripes. (K) The width of adult light and dark stripes is not affected in adult *ltk^{mne}* when compared to wild type. Each line represents average for one fish. (L) six dpf *mne* larvae exhibit ectopic iridophores, as compared to wild-type larvae.



ure 1A–C). The number of iridophores on the fins is increased as well, as to form almost an uninterrupted sheet of iridophores in the space between fin rays in the light stripes (Figure 1F,G), as opposed to single iridophores in wild type (Hirata et al., 2005). The mutant is homozygous viable, and its phenotype is stronger in homozygous fish.

Occasionally, homozygotes show an overgrowth of iridophores in one or both eyes (Figure 1H), covering the pupil. Further, the abdominal cavity of adult *mne* fish is completely covered by a dense sheet of iridophores (Figure 1I).

Adult *mne* display an apparently normal striped pattern in the skin, albeit at times the dark stripes display rough, undulating borders. To assess the width of the dark and light stripes, 4 different stripes were measured in three consecutive segments – the first two dark stripes (1D and 1V), the first light stripe (X0) and the second light stripe (X1V) located ventrally to 1V (Figure 1J and Frohnhöfer et al., 2013). These measurements indicate that there is no significant change in the width of the light and dark stripes in the trunk of heterozygous and homozygous mutant fish when compared to wild type (Figure 1K).

In larvae, iridophores are arranged in a dorsal and a ventral stripe – on average one iridophore per segment. In addition, *mne* mutant larvae display scattered clusters of ectopic iridophores, located inside the body (Figure 1L).

The mutation was mapped to the region of chromosome 17 between markers z9831 (43.5 cM, 26.5 Mb) and z11202 (48.8 cM, 38 Mb), according to Ensembl Zebrafish release 82). *shady*, a recessive mutant exhibiting loss of iridophores in larvae as well as adults (Kelsh et al., 1996) encodes Leucocyte tyrosine kinase (Ltk) (Lopes et al., 2008). *ltk* is located in the middle of the mapping region (31.4 Mb) (Figure 2A). We sequenced *ltk* cDNA from *mne* mutants and detected an F993I change in the kinase domain of the protein (Figure 2B,C), which is highly conserved throughout the tyrosine kinase family (Figure 2D). In subsequent crosses, no segregation of the *mne* phenotype and the *ltk* lesion was detected. This suggests that the supernumerary iridophores in the dominant *mne* phenotype are caused by a gain-of-function mutation in the *ltk* gene. Subsequently, the mutant allele will be referred to as *ltk^{mne}*.

To investigate the phenotype in the absence of a functional *ltk* allele, transallelic *ltk^{mne}/-* animals were produced. *ltk^{mne}/ltk^{shd}* individuals exhibit a phenotype close to wild type, only a slight increase of iridescence in dorsal scales is observed, weaker than in heterozygous *ltk^{mne}/+* animals (Figure 1E). Homozygous *ltk^{mne}* fish exhibit a stronger phenotype than heterozygous animals, suggesting that the *ltk^{mne}* allele encodes a hyperactive Ltk, and the strength of the phenotype depends on the overall Ltk activity.

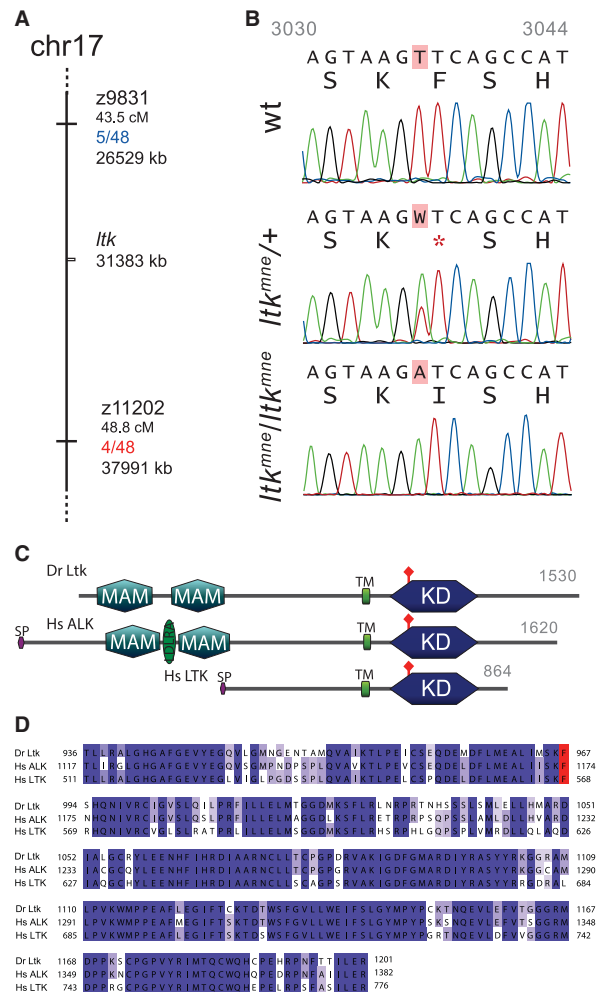


Figure 2. *mne* encodes Ltk. (A) Scheme of meiotic mapping of *ltk^{mne}*. Marked are z-markers with their genomic and genetic coordinates. The numbers of recombinants among all fish tested are given in red and blue. (B) DNA sequence traces of *ltk* from mutants and wild type (Ensembl transcript ID: ENSDART0000061547). Red rectangles mark the mutated residues. (C) Scheme of Ltk protein of *Danio rerio* (UniProt ID: F1QVU0) and human ALK (Q9UM73) and LTK (P29376). SP – signal peptide, MAM – MAM domain, TM – transmembrane region, KD – tyrosine protein kinase catalytic domain. Red diamond – position of F993 in Dr Ltk, and corresponding phenylalanine in human proteins. (D) Multiple protein alignment of kinase domains of zebrafish Ltk and human ALK and LTK. Intensity of colour corresponds to the conservation level. Red square – F993 in *Danio rerio* and corresponding phenylalanine.

Ltk regulates specification, survival and proliferation of iridophores

Further evidence that *mne* is a *shd* allele comes from the sensitivity of the phenotype to inhibitor treatment. TAE684 (TAE) has been shown to be a specific inhibitor of zebrafish Ltk and Alk (Colanesi et al., 2012; Rodrigues et al., 2012). To test whether it affects the *ltk^{mne}* phenotype, we grew wild-type and *ltk^{mne}/ltk^{mne}* larvae in a medium containing TAE from 82 to 105 hpf (N = 5; Figure 3A). Numbers of iridophores in TAE and

mock-treated wild-type larvae did not differ significantly, whereas TAE treatment led to a reduction of iridophore numbers in mutants. When fish were treated from 9 to 72 hpf with daily changes of the medium, the effect was much stronger, resulting in complete disappearance of iridophores (N = 7; Figure 3B,C). In this experiment iridophores were labelled with *Tg(TDL358:GFP)* and *Tg(sox10:RFP)*, the former driving expression of GFP in iridophores and the latter labelling neural crest-derived tissues. These results indicate that Ltk is required for the maintenance of iridophores.

Larval wild-type and *ltk^{mne}* fish did not show a significant difference in numbers of clusters of iridophores in the ventral or dorsal stripes of the body (entopic iridophores, found in both wild type and mutant) (Figure 3C, mock treatment). Ectopic iridophore clusters in the mutants were frequently found close to or in contact with dorsal root ganglia (DRG) in four dpf fish (six of 10 clusters in 11 fish, Figure 3D). Some ectopic iridophores are located in ventral parts of the larvae and might give rise to the sheet of iridophores covering the abdominal cavity (Figure 1I). These data point to an instructive role of Ltk in specification of iridophores from the neural crest and subsequent neural crest-derived iridophore progenitors. It is plausible that in *ltk^{mne}* mutants additional precursors for ectopic iridophores are produced, although the possibility that these arise from entopic iridophores moving to abnormal positions cannot be excluded.

Ectopic iridophore clusters inside the body persist and increase their size in metamorphic (Figure 3E) and adult fish (Figure 1I, arrowhead). The increase of iridophore number in these clusters is achieved, at least partially, by cell division as shown by BrdU incorporation experiments on three dpf *ltk^{mne}/+* larvae (Figure 3F). Four dpf *ltk^{mne}* larvae exhibit larger entopic clusters, as compared to wild type, suggesting larger number of cells (Figure 3G). BrdU incorporation showed that in three dpf *ltk^{mne}/+* larvae 9 of 93 entopic iridophore clusters contained dividing cells (9.6%), in a contrast to 1 of 24 clusters in wild-type animals (4.1%). Interestingly, four dpf mutant larvae exhibited proliferation in only 4/89 clusters, whereas in wild type no division was observed in 61 clusters. This suggests a gradual decrease in iridophore proliferation during larval development. To estimate the effect of *ltk^{mne}* on iridophore proliferation during the formation of the first light stripe, we quantified the change in the number of iridophores during a time-window of 24 h at the onset of metamorphosis in 14 dpf fish carrying both *Tg(TDL358:GFP)* and *Tg(sox10:RFP)* transgenes (N = 7; Figure 3H). *ltk^{mne}* did not show a significant difference in iridophore proliferation rate as compared to wild type (Figure 3I). These data suggest that Ltk controls iridophore ability to divide, but not the division rate, because *ltk^{mne}* iridophores continue to proliferate when their wild-type counterparts cease to do so.

TAE treatments suggest that the iridophore lineage requires Ltk for survival during metamorphosis as well as

larval stages: wild type and *ltk^{mne}* display reduction in the numbers of metamorphic iridophores after 24 h of treatment with TAE (Figures 3H,I).

Thus we suggest that the overall increase in iridophore numbers in mutants is due to a combination of increased number of iridophore progenitors, enhanced survival of iridophores and retention of proliferation activity.

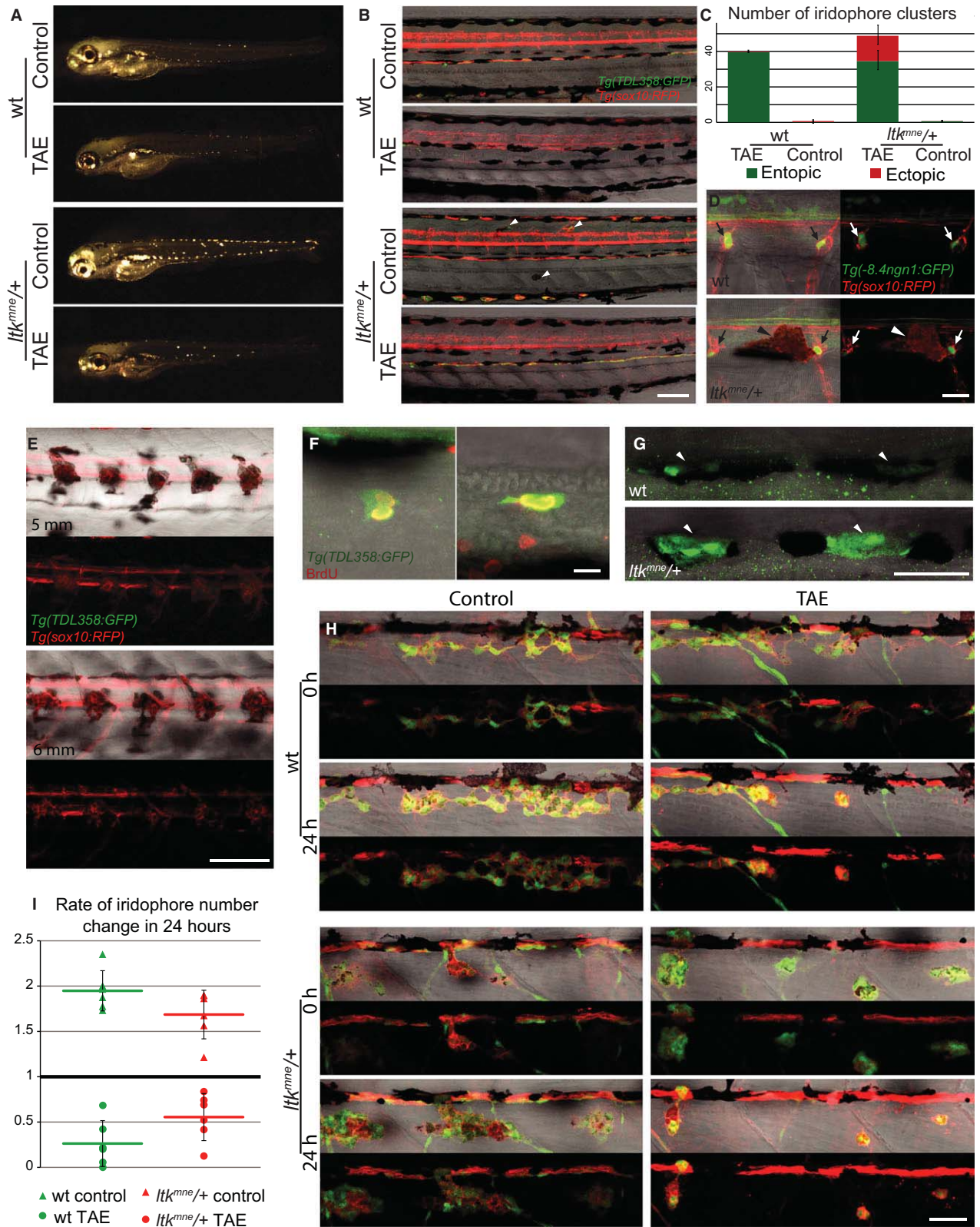
***ltk^{mne}* iridophores display normal cell–cell interactions during body stripe patterning**

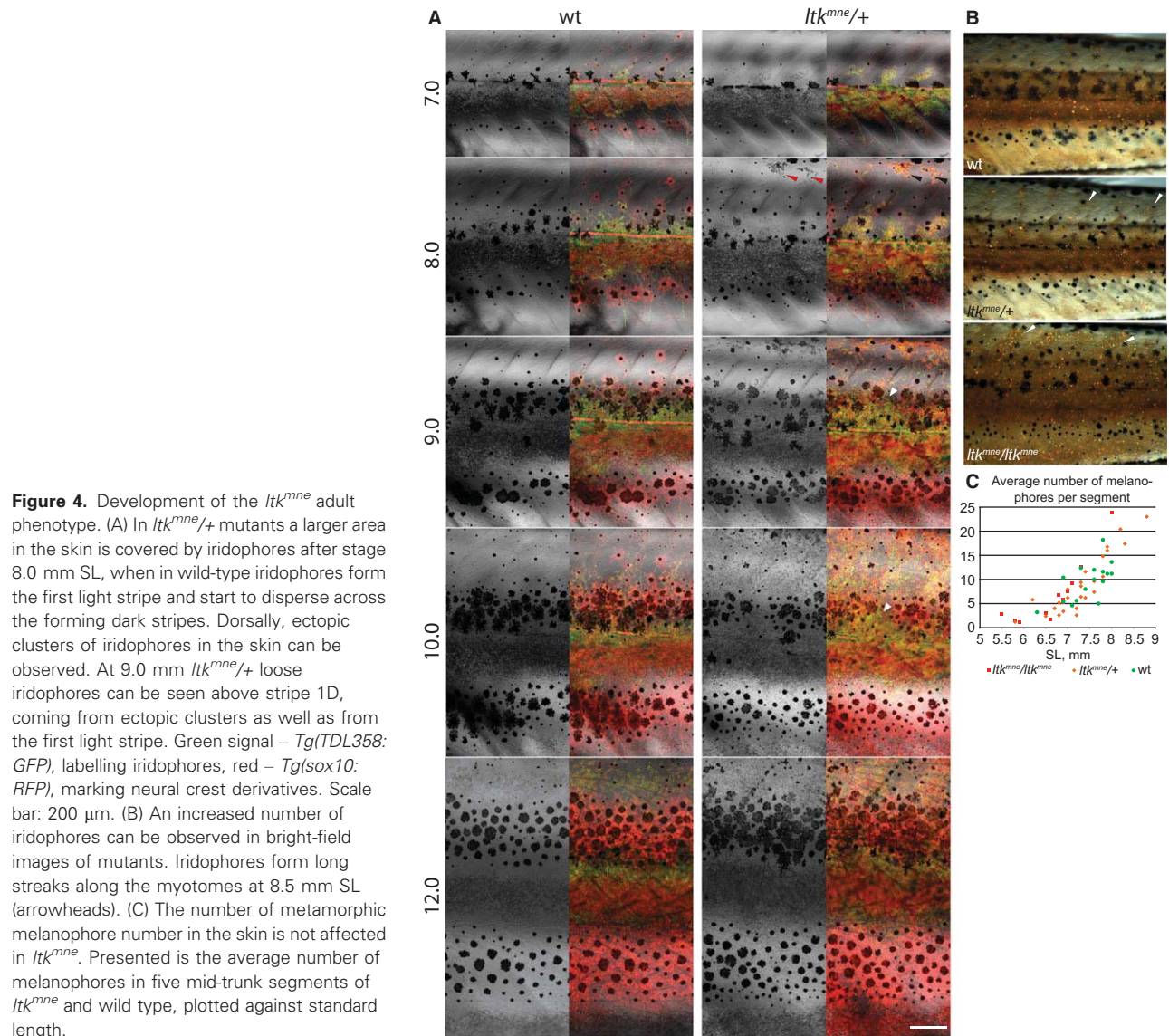
To assess the behaviour of iridophores during metamorphosis, *Tg(TDL358:GFP);Tg(sox10:RFP)* transgenic fish were imaged repeatedly during the formation of the first dark stripes (7–12 mm Standard length (SL)). In early metamorphosis, the distribution of the iridophores in both wild type and *ltk^{mne}* was similar – clusters of iridophores appeared along the horizontal myoseptum and merged to form the first light stripe (Figure 3H). However, at 7 mm SL iridophores in *ltk^{mne}* extended further ventrally compared to wild type, instead of restricting themselves to the borders of the developing first light stripe (Figure 4A). Subsequently, at 8 mm SL additional clusters of iridophores appeared dorsally and ventrally (arrowheads). By the 9 mm stage, the borders of the first light stripe started to sharpen and look similar to wild type. In some cases, dense iridophores in the dark stripe area could be observed until 10–11 mm SL (Figure 4A, arrowheads). At 10 mm SL, the scales dorsal to the 1D stripe exhibited large numbers of iridophores. By 12 mm SL, the *ltk^{mne}* stripe pattern is indistinguishable from wild type. However, increased numbers of iridophores and melanophores persist on the dorsal scales (Figure 4A). These data are corroborated by the observation of ectopic iridophores on the trunk in bright-field images (Figure 4B). Our observations indicate an increase in iridophore numbers during early metamorphosis, which is regulated later to achieve a normal cell density in the adult pattern.

To test whether *ltk^{mne}* is affecting the number of melanophores during metamorphosis, the average number of melanophores per segment was assessed in developing metamorphic fish (Figure 4C). When compared to wild type, neither homozygous, nor heterozygous *ltk^{mne}* showed significant differences in melanophore numbers. Meaningful comparison of the number of iridophores in metamorphic fish has proven to be challenging due to the substantial variation in iridophore numbers even in the adjacent myotomes of the same fish; however, the stripe width measurements suggest a number within a normal range.

Adult fish have increased number of iridophores and melanophores on scales

The green sheen of mutant fish seems to be largely derived from supernumerary iridophores on the scales and dorsum. Scales isolated from heterozygous *ltk^{mne}/+* fish along the dorso-ventral axis display an increased area occupied by iridophores when compared to their





wild-type counterparts (Figure 5A). The iridophores also seem to be packed more densely in the mutants (Figure 5A, dorsal). In homozygous *ltk^{mne}* fish, the coverage of scales with iridophores is increased even further

(data not shown). Melanophores on the dorsal scales are present in larger numbers and co-localize with iridophores. This effect is even more profound in homozygous fish (Figure 5B). It is plausible that melanophores on

Figure 3. *Ltk* inhibitor TAE684 partially rescues the *ltk^{mne}* phenotype and decreases the number of iridophores. (A) The number of iridophores is reduced in *ltk^{mne}/+* larvae treated with ALK inhibitor TAE684 from 82 to 105 hpf. N = 5. (B) A massive reduction in iridophore numbers is observed in wild-type and *ltk^{mne}/+* larvae, treated with TAE684 from 9 to 72 hpf. Green signal – *Tg(TDL358:GFP)*, labelling iridophores, red – *Tg(sox10:RFP)*, marking neural crest derivatives. Arrowheads: ectopic iridophores in *ltk^{mne}* larvae. N = 8. Scale bar: 100 μ m. (C) The increased number of iridophores in three dpf *ltk^{mne}/+* larvae is due to ectopic iridophores. Continuous TAE treatment (B) abolished all iridophores both in wild type and *ltk^{mne}/+*. Shown is the number of single iridophores and iridophore clusters posterior to the developing swim bladder. N = 7–9. (D) Clusters of ectopic *ltk^{mne}* iridophores (arrowhead) are frequently located close to or in direct contact with DRG (arrows, shown are three individual four dpf larvae). Green – *Tg(-8.4ngn1:GFP)* driving the expression of GFP in DRG neurons, red – *Tg(sox10:RFP)*. Scale bar: 25 μ m. (E) Larval ectopic iridophores inside the trunk continue to proliferate and stay clustered in metamorphic fish. Scale bar: 200 μ m. (F) *ltk^{mne}* iridophores in ectopic clusters are able to divide, as shown by BrdU incorporation in fish carrying *Tg(TDL358:GFP)*. Scale bar: 25 μ m. (G) *ltk^{mne}* fish exhibit larger ectopic iridophore clusters (arrowheads) as compared to wild type. Shown is antibody staining against GFP of fish carrying *Tg(TDL358:GFP)*. Scale bar: 10 μ m. (H) TAE684 treatment for 24 h causes a reduction in iridophore numbers in metamorphic fish. N = 7. Scale bar: 50 μ m. (I) *ltk^{mne}* metamorphic iridophores do not divide at a significantly different rate, when compared to wild type. Plotted is the ratio of metamorphic iridophore numbers after/before treatment with TAE for 24 h.

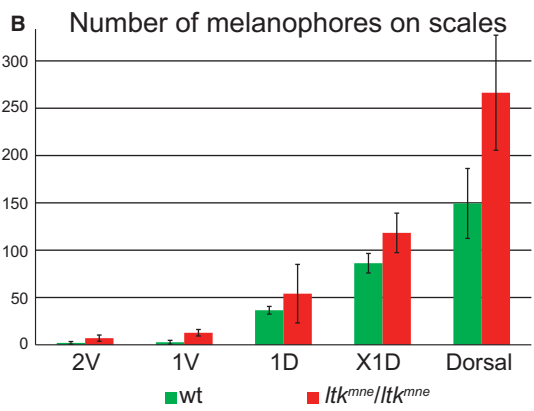
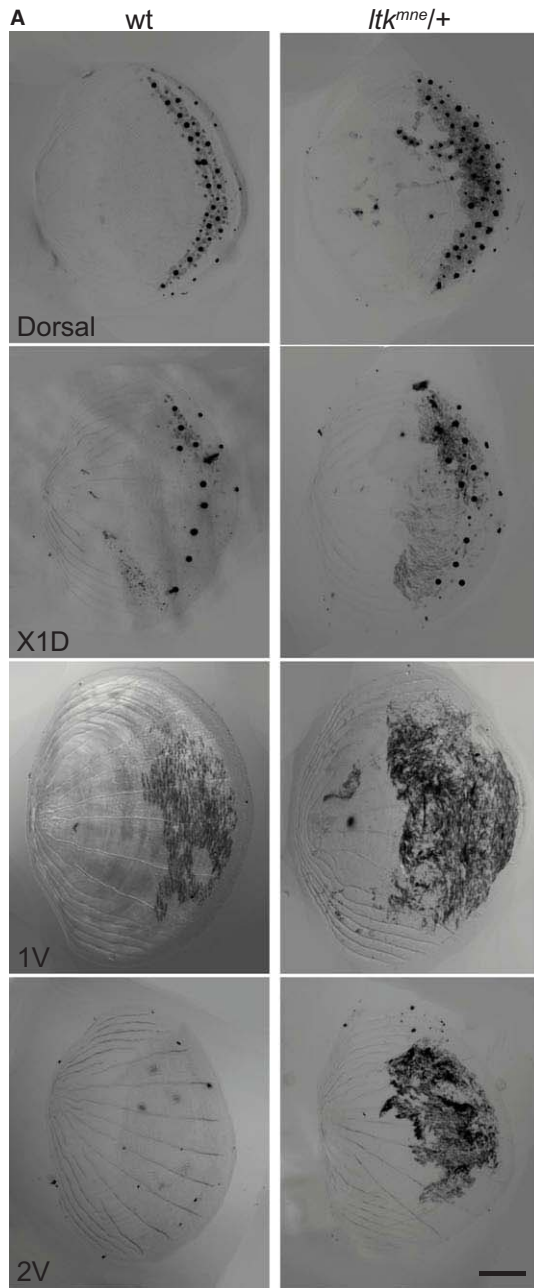


Figure 5. Adult *Itk^{mne}* fish exhibit increased numbers of iridophores and melanophores on scales. (A) All *Itk^{mne}/+* scales exhibit large areas covered by iridophores, which are accompanied dorsally by melanophores. Dorsal – dorsal-most scale, X1D, 1V, 2V – stripe covered by a scale. Scale bar: 200 μ m. (B) All *Itk^{mne}/Itk^{mne}* scales exhibit increased number of melanophores. Evaluated were 3–8 scales for each group from 1 to 2 individuals. The error bars represent standard deviation.

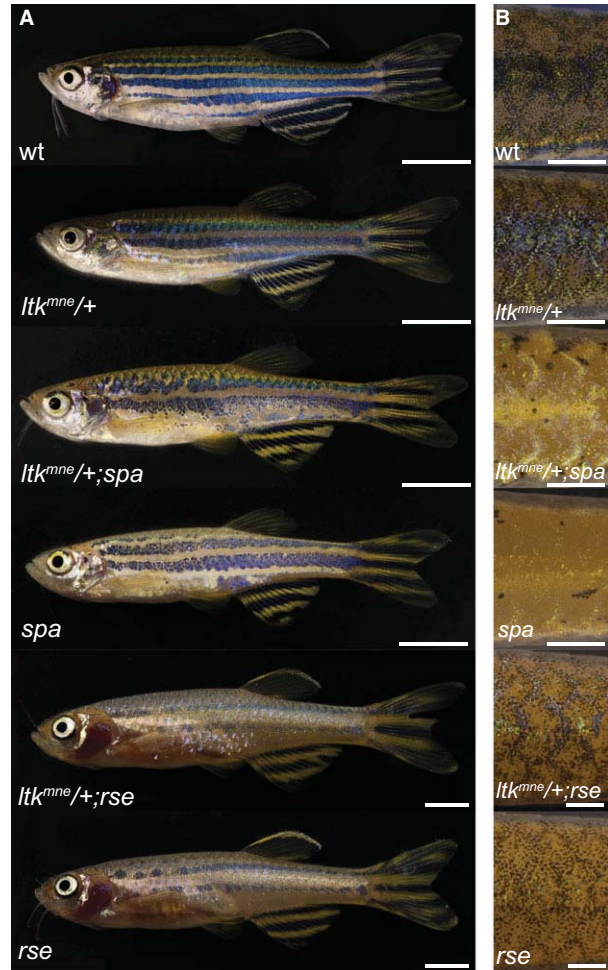


Figure 6. *Itk^{mne}* acts independently of *sparse* and *rose*. (A) Double mutants of *Itk^{mne};spa* and *Itk^{mne};rse* exhibit superpositions of the corresponding phenotypes. Scale bar: 5 mm. (B) Dorsal view. Scale bar: 1 mm.

scales are regulated differently from hypodermal melanophores.

***Ltk* specifically regulates iridophores**

As discussed above, the major *Itk^{mne}* adult phenotype is increased numbers of iridophores on the scales. To test if this is due to the formation of excess iridophores at the expense of other pigment cell types, we studied the genetic interaction between *Itk^{mne}* and *sparse* (*spa*). Mutations in *spa/kita* affect a subset of melanophores and display a strong reduction in the number of

melanophores on the scales and on the dorsum (Johnson et al. 1995). If increased iridophores in *ltk^{mne}* develop from *spa*-dependent precursors, then *ltk^{mne};spa* double mutants should display a *spa* phenotype and decreased numbers of iridophores in the dorsum and the trunk. We do not observe this, despite the expected reduction in the number of melanophores in *ltk^{mne};spa*, the excess iridophores remain (Figure 6). This suggests that the *Ltk* specifically regulates iridophores.

Ltk and Ednrba regulate distinct aspects of iridophore behaviour

During stripe pattern formation, iridophores undergo proliferation, dispersal and cell shape transitions; at the genetic level, these processes are regulated by two main signalling receptors – *Ednrba* and *Ltk*. Mutations in *rose (rse)/ednrba* lead to a severe reduction in iridophore numbers, specifically a reduction in dense iridophores. Due to the lack of dense iridophores melanophores are restricted to the two early stripes (1D and 1V) in both *shd* and *rse*, and their numbers are much reduced. If the primary defect in *rose* is a reduced number of iridophores, then supplying excess iridophores should revert the phenotype. However, if it is due to a primary function of *rse* during the cell shape transitions of iridophores, then we should observe no rescue even when excess iridophores are supplied. To distinguish between these two possibilities, we generated double mutants *ltk^{mne};rse*, which display a combination of *ltk^{mne}* and *rse* phenotypes – increased numbers of iridophores and melanophores on scales and reduced numbers of trunk melanophores and iridophores (Figure 6). Taken together with the results of BrdU incorporation experiments, this observation suggests that *rse* and *ltk^{mne}* affect iridophores independently: *Ltk* regulates iridophore proliferation, whereas *Ednrba* might have a primary function in iridophore cell shape transition.

***ltk^{mne}* iridophores may have a growth advantage over wild-type iridophores**

Recently, it has been shown that iridophore proliferation and coverage of the skin is regulated by homotypic competition between iridophores (Walderich et al., 2016). Our data indicate that *Ltk* regulates iridophore numbers by promoting iridophore establishment, proliferation and survival. This suggests that the hyperactive *Ltk* might provide a selective advantage to *ltk^{mne}* iridophores

compared to wild-type iridophores. To assess the behaviour of *ltk^{mne}* cells in a wild-type environment, we performed blastomere transplantation. As recipients, we used *albino* mutants, which lack pigment in

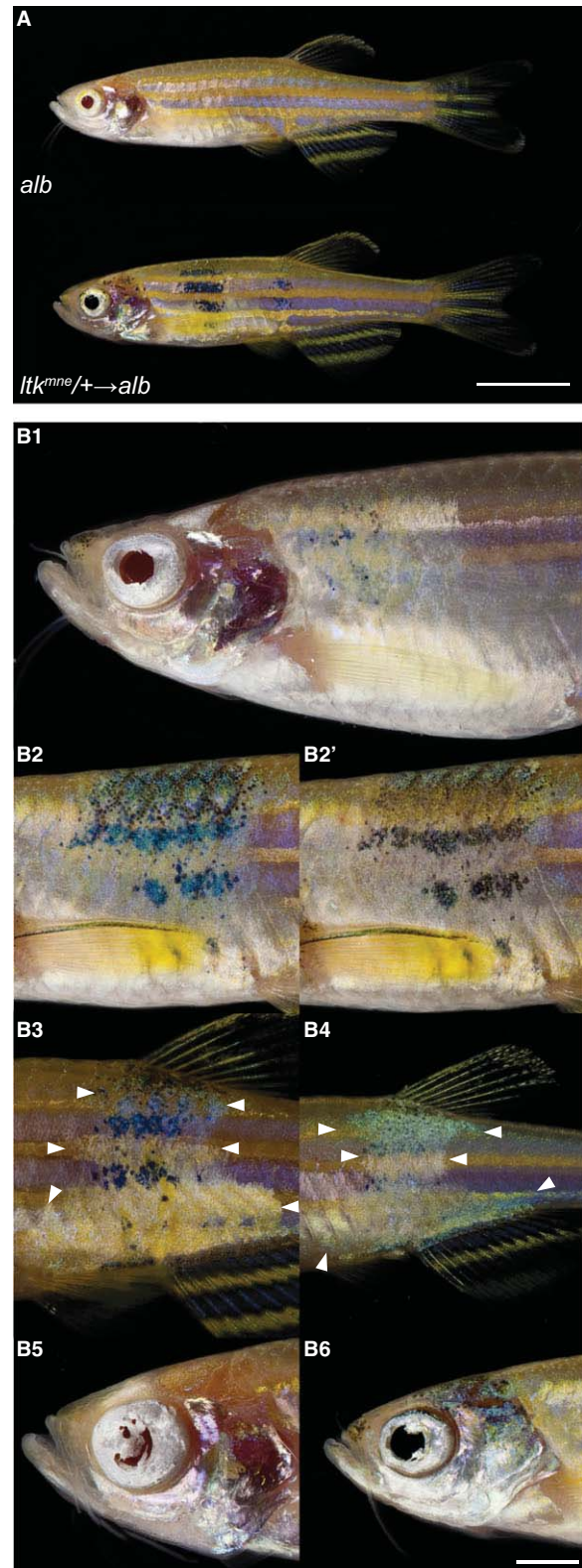


Figure 7. *ltk^{mne}* iridophores lead to overgrowth in an *ltk⁺* environment. (A) Blastula transplantations from *ltk^{mne}* into *albino* hosts resulted mostly in a normal striped pattern in the chimeras. Scale bar: 5 mm. (B) In some cases *ltk^{mne}/albino* chimeras developed large overgrowths of iridophores (B1-B4), which persisted when scales were removed from affected area (B2'). Frequently such overgrowths were spreading out further along the antero-posterior axis on the ventral and dorsal sides (arrowheads). Overgrowths of iridophores in the eyes and heads (B5, B6). Scale bar: 2 mm.

melanophores but are normal otherwise (Dooley et al., 2013b), thereby allowing easy identification of clones (Figure 7A). In most of the cases (28/46), chimeric fish exhibited mixed donor-derived melanophore and iridophore clusters spanning 2–5 segments and spreading vertically, contributing to all stripes along the dorso-ventral axis, typical for such transplantations (Walderich et al., 2016). These clusters displayed the characteristic scale pattern of *ltk^{mne}*, indicating cell-autonomous function of *ltk* in iridophores. However, in some cases (12/46) a novel phenotype, which can be described as iridophore overgrowth, was observed in the clusters (Figure 7B). They displayed a sheet of iridophores that spread out over several segments along anterior–posterior axis especially in the ventral or dorsal region of the chimeric fish (Fig. 7B3, 4, arrowheads). These clones presented obscure stripe borders and contained fewer donor-derived melanophores (compare Figure 7A and B2), in some cases only 10–20 melanophores (Figure 7B2–B4). After removal of scales, the green sheen was lost, but the overgrowth phenotype persisted (Figure 7B2, B2') indicating that overgrowth of iridophores occurred in the skin, along with increased iridophore numbers in scales. In some cases (10/46), extensions of iridophore sheets over the pupils were observed (Figure 7B5, 7B6). This phenotype was also occasionally observed in the *ltk^{mne}* mutants (Fig 1H). However, an overgrowth in the skin has never been observed in mutants. These data suggest that when presented with an environment with normal Ltk activity, the iridophores expressing the overactive *ltk^{mne}* allele exhibit overgrowth behaviour due to a growth advantage.

Discussion

Moonstone fish exhibit ectopic iridophores inside the body during larval stages and entering in the skin at the onset of metamorphosis. Adults display a normal striped pattern but an increased number of iridophores on the scales and fins, which gives the fish a striking green-blue sheen. Ectopic iridophore sheets are also observed in the viscera and occasionally in the eye. No effect on other pigment cell types was observed, besides an increase of melanophore numbers on scales. We show that *moonstone* is a gain-of-function allele of *ltk* carrying a mutation in a highly conserved position of the kinase domain. An inhibitor of ALK – TAE684, shown to inhibit zebrafish Ltk as well, alleviated the *ltk^{mne}* phenotype and caused a reduction in the number of iridophores in metamorphic mutants and wild-type fish. Transallelic *ltk^{mne}*- animals display the phenotype weaker than or comparable to *ltk^{mne}/+*, suggesting that Ltk acts in a dosage-dependent manner. Intriguingly, in an *ltk⁺* environment, *ltk^{mne}* mutant iridophores sometimes produce large homogeneous overgrowths in the skin.

Several genes were shown to regulate different aspects of iridophore development, such as establishment, proliferation and cell shape transition. *schachbrett*/

tjp1a is expressed in iridophores and required for proper transition of iridophores from the dense to the loose form (Fadееv et al., 2015). It has been reported that endothelin signalling regulates iridophore number (Parichy et al., 2000). However, mutations of *rose* (*ednrba*) and *karneol* (*ece 2*) specifically abolish dense iridophores, as loose iridophores can still be observed even in the strongest mutant alleles. This suggests that the endothelin pathway has a function in iridophore shape transitions. *ltk^{mne}* does not rescue the *rose* phenotype, and double mutants show the superposition of the two phenotypes, indicating independent roles in iridophore development for both genes. We confirm the requirement for *ltk* in iridophore establishment and suggest a novel role in proliferation and survival, as gain-of-function *ltk^{mne}* leads to increased iridophore numbers, and specific inhibitors cause disappearance of existing iridophores.

We propose a role for Ltk in iridophore homotypic interactions (Walderich et al., 2016), as *ltk^{mne}* iridophores can form large clusters in an *ltk⁺* environment, outcompeting wild-type iridophores. In addition, *ltk^{mne}* displays supernumerary iridophores in regions devoid of iridophores on anterior regions of scales and in the eye. However, interactions with other pigment cells do not seem to be affected, as *ltk^{mne}* iridophores are able to participate in a normal striped pattern. It is possible that MAM domains, present in the extracellular part of hALK and zebrafish Ltk and Alk (Fig 2C), mediate homotypic iridophore interactions in zebrafish. MAM domains have been shown to participate in homotypic interactions in insect cell culture (Cismasiu et al., 2004; Zondag et al., 1995; Brady-Kalnay and Tonks, 1994).

Data on the physiological functions of ALK and LTK in vertebrates are scarce, studies mostly concentrating on their tumorigenic properties. LTK and ALK mutations in mice and humans at the same conserved position as in *ltk^{mne}* have been shown to be involved in several types of cancer (De Brouwer et al., 2010; Martinsson et al., 2011; Heukamp et al., 2012; Chen et al., 2008). Notably, knockdown of ALK lead to a decreased proliferation rate of neuroblastoma cells (Mossé et al., 2008), supporting our suggestion for a role of the Ltk tyrosine kinase receptor in proliferation control of iridophores. We describe the function of Ltk in particular aspects of cellular behaviour in the context of pigment cells in an in vivo system. We suggest that the *ltk^{mne}* larvae can provide an easily detectable readout in drug screens for Alk and Ltk inhibitors.

Methods

Zebrafish maintenance

Fish were bred and maintained as described (Brand et al., 2002). Fish of the following genotypes were used: Tu, WIK, TE wild-type strains (Tübingen zebrafish stock centre), *shady^{9s1}* (Lopes et al., 2008), *sparse^{b134}* (Kelsh et al., 1996), *rose^{tLF802}* (Frohnhofer et al., 2013), *albino^{b4}* (Dooley et al., 2013b), *Tg(TDL358:GFP)*, *Tg(sox10:mRFP)* (M.

Levesque; C.N.V. laboratory), *Tg(-8.4ngn1:GFP)* (Blader et al., 2003). Fish were staged according to the normal table of zebrafish development (Parichy et al., 2009).

Mutagenesis

The allele *mne^{dtwc3}/WIK* was identified in a screen for mutants induced with N-ethyl-N-nitrosourea (N5809, Sigma-Aldrich, Louis, MO, USA) in Tü wild-type background. Mutagenesis was carried out as described previously (Rohner et al., 2011). Subsequently, fish were crossed to TE fish and later maintained by regular outcrossing.

Mapping and alleles testing

mne^{dtwc3}/WIK fish were incrossed and used for meiotic mapping as described previously (Geisler 2002). The mutation was mapped to the region between microsatellite markers z9831 (43.5 cM) and z11202 (48.8 cM) on chromosome 17. To check for the presence of lesions in *ltk*, RNA was extracted from fin blastema of adult wild type and heterozygous *mne* fish using TRIzol reagent (15596, Thermo Fisher Scientific, Waltham, MA, USA). cDNA was obtained using Omniscript RT kit (205111, QIAGEN, Venlo, the Netherlands). For amplifying and sequencing the *ltk* coding sequence, the following primers were used:

Tue1013 ATGAAGACACCAAGCTCATC
 Tue1014 GCTGGATCAGGATTTGACG
 Tue1015 AGACATCGCTCTTGGCTGTC
 Tue1016 CCATGCTCCAGAAGTAGTTC
 Tue1017 GACCAGGACAAGTCAAAGG
 Tue1018 CGTCCAAAGCTCTCTAGGAC
 Tue1430 ACTGGAGGAGACTGGTTTATC
 Tue1431 TGTTCTTCAGAGTTGTGCC
 Tue1432 TGGGGATTTCAATGGAACAG
 Tue1433 TCAGCAAAGGAAGTGGTTG

Taq polymerase S (M3001.0250, Genaxxon, Ulm, Germany) was used for amplification, and products were cloned into pGEM-T Easy (A360, Promega Fitchburg, WI, USA) and sequenced using Big Dye Terminator v3.1 kit (4337455, Thermo Fisher Scientific).

Transplantations

Chimeras were produced as described (Kane and Kishimoto, 2002) using mid-blastula stage (1000 cell stage) embryos, transplanting 30–60 cells.

BrdU incorporation and immunohistochemistry

Experiments were carried out using three, four and five dpf fish as described before (Singh et al., 2014).

Image acquisition

We used Zeiss LSM 780 NLO confocal microscope and Canon 5D Mk II camera to obtain images. Fiji (Schindelin et al., 2012), Adobe Photoshop and Adobe Illustrator CS6 were used for image processing and analysis. Maximum intensity projection was made for fluorescent channels of confocal scans. For bright-field images, we used 'stack focuser' plugin or a single slice on an appropriate depth. For adult fish photos, multiple RAW camera images were taken in different focal planes and auto-align and auto-blend functions of Photoshop were used. Blemishes on the black background in the photos were removed using the brush tool, without affecting the image of the fish. Repeated imaging of metamorphic fish and anaesthesia was performed as described previously (Singh et al., 2014).

Melanophore counts

Melanophores in metamorphic fish were counted in five segments in the middle 70% of the myotome starting with the one above the first ray of the anal fin and proceeding posteriorly.

Multiple alignments

Multiple protein alignment was obtained using MUSCLE (Edgar, 2004) and visualized using JALVIEW (Waterhouse et al., 2009).

TAE treatment

TAE684 (NVP-TAE684) (HY-10192, MedChem Express) was diluted in dimethylsulphoxide (DMSO; Sigma-Aldrich Louis, MI, USA) to a final concentration of 7.5 mM. Fish were treated in the fish medium containing 50 μM gentamycin (NH09, Carl Roth GmbH + Co. KG, Karlsruhe, Germany) and 0.8% DMSO with 6 μM TAE or without for controls. Thirty embryos were treated in 40 ml of the medium in a 30 mm Petri dish. Larvae were treated individually in 10 ml of the medium in six well plates.

Acknowledgements

We thank U. Irion for discussion and comments on the project and P. Panza, A. Dinwiddie for comments on the manuscript. We thank H.-M. Maischein for help with blastomere transplantations, C. Liebig for support in light microscopy, B. Walderich and the fish facility for great support. This work was financially supported by the Max-Planck Society for the Advancement of Science and by ZF-HEALTH grant (Project number 242048).

Author contribution

CNV and JK conceived the project; JK and AF isolated, mapped and cloned the mutant; AF and APS carried out the experiments; CNV, APS and AF analysed the data and wrote the manuscript.

Conflict of interest

The authors declare that they have no conflict of interest.

References

- Ben-Neriah, Y., and Bauskin, A.R. (1988). Leukocytes express a novel gene encoding a putative transmembrane protein-kinase devoid of an extracellular domain. *Nature* 333, 672–676.
- Bernards, A., and de la Monte, S.M. (1990). The *Ltk* receptor tyrosine kinase is expressed in pre-B lymphocytes and cerebral neurons and uses a non-AUG translational initiator. *EMBO J.* 9, 2279–2287.
- Blader, P., Plessy, C., and Strähle, U. (2003). Multiple regulatory elements with spatially and temporally distinct activities control neurogenin1 expression in primary neurons of the zebrafish embryo. *Mech. Dev.* 120, 211–218.
- Brady-Kalnay, S.M., and Tonks, N.K. (1994). Identification of the homophilic binding site of the receptor protein tyrosine phosphatase PTP mu. *J. Biol. Chem.* 269, 28472–28477.
- Brand, M., Granato, M., and Nüsslein-Volhard, C. (2002). Keeping and raising zebrafish. In *Zebrafish, Practical Approach*, Nüsslein-Volhard C and Dahm R. eds. (New York: Oxford University Press), pp. 7–38.
- Budi, E.H., Patterson, L.B., and Parichy, D.M. (2011). Post-embryonic nerve-associated precursors to adult pigment cells: genetic

- requirements and dynamics of morphogenesis and differentiation. *PLoS Genet.* 7, e1002044.
- Carén, H., et al. (2008). High incidence of DNA mutations and gene amplifications of the ALK gene in advanced sporadic neuroblastoma tumours. *Biochem. J.* 416, 153–159.
- Challa, A.K., and Chatti, K. (2013). Conservation and early expression of zebrafish tyrosine kinases support the utility of zebrafish as a model for tyrosine kinase biology. *Zebrafish* 10, 264–274.
- Chand, D., et al. (2013). Cell culture and *Drosophila* model systems define three classes of anaplastic lymphoma kinase mutations in neuroblastoma. *Dis. Model. Mech.* 6, 373–382.
- Chen, Y., et al. (2008). Oncogenic mutations of ALK kinase in neuroblastoma. *Nature* 455, 971–974.
- Cismasiu, V.B., et al. (2004). The MAM (Meprin/A5-protein/PTPmu) domain is a homophilic binding site promoting the lateral dimerization of receptor-like protein-tyrosine phosphatase μ . *J. Biol. Chem.* 279, 26922–26931.
- Colanesi, S., et al. (2012). Small molecule screening identifies targetable zebrafish pigmentation pathways. *Pigment Cell Melanoma Res.* 25, 131–143.
- De Brouwer, S., et al. (2010). Meta-analysis of neuroblastomas reveals a skewed ALK mutation spectrum in tumors with MYCN amplification. *Clin. Cancer Res.* 16, 4353–4362.
- Dirks, W.G., et al. (2002). Expression and functional analysis of the anaplastic lymphoma kinase (ALK) gene in tumor cell lines. *Int. J. Cancer* 100, 49–56.
- Dooley, C.M., et al. (2013a). On the embryonic origin of adult melanophores: the role of ErbB and Kit signalling in establishing melanophore stem cells in zebrafish. *Development* 140, 1003–1013.
- Dooley, C.M., et al. (2013b). Slc45a2 and V-ATPase are regulators of melanosomal pH homeostasis in zebrafish, providing a mechanism for human pigment evolution and disease. *Pigment Cell Melanoma Res.* 26, 205–217.
- Edgar, R.C. (2004). MUSCLE: multiple sequence alignment with high accuracy and high throughput. *Nucleic Acids Res.* 32, 1792–1797.
- Fadееv, A., et al. (2015). Protein, tight junction 1a regulates pigment cell organisation during zebrafish colour patterning. *eLife* 4, 1–17.
- Fass, D., et al. (1997). Molecular basis of familial hypercholesterolaemia from structure of LDL receptor module. *Nature* 388, 691–693.
- Forbes, S.A., et al. (2015). COSMIC: exploring the world's knowledge of somatic mutations in human cancer. *Nucleic Acids Res.* 43 (D1), D805–D811.
- Frohnhofer, H.G., et al. (2013). Iridophores and their interactions with other chromatophores are required for stripe formation in zebrafish. *Development* 140, 2997–3007.
- Geisler, R. (2002). Mapping and cloning. In *Zebrafish, A Practical Approach*, C., Nüsslein-Volhard, and R., Dahm, eds. (New York, NY: Oxford University Press), 261, 175–212.
- George, R.E., et al. (2008). Activating mutations in ALK provide a therapeutic target in neuroblastoma. *Nature* 455, 975–978.
- Heukamp, L.C., et al. (2012). Targeted expression of mutated ALK induces neuroblastoma in transgenic mice. *Sci. Transl. Med.* 4, 141ra91.
- Hirata, M., et al. (2003). Pigment cell organization in the hypodermis of zebrafish. *Dev. Dyn.* 227, 497–503.
- Hirata, M., Nakamura, K.-I., and Kondo, S. (2005). Pigment cell distributions in different tissues of the zebrafish, with special reference to the striped pigment pattern. *Dev. Dyn.* 234, 293–300.
- Irion, U., et al. (2014). Gap junctions composed of connexins 41.8 and 39.4 are essential for colour pattern formation in zebrafish. *eLife* 3, 1–16.
- Irion, U., Singh, A.P., and Nüsslein-Volhard, C. (2016). The Developmental Genetics of Vertebrate Color Pattern. doi:10.1016/bs.ctdb.2015.12.012. [Epub ahead of print].
- Janoueix-Lerosey, I., et al. (2008). Somatic and germline activating mutations of the ALK kinase receptor in neuroblastoma. *Nature* 455, 967–970.
- Johnson, S.L., Africa, D., Walker, C., and Weston, J.A. (1995). Genetic control of adult pigment stripe development in zebrafish. *Dev. Biol.* 167, 27–33.
- Kane, D.A., and Kishimoto, Y. (2002) Cell labelling and transplantation techniques. *Zebrafish, Practical Approach*. Nüsslein-Volhard C and Dahm R. eds. (New York: Oxford University Press), pp. 95–120.
- Kelsh, R.N., et al. (1996). Zebrafish pigmentation mutations and the processes of neural crest development. *Development* 123, 369–389.
- Kelsh, R.N., et al. (2009). Stripes and belly-spots – a review of pigment cell morphogenesis in vertebrates. *Semin. Cell Dev. Biol.* 20, 90–104.
- Kirschbaum, F. (1975). Investigations on color pattern of zebra fish *Brachydanio-Rerio* (Cyprinidae, Teleostei). *Roux Arch. Dev. Biol.* 177, 129–152.
- Krauss, J., et al. (2013). Transparent, a gene affecting stripe formation in Zebrafish, encodes the mitochondrial protein Mpv17 that is required for iridophore survival. *Biol. Open* 2, 703–710.
- Krauss, J., et al. (2014). Endothelin signalling in iridophore development and stripe pattern formation of zebrafish. *Biol. Open* 3, 503–509.
- Liao, E.H., et al. (2004). An SCF-like ubiquitin ligase complex that controls presynaptic differentiation. *Nature* 430, 345–350.
- Lopes, S.S., et al. (2008). Leukocyte tyrosine kinase functions in pigment cell development. *PLoS Genet.* 4, e1000026.
- Lorén, C.E., et al. (2001). Identification and characterization of DAlk: a novel *Drosophila melanogaster* RTK which drives ERK activation in vivo. *Genes Cells* 6, 531–544.
- Maderspacher, F., and Nüsslein-Volhard, C. (2003). Formation of the adult pigment pattern in zebrafish requires leopard and obelix dependent cell interactions. *Development* 130, 3447–3457.
- Mahalwar, P., et al. (2014). Local reorganization of xanthophores fine-tunes and colors the striped pattern of zebrafish. *Science* 345, 1362–1364.
- Martinsson, T., et al. (2011). Appearance of the novel activating F1174S ALK mutation in neuroblastoma correlates with aggressive tumor progression and unresponsiveness to therapy. *Cancer Res.* 71, 98–105.
- McMenamin, S.K., et al. (2014). Thyroid hormone-dependent adult pigment cell lineage and pattern in zebrafish. *Science* 345, 1358–1361.
- Mossé, Y.P., et al. (2008). Identification of ALK as a major familial neuroblastoma predisposition gene. *Nature* 455, 930–935.
- Müller-Tidow, C., et al. (2005). Identification of metastasis-associated receptor tyrosine kinases in non-small cell lung cancer. *Cancer Res.* 65, 1778–1782.
- Nakamasu, A., et al. (2009). Interactions between zebrafish pigment cells responsible for the generation of Turing patterns. *Proc. Natl. Acad. Sci.* 106, 8429–8434.
- Palmer, R.H., and Hallberg, B. (2015). Receptor Tyrosine Kinases: Family and Subfamilies. Available at: <http://link.springer.com/10.1007/978-3-319-11888-8>.
- Parichy, D.M., et al. (2000). Mutational analysis of endothelin receptor b1 (rose) during neural crest and pigment pattern development in the zebrafish *Danio rerio*. *Dev. Biol.* 227, 294–306.
- Parichy, D.M., et al. (2009). Normal table of postembryonic zebrafish development: staging by externally visible anatomy of the living fish. *Dev. Dyn.* 238, 2975–3015.
- Patterson, L.B., and Parichy, D.M. (2013). Interactions with iridophores and the tissue environment required for patterning melanophores and xanthophores during zebrafish adult pigment stripe formation. *PLoS Genet.* 9, e1003561.

- Rodrigues, F.S.L.M. et al. (2012). A Simple, Highly Visual in Vivo Screen for Anaplastic Lymphoma Kinase Inhibitors. *ACS Chem. Biol.* **7**, 1968–1974.
- Rohner, N., et al. (2011). Enhancing the efficiency of N-ethyl-N-nitrosourea-induced mutagenesis in the zebrafish. *Zebrafish* **8**, 119–123.
- Roll, J.D., and Reuther, G.W. (2012). ALK-activating homologous mutations in LTK induce cellular transformation. *PLoS ONE* **7**, e31733.
- Schindelin, J., et al. (2012). Fiji: an open-source platform for biological-image analysis. *Nat. Methods* **9**, 676–682.
- Shiota, M., et al. (1994). Hyperphosphorylation of a novel 80 kDa protein-tyrosine kinase similar to Ltk in a human Ki-1 lymphoma cell line, AMS3. *Oncogene* **9**, 1567–1574.
- Singh, A.P., and Nüsslein-Volhard, C. (2015). Zebrafish stripes as a model for vertebrate colour pattern formation. *Curr. Biol.* **25**, R81–R92.
- Singh, A.P., Schach, U., and Nüsslein-Volhard, C. (2014). Proliferation, dispersal and patterned aggregation of iridophores in the skin prefigure striped colouration of zebrafish. *Nat. Cell Biol.* **16**, 607–614.
- Toyoshima, H., et al. (1993). Differently spliced cDNAs of human leukocyte tyrosine kinase receptor tyrosine kinase predict receptor proteins with and without a tyrosine kinase domain and a soluble receptor protein. *Proc. Natl Acad. Sci.* **90**, 5404–5408.
- Walderich, B., Singh, A.P., Mahalwar, P., and Nüsslein-Volhard, C. (2016). Homotypic cell competition regulates proliferation and tiling of Zebrafish pigment cells during colour pattern formation. *Nat. Commun.*, accepted on 30 March 2016.
- Waterhouse, A.M., et al. (2009). Jalview Version 2—a multiple sequence alignment editor and analysis workbench. *Bioinformatics* **25**, 1189–1191.
- Zondag, G.C.M., et al. (1995). Homophilic interactions mediated by receptor tyrosine phosphatases μ and κ . a critical role for the novel extracellular MAM domain. *J. Biol. Chem.* **270**, 14247–14250.

2.3 Publication 3

Kottler, V.A.*, Fadeev, A., Weigel, D., and Dreyer, C. (2013) Pigment pattern formation in the guppy, *Poecilia reticulata*, involves the Kita and *Csf1ra* receptor tyrosine kinases. *Genetics* 194.3 (2013): 631-646

*Corresponding author

The wide variation in the ornamental pattern in male guppies, *Poecilia reticulata*, has attracted the attention of researchers for almost a century (Winge, 1922, 1927). However many of the techniques that are available in other model organisms, such as transplantation, *in situ* hybridisation and the generation of transgenic lines, are either impossible or extremely difficult to use in guppies. The available data on pigment pattern formation in zebrafish are of particular value for the guppy research. The present study focuses on two guppy mutants: *golden* and *blue* (Figure 1). *Golden* guppies lack melanophores at birth but eventually develop a rudimentary pattern of melanophores, whereas the *blue* mutants lack xanthophores throughout development (Dzwillo, 1959; Goodrich *et al*, 1944; Winge & Ditlevsen, 1947; Haskins & Druzba, 1938). A candidate gene approach, based on zebrafish mutants that exhibit similar phenotypes, was used to elucidate the genetic nature of these phenotypes.

The *pfeffer/csf1ra* mutant in zebrafish lacks xanthophores, similarly to *blue*. Guppy orthologs of *csf1ra* were identified, and its cDNA from the *blue* mutants was sequenced. A complex mutation, comprised of a deletion of 5 bp and an insertion of a 7bp fragment, was observed in the *blue* guppy mutants (Figure 2). To confirm that *blue* is indeed a *csf1ra* allele, the genetic linkage was tested. Backcrosses were performed and the progeny was checked for the lesion in *csf1ra*. All fish with the wild type phenotype were heterozygous for the mutation in *csf1ra*. All *blue* fish were homozygous for the mutation. The absence of segregation of the phenotype and the *csf1ra* mutation confirms the notion that the *blue* mutant is indeed *csf1ra*. Interestingly, a careful examination of the *blue* and *golden;blue* mutants showed a small number of xanthophores.

A similar logic was applied to the *golden* mutants. Two zebrafish mutants, *sparse/kita* and *sparse-like/kitla*, exhibit a reduced number of melanophores, similarly to guppy *golden*. Guppy orthologs of *kita* and *kitla* were identified, and their cDNA from the *golden* mutants was sequenced. No lesions were found in *kitla*. On the other hand, *kita* carried insertions of 17, 36 or 53 bp in the coding sequence or deletions of parts of exon 6, depending on the particular allele (Figure 2). Similarly to the *blue* mutations, an examination of backcrosses showed that the *golden* phenotype did not segregate from mutations in *kita*. Further analysis of the *golden* phenotype suggested the presence of two melanophore populations. The first population is *kita*-dependent and emerges before birth, whereas the second population is independent of *kita* and appears after birth. Both populations contribute to the inconspicuous gender-unspecific pattern, shared by males and females, as both adult mutant males and females exhibit melanophores.

Currently it is almost impossible to test whether these mutations are cell-autonomous in guppies, but data from zebrafish yield some clues. A thorough analysis of male-specific patterns shows that the *csf1ra* mutants, which lack orange ornaments, exhibit strong displacement of the dark elements of the pattern, which are composed of melanophores. This suggests that melanophores cannot faithfully reproduce the wild type pattern on their own, and that interactions between different pigment cell types are crucial for pattern formation in the guppy, a finding similar to what is known in zebrafish.

In contrast, *kita* mutations, which affect melanophores, produce only weak changes in the orange colouration and alter the dark elements more subtly and reproducibly than the *csf1ra* mutation. Similarly, *sparse/kita* mutants in zebrafish exhibit less than half the number of melanophores compared to wild type, but they still retain the striped pattern. This also suggests that the male-specific melanophore population is largely *kita*-independent.

In summary, the present study demonstrates a partial conservation of *kita* and *csf1ra* functions in guppy and zebrafish and suggests similarities in genetic mechanisms that govern the process of pigment cell pattern formation across the ray-finned fish (*Actinopterygii*).

Pigment Pattern Formation in the Guppy, *Poecilia reticulata*, Involves the Kita and *Csf1ra* Receptor Tyrosine Kinases

Verena A. Kottler,^{*,1} Andrey Fadeev,[†] Detlef Weigel,^{*} and Christine Dreyer^{*,1}

^{*}Department of Molecular Biology and [†]Department of Genetics, Max Planck Institute for Developmental Biology, 72076 Tübingen, Germany

ABSTRACT Males of the guppy (*Poecilia reticulata*) vary tremendously in their ornamental patterns, which are thought to have evolved in response to a complex interplay between natural and sexual selection. Although the selection pressures acting on the color patterns of the guppy have been extensively studied, little is known about the genes that control their ontogeny. Over 50 years ago, two autosomal color loci, *blue* and *golden*, were described, both of which play a decisive role in the formation of the guppy color pattern. Orange pigmentation is absent in the skin of guppies with a lesion in *blue*, suggesting a defect in xanthophore development. In *golden* mutants, the development of the melanophore pattern during embryogenesis and after birth is affected. Here, we show that *blue* and *golden* correspond to guppy orthologs of *colony-stimulating factor 1 receptor a* (*csf1ra*; previously called *fms*) and *kita*. Most excitingly, we found that both genes are required for the development of the black ornaments of guppy males, which in the case of *csf1ra* might be mediated by xanthophore–melanophore interactions. Furthermore, we provide evidence that two temporally and genetically distinct melanophore populations contribute to the adult camouflage pattern expressed in both sexes: one early appearing and *kita*-dependent and the other late-developing and *kita*-independent. The identification of *csf1ra* and *kita* mutants provides the first molecular insights into pigment pattern formation in this important model species for ecological and evolutionary genetics.

THE guppy (*Poecilia reticulata*) is thought to be among the most color-polymorphic vertebrates (Endler 1983). Male guppies have an outstanding degree of variation in their ornamental patterns, which are shaped by a complex interplay between natural and sexual selection in wild populations. Along with introduction experiments, studies on guppy life-history traits, mate choice behavior, and predator–guppy as well as guppy–environment interactions have demonstrated that guppy populations can adapt rapidly to new environments (for an overview, see Magurran 2005).

The guppy is therefore a prime model organism for the study of “evolution in action.”

Despite our wealth of knowledge about the ecological importance of coloration, the genes and developmental pathways underlying guppy pigment pattern formation are unknown. Both forward and reverse genetic studies are hampered by the fact that guppies are livebearers with internal fertilization, an average gestation period of 3–4 weeks, and a relatively small brood size (Houde 1997). The genetic basis of sex determination is highly variable within the Poeciliid family, to which the guppy belongs. The guppy itself has incipient X and Y chromosomes that include a non-recombining part (Traut and Winking 2001). Only males develop highly polymorphic ornaments during puberty, which are under hormonal control (Houde 1997). The genetic analysis of male guppy ornaments first attracted attention >80 years ago, when Winge described a total of 18 putative ornamental loci, of which 17 showed sex-linked inheritance and 9 were strictly Y-linked (Winge 1922, 1927). Many more pigment pattern loci, which can be Y-linked, X-linked, XY-linked, or autosomal, have since been described (Lindholm and Breden 2002). Ornamental traits linked to the sex

Copyright © 2013 by the Genetics Society of America
doi: 10.1534/genetics.113.151738

Manuscript received March 27, 2013; accepted for publication April 27, 2013

Available freely online through the author-supported open access option.
Supporting information is available online at <http://www.genetics.org/lookup/suppl/doi:10.1534/genetics.113.151738/-/DC1>.

Data for File S1 and File S2 are available at ftp://ftp.tuebingen.mpg.de/ebio/csf1ra_kita_mutants

Sequence data from this article have been deposited under GenBank accession nos. KC143122 (*csf1ra*); KC143123 (*csf1ra blue* allele); KC143124 (*kita*); KC143125 (*kita*); and KC143126

(part of *kita* genomic locus in *golden* mutants).

¹Corresponding authors: Max Planck Institute for Developmental Biology, Department of Molecular Biology, Spemannstr. 35-39, 72076 Tübingen, Germany. E-mail: verena.kottler@tuebingen.mpg.de; E-mail: christine.dreyer@tuebingen.mpg.de

chromosomes are typically expressed only in males, but females can develop some male color patterns when treated with testosterone (Clemens *et al.* 1966; Lindholm and Breden 2002). An analysis of quantitative trait loci (QTL) has confirmed that most male color traits are controlled by multiple genes, including genes on autosomes (Tripathi *et al.* 2009b). In contrast to the sex-specific genes, several autosomal color factors behave as ordinary Mendelian recessive genes and are expressed in both sexes (Goodrich *et al.* 1944; Dzwillo 1959; Lindholm and Breden 2002).

The pigment pattern of the guppy consists of three to four different types of neural crest-derived chromatophores: black melanophores, yellow/orange to reddish xanthophores, blue iridescent iridophores, and, possibly, white leukophores (Takeuchi 1976; Tripathi *et al.* 2008). Guppy embryos are staged according to the differentiation of their eyes. In the middle-eyed stage, the retina is fully pigmented and the first melanophores differentiate on the head above the midbrain (Martyn *et al.* 2006). More melanophores appear during the late-eyed stage and form dark stripes along the lateral midline, on the back, and on the belly (Martyn *et al.* 2006). In the very late-eyed stage shortly before birth, a rhombic reticulate pattern consisting of melanophores emerges on the trunk (Martyn *et al.* 2006). It has also been referred to as a ground, diamond, or camouflage pattern (Goodrich *et al.* 1944; Martyn *et al.* 2006; Tripathi *et al.* 2008). All pigment cell types are present in wild-type embryos at birth and contribute to the newborn pattern (Figure 1A); *e.g.*, the yolk is partially covered by iridophores and melanophores, while xanthophores are widely dispersed (Martyn *et al.* 2006).

The reticulate pattern of very late-eyed embryos and newborn guppies appears to persist into adulthood (Tripathi *et al.* 2008). This pattern is expressed in both sexes, but becomes overlain in males by male-specific ornaments (Figure 1, B–E). Two different melanophore types occur in adult wild-type guppies: large, roundish corolla and more heterogeneously shaped dendritic melanophores (Goodrich *et al.* 1944). The reticulate pattern is composed of corolla melanophores in deep skin layers, which are additionally arranged irregularly over the whole body, whereas dendritic melanophores are distributed superficially and are associated with the scales (Figure 1E) (Goodrich *et al.* 1944; Winge and Ditlevsen 1947).

Two autosomal color loci that are expressed in male and female guppies are *blue* and *golden* [also known as *fredlini* (Haskins and Druzba 1938; Winge and Ditlevsen 1947) and not to be confused with the zebrafish (*Danio rerio*) *golden* locus (Lamason *et al.* 2005)]. The mutations in both genes occurred spontaneously and act recessively (Goodrich *et al.* 1944; Dzwillo 1959). *Blue* mutants lack orange pigmentation in their skin, indicating a xanthophore defect (Figure 1) (Dzwillo 1959).

In *golden* mutants, the development of the melanophore pattern during embryogenesis and after birth is affected (Haskins and Druzba 1938; Goodrich *et al.* 1944; Winge and Ditlevsen 1947). Golden guppies of both sexes lack

melanophores in the skin at birth and have only a few peritoneal melanophores above the swim bladder (Figure 1A), but eventually develop an incomplete reticulate pattern, which gives them a “coarsely mottled appearance” (Goodrich *et al.* 1944; Winge and Ditlevsen 1947). Corolla melanophores are restricted to the reticulate pattern in *golden* mutants, which also have only a very few dendritic melanophores (Figure 1E) (Haskins and Druzba 1938; Goodrich *et al.* 1944; Winge and Ditlevsen 1947). *golden* mutant females have only half of the normal number of melanophores in total (Goodrich *et al.* 1944). *golden* mutant males develop male-specific ornaments (Figure 1, B and C) (Haskins and Druzba 1938).

Among teleost fish, pigment pattern formation has been most extensively studied in zebrafish. Zebrafish undergo a complex pigment pattern metamorphosis during the transition from the embryonic/early larval to the juvenile/early adult stage (Johnson *et al.* 1995; Parichy and Turner 2003a,b; Kelsh *et al.* 2009; Parichy *et al.* 2009; Budi *et al.* 2011). The two type III receptor tyrosine kinases encoded by *kita* and its ancient paralog *colony-stimulating factor 1 receptor a* (*csf1ra*; previously called *fms*) (Braasch *et al.* 2006) play key roles during the establishment of the adult zebrafish pigment pattern: early metamorphic melanophores require *kita* for their development, while late metamorphic melanophores depend on *csf1ra* and *endothelin receptor b1a* (*ednrb1a*) (Parichy *et al.* 1999, 2000a,b; Parichy and Turner 2003b). *Csf1ra* is also crucial for xanthophore development (Parichy *et al.* 2000a; Parichy and Turner 2003b). In other teleost species, the functions of *kita* and *csf1ra* are less well understood; comparative studies including interspecies hybrids suggest some functional diversification of both receptor tyrosine kinases even within the *Danio* genus (Quigley *et al.* 2005; Parichy 2006; Mills *et al.* 2007).

Here, we present evidence that *golden* and *blue* correspond to guppy orthologs of *kita* and *csf1ra*. Both an early *kita*-dependent and a later-appearing *kita*-independent melanophore population contribute to the adult reticulate pattern in this species. In contrast to zebrafish, *csf1ra* is not required for the development of the late-appearing *kita*-independent melanophores. *Csf1ra*, however, is essential for xanthophore development and the formation of the male-specific melanophore pattern, which also requires *kita*.

Materials and Methods

Fish husbandry

All fish were maintained at 25° in a 12-hr light and dark cycle and fed 6 days a week with *Artemia*. No more than eight fish were kept per 1.5-liter tank. We used virgins for crosses, as guppy females are capable of storing sperm.

Strains

Guppies of the following inbred strains were used in this study; available phenotypes other than wild-type are shown in parentheses: Maculatus (MAC) (*golden*) (Tripathi *et al.*

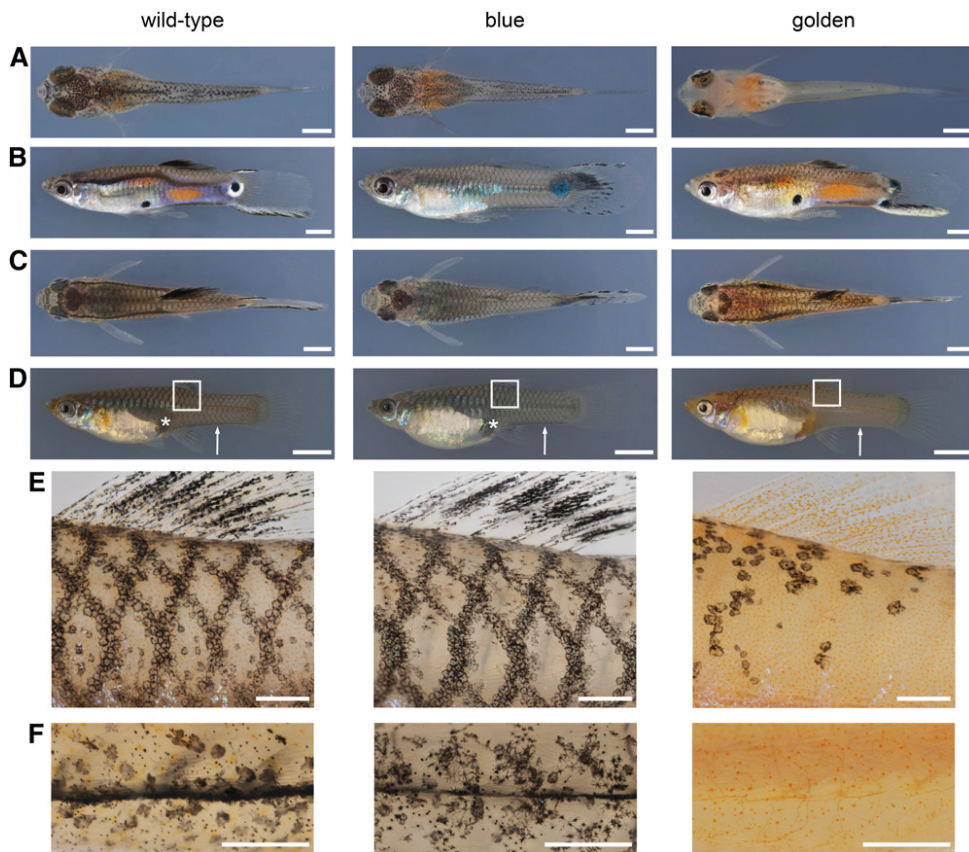


Figure 1 Blue and golden phenotypes. (A) Dorsal aspect of newborns. (B) Lateral aspect of adult males. (C) Dorsal aspect of adult males. (D) Lateral aspect of adult females. (E) Details of areas boxed in D showing the reticulate pattern. (F) Ventral view of the caudal peduncle of females (indicated by white arrows in D). *golden* mutants of both sexes lack a ventral black stripe and have only a few melanophores on the anterior head, including the choroid of the eyes. Golden females lack the female pigment spot above the anal fin (white asterisks in D). Individuals shown are from the BDZW1 (wild type, golden) and BDZW2 (blue) background. Bars: (A) 1 mm; (B and C) 2 mm; (D) 5 mm; (E and F) 0.5 mm.

2008); BDZW1 (golden, golden blue) and BDZW2 (blue only) (Dzwillo 1959); *Armatus* (golden) (Winge 1927); Guanapo and Quare6 (Reznick and Endler 1982); Quare6 family II 215-3 (Tripathi *et al.* 2008); and Cumaná (Alexander and Breden 2004). *Maculatus*, BDZW1, BDZW2, and *Armatus* are domesticated strains that have been bred in captivity for >50 years [in our laboratory since 2003 (*Maculatus*, BDZW1) and 2011 (*Armatus*, BDZW2)]; the others are derived from wild individuals caught in Trinidad (Guanapo and Quare rivers) and Venezuela (Cumaná region). Quare and Cumaná guppies were obtained in 2003 and Lower Guanapo (Twin Bridge) fish in 2009. All guppy strains are kept separately in small groups, usually consisting of two to three females and four to five males per tank and are allowed to reproduce freely, except for the Guanapo fish that are inbred by brother–sister mating.

blue was found in two strains that likely both were derived from the original population of *blue* mutants described by Dzwillo in 1959. We renamed them BDZW1 and BDZW2 for clarity. BDZW1 was obtained under the name “Blau” and comprised individuals heterozygous for *golden* and *blue*; BDZW2 (“Dzwillo 1959 Blau”) fish were all homozygous for *blue*.

Phylogenetic analyses

Only unambiguously annotated sequences were used for the analyses (ORF begins with a start codon; number of exons are as predicted for other species; and introns begin and end

with splice sites). Sequences were aligned with Clustal Omega (v1.1.0) (Goujon *et al.* 2010; Sievers *et al.* 2011). Maximum-parsimony and maximum-likelihood phylogenetic trees were constructed by the PhylipParsimony algorithm (Felsenstein 1989) via the SplitsTree4 (v4.12.8) interface (Huson and Bryant 2006) and by PhyML (Guindon *et al.* 2010), respectively. The topologies of the maximum-likelihood trees were not fully resolved (therefore not shown), but, as the maximum-parsimony trees, they suggest that the sequenced guppy ORFs are most similar to *kita*, *kit ligand a* (*kitla*), and *csf1ra* of other teleost species.

Complementary DNA analyses

We used polymerase chain reaction (PCR) to amplify genes of interest from first-strand complementary DNA (cDNA). Total RNA was extracted from 10 to 15 pooled early to very-late eyed embryos with TRIzol (Invitrogen) according to the manufacturer’s instructions. Total RNA was then directly used for first-strand cDNA synthesis using PrimeScript Reverse Transcriptase (TaKaRa) and the oligo(dT) primer 5’-ATTCTAGAGGCCGAGGCGGCCGACATGT(18)VN-3’. We added 1 U/μl SUPERaseIn RNase Inhibitor (Ambion) to each reaction. First-strand cDNA was used as template for PCR, which was carried out with Advantage 2 Polymerase Mix (Clontech) according to the manufacturer’s instructions. PCR program was 10 cycles touchdown [95° for 15 sec, T_m (melting temperature) of primers (lower one) + 5° –0.5°/cycle for 30 sec, 68° for 2–5 min] followed by 27 cycles

without touchdown (95° for 15 sec, Tm for 30 sec, 68° for 2–5 min]. Elongation time was adapted to the length of the expected product (~1 min/kb). Primer sequences and methods used for full-ORF amplification of candidate genes are listed in Supporting Information, Table S1. PCR products were analyzed by gel electrophoresis, purified with MinElute Gel Extraction Kit (QIAGEN), and subsequently cloned into pGEM-T Easy vector (Promega) following the manufacturer's instructions. Plasmid DNA was purified with Wizard Plus SV Minipreps DNA Purification System (Promega) according to the instruction manual and sequenced.

To investigate whether the *kita* transcripts V1–V6 cosegregate with the golden phenotype, we prepared first-strand cDNA from adult individuals as described before. Total RNA for cDNA synthesis was extracted separately from liver tissue of the parental male and the parental female and from pooled liver tissue of seven wild-type N2 fish and 11 golden N2 fish. Liver tissue was used as total RNA isolated from liver usually is of very high quality (personal observation). We used primers in exon 5 (forward: 5'-GATGCTGGGAGT TACAAATGCGTAG-3') and exon 9 (reverse: 5'-AAACAGT ATGTAGGCTTGCTCTCC-3') for PCR amplification with Advantage 2 Polymerase Mix (Clontech) and cloned the products into pGEM-T Easy vector (Promega). We sequenced the purified plasmid DNA of 24 colonies per parent and N2 pool to identify wild-type and *golden* mutant *kita* transcripts.

Real-time quantitative PCR

Total RNA for real-time quantitative PCR was prepared as described above from skin of adult wild-type, golden, and blue females that were 6–9 months old. Following DNaseI treatment, first-strand cDNA was prepared from 830 ng of total RNA primed with oligo(dT)₁₈ using the RevertAid First Strand cDNA Synthesis Kit (Thermo Scientific) according to the manufacturer's instructions. First-strand cDNA was diluted 10-fold for real-time quantitative PCR that was conducted with Platinum SYBR Green qPCR SuperMix-UDG (Invitrogen) on a CFX384 Touch Real-Time PCR Detection System (Bio-Rad) according to the instruction manuals provided by the manufacturers. PCR program was 95° for 3 min, 40 times (95° for 10 sec, 60° for 10 sec, 72° for 5 sec), and 95° for 10 sec. Expression of *csf1ra*, *csf1rb*, *kita*, and *kitb* was determined by using three biological replicates with three technical repetitions each. Expression of the target genes was normalized to *glyceraldehyde-3-phosphate dehydrogenase* expression. Standard deviation and normalized expressions ($\Delta\Delta C_q$) were calculated with CFX Manager software. Primer sequences and efficiencies (Pfaffl 2001; Vandesompele *et al.* 2002) are given in Table S2.

Genomic DNA analyses

Genomic DNA was prepared with DNeasy Blood and Tissue Kit (Qiagen) from trunk tissue of adult guppies. We used 100 ng of DNA per PCR reaction. If not mentioned otherwise, Advantage 2 Polymerase Mix (Clontech) was used to carry out the PCRs. *Kita*^{insert} was first amplified using

a forward primer in exon 6 (5'-TGTCTCTGAACGTTAG CATGGAG-3') and a reverse primer in exon 7 (5'-ACACG GAGAAGTTCTGCTTTACC-3') of *kita* (elongation time: 5 min). To test whether *kita*^{insert} and the golden phenotype are associated, we designed PCR assays for *kita*^{insert} and *kita*^{wt} using Phusion High-Fidelity DNA Polymerase (New England Biolabs) according to the manufacturer's instructions. Details can be found in Table S3. PCR products were analyzed by gel electrophoresis. PCR products of *csf1ra*^{wt} and *csf1ra*^{indel} were purified with 0.2 U/ μ l FastAP Thermosensitive Alkaline Phosphatase (Fermentas) and 2 U/ μ l exonuclease I (Fermentas) (37° for 15 min, 85° for 15 min) and subsequently sequenced. Primer sequences are given in Table S3.

Sequence analysis

Purified plasmid DNA and PCR products were sequenced with BigDye Terminator v3.1 Cycle Sequencing Kit (Applied Biosystems) on a DNA Analyzer ABI Prism 3730XL (Applied Biosystems). Sequences were analyzed using the Staden package (Pregap4 v1.5 and Gap4 v4.10; <http://staden.sourceforge.net/>) and inspected manually. Exon–intron structures were predicted according to the gene structure of *kitla*, *kita*, and *csf1ra* of other teleost species (for species, see Table S1; exon–intron structure was inferred from <http://www.ensembl.org>).

Imaging

Photos of whole embryos or details of adult fish were taken with a Leica MZFLIII dissecting microscope connected to a Zeiss AxioCam HRc color camera and processed with AxioVision Software Release 4.7.2. Photos of fish after birth and adult fish were taken with a Canon EOS 10D digital camera using a Canon Macro Photo Lens MP-E 65 mm or Canon Macro Lens EF 100 mm. Adult males were at least 4 months old to ensure that their pigment pattern was fully developed. All photos were taken under incident light conditions. Fish were anesthetized in 0.1% (w/v) tricaine (ethyl 3-aminobenzoate methanesulfonate salt) solution (pH 7) before imaging. The background of most images was equalized with Adobe Photoshop software version 12.1; all original images are available upon request.

Analysis of melanophores

To analyze melanophore pattern development, photos of the same fish were taken every 3 days (day 1–40 after birth). Each fish was kept separately in a 1.5-liter tank. Fish were briefly anesthetized in 0.04% tricaine solution before imaging. Their siblings were kept as control; none of the imaged fish showed retarded development. Newly arising melanophores were detected by comparing consecutive images to each other.

To analyze the number of melanophores, fish were immersed in standard E2 solution (Nusslein-Volhard and Dahm 2002) containing 2.4 mg/ml epinephrine for ~5 min to contract melanosomes. Afterward, fish were anesthetized, and the right side under the dorsal fin, as well as the complete

fish, were imaged. Melanophores were counted manually utilizing Adobe Photoshop software version 12.1. The number of melanophores was plotted against the area in square millimeters using Microsoft Excel for Mac 2011 version 14.2.3.

Results

Identification of golden as kita:

We used a candidate gene approach to identify *golden* at the molecular level. Based on a comparison with zebrafish pigment pattern mutants, we investigated two potential candidates for *golden*, *kita*, and *kitla* (also called *stem cell/steel factor*). *Kitla* is the ligand for the *Kita* receptor, and together the two are required for melanophore migration and survival in zebrafish (Hultman *et al.* 2007). While only one copy of *kit* and *kitl* exists in mouse and humans, two copies of each gene are present within the Teleostei. These copies can be considered as “ohnologs” since they are derived from ancestral *kit* and *kitl* genes that were duplicated during the teleost-specific whole-genome duplication event (Mellgren and Johnson 2005; Braasch *et al.* 2006; Hultman *et al.* 2007). Mutations in zebrafish *kita*, as in *golden*, greatly reduce melanophore number (Parichy *et al.* 1999). *Kita* is located on guppy autosomal linkage group 4 (Tripathi *et al.* 2008). *Kitla* has not been mapped so far.

To amplify the guppy orthologs of *kita* and *kitla*, we used rapid amplification of cDNA ends (Table S1). Phylogenetic analyses demonstrated that the obtained full-ORF sequences are orthologous to *kita* (GenBank accession no. KC143124) and *kitla* (GenBank accession no. KC143125) of other teleost species (Figure 2A and Figure S1). We also identified a potential guppy *kitb* ortholog by performing BLAST searches of zebrafish *kitb* against a preliminary genome and transcriptome assembly of the guppy (E. Sharma, A. Künstner, B. A. Fraser, M. Hoffmann, V. A. Kottler, G. Zipprich, D. Weigel, and C. Dreyer, unpublished data) (Figure 2A) (Altschul *et al.* 1990). We could not determine whether a guppy *kitlb* ortholog exists, as BLAST yielded no significant results.

Golden mutant guppies did not have any obvious polymorphisms in the *kitla* ORF. In contrast, among cDNAs from *golden* fish of the MAC and BDZW1 backgrounds, we found a total of six different *kita* splice variants, none of which was wild type. Most of these variants contained inserts with a length of 17, 36, or 53 bp and/or lacked parts of or the complete exon 6 (Figure 2B and Table S4). Exons 7 and 8 were additionally absent in two variants (Figure 2B and Table S4). In all cases, these alterations cause frameshifts and truncate the ORF. These *kita* variants are likely non-functional since the encoded proteins would lack the transmembrane, juxtamembrane, and split kinase domains, all of which are required for normal protein function (Mol *et al.* 2003).

Analysis of genomic DNA indicated that *kita* exon 6 of *golden* mutants has an insertion of 1678 bp. This insertion consists of two potential short exons of 17- and 36-bp length that surround a 1625-bp intron delineated by 5' GT-AG 3'

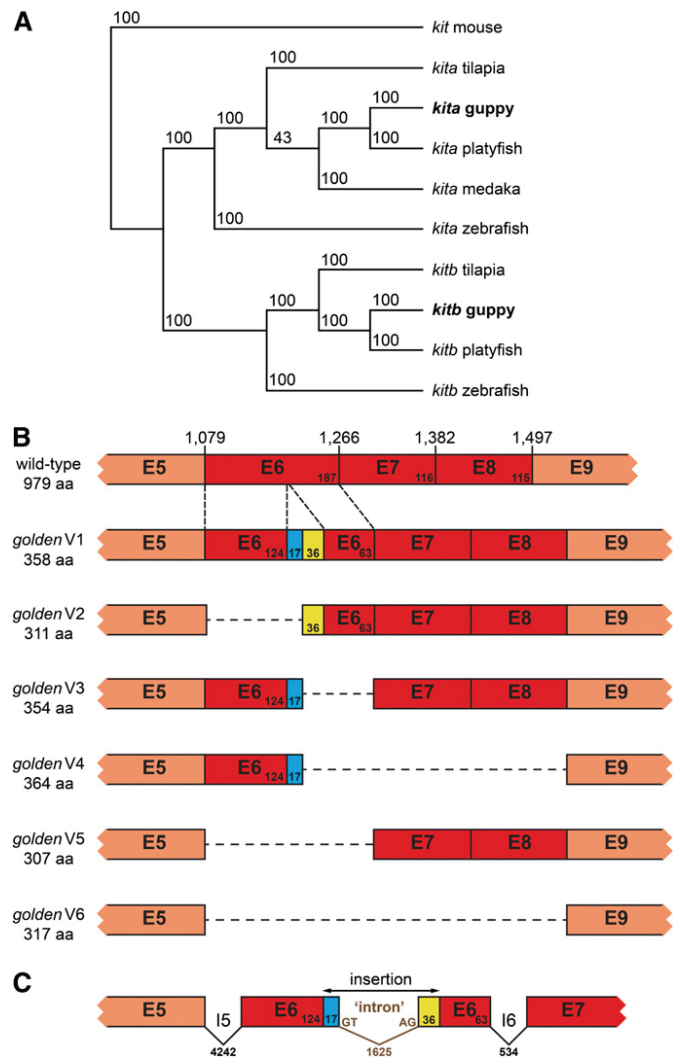


Figure 2 *golden* is an ortholog of *kita*. (A) Maximum-parsimony phylogenetic tree of *kita* and *kitb* ORF sequences. Mouse *kit* was used as an outgroup. Bootstrap support values from 100 replicates are shown. Accession numbers of sequences are the following: guppy *kita*, KC143124; medaka (*Oryzias latipes*) *kita*, ENSORLT0000000707; mouse (*Mus musculus*) *kit*, NM_021099; platyfish (*Xiphophorus maculatus*) *kita*, ENSXMAT00000013579; platyfish *kitb*, ENSXMAT00000017731; tilapia (*Oreochromis niloticus*) *kita*, ENSONIT00000003735; tilapia *kitb*, XM_003452144; zebrafish *kita*, NM_131053; and zebrafish *kitb*, NM_001143918. Guppy *kitb* sequence is available upon request. (B) Exons 5–9 of *kita* cDNAs sequenced from wild-type and *golden* mutant [variants (V) 1–6] backgrounds; exons affected by splicing defects are shown in dark red. Length in amino acids (aa) of the respective predicted protein is shown on the left. Numbers above wild type refer to the wild-type *kita* cDNA sequence deposited at GenBank (KC143124) and demarcate the last nucleotide of each exon. (C) Part of *kita* genomic locus in *golden* mutants (*kita^{insert}*) (GenBank accession no. KC143126). Numbers refer to base pairs. Exons (E), introns (I), and inserted sequence are not drawn to scale.

canonical splice sites (Figure 2C). The splice sites within the novel intron seem to be recognized by the spliceosome and lead to mis-splicing of the *kita* pre-messenger RNAs (mRNAs) in the *golden* mutants. Depending on which splice sites are used, this leads to short insertions or removal of parts of exon

6 or of exons 6–8 from the mature transcript. Comparison with a preliminary genome assembly of the guppy (A. Künstner, E. Sharma, B. A. Fraser, M. Hoffmann, V. A. Kottler, D. Weigel, and C. Dreyer, unpublished data) suggests that >50 copies similar to the 1678-bp insertion, which all include a long terminal repeat of ~300 bp, exist (data not shown).

To confirm that *kita*^{insert} corresponds to *golden*, we tested for genetic linkage. Forty *golden* mutant fish from the MAC, BDZW1, and Armatus (ARM) backgrounds were homozygous for *kita*^{insert} and complementation test crosses between the strains demonstrated allelism (Figure S2B and S1C). In 28 wild-type MAC, BDZW1, and ARM individuals, only *kita*^{wt} could be detected. This indicates that *kita*^{insert} was likely introduced into several guppy strains by breeders because of the golden coloration. Next, we investigated whether *kita*^{insert} is also linked to the golden phenotype in a segregating backcross N2 population: we crossed a *golden blue* double-mutant female of the BDZW1 strain to a wild-type male from the Guanapo river in Trinidad; F₁ males were then backcrossed to produce X^{BDZW1}X^{BDZW1}/X^{BDZW1}Y^{GU} N2 individuals. Forty-six golden and golden blue N2 fish were homozygous for *kita*^{insert}, while 12 wild-type and blue fish were heterozygous *kita*^{insert}/*kita*^{wt}. In addition, we could amplify only *kita*^{insert} variants from pooled cDNA of *golden* mutant N2 offspring. Taken together, all of these results make it very likely that guppy *golden* is allelic to *kita*.

Identification of blue as *csf1ra*:

We hypothesized *csf1ra* to be a candidate for *blue*, since *blue* mutants lack xanthophores as do *csf1ra* mutants of zebrafish (Dzwillo 1959; Parichy *et al.* 2000a). *Csf1ra* and *csf1rb* ohnologs have been identified in several teleost species (Braasch *et al.* 2006). *csf1ra* has previously been mapped to guppy autosomal linkage group 10 (Tripathi *et al.* 2008).

Rapid amplification of cDNA ends was used to amplify the guppy *csf1ra* ortholog (Table S1). Phylogenetic analyses showed that the sequenced cDNA is closely related to *csf1ra* of other teleost species (Figure 3A). We also identified a presumptive guppy *csf1rb* ortholog within a preliminary genome and transcriptome assembly of the guppy (E. Sharma, A. Künstner, B. A. Fraser, M. Hoffmann, V. A. Kottler, G. Zipprich, D. Weigel, and C. Dreyer, unpublished data) (Figure 3A).

Blue mutant guppies carry a complex change in exon 17 of *csf1ra*, with a deletion of 5 bp and an insertion of 7 bp (Figure 3B). This indel causes a frameshift and truncates the ORF. The predicted protein lacks part of the second half of the split kinase domain, which is required for the activity of type III receptor tyrosine kinases (Yarden and Ullrich 1988; Mol *et al.* 2003). A similar mutation in zebrafish, *fms*^{j4blue}, inactivates *csf1ra* and leads to loss of xanthophores (Parichy *et al.* 2000a).

We used the same cross as above to test for linkage of *csf1ra* and *blue*. Forty-six blue and golden blue N2 fish were homozygous for *csf1ra*^{indel}, while 12 wild-type and golden N2 individuals tested were heterozygous *csf1ra*^{indel}/*csf1ra*^{wt}. Consistent with this, 24 *golden blue* mutant guppies of the

BDZW1 strain were homozygous for *csf1ra*^{indel}, whereas only *csf1ra*^{wt} could be identified in 12 wild-type and golden fish of the same population. Another *blue* strain obtained from a hobby breeder, BDZW2, was also homozygous for the *csf1ra*^{indel} allele, and complementation test crosses to BDZW1 confirmed allelism (Figure S2A). *blue* is therefore likely to be the guppy ortholog of *csf1ra*, with the same *csf1ra*^{indel} mutation present in both strains tested.

In zebrafish, *csf1ra* promotes the migration of the xanthophore precursors from the neural crest (Parichy *et al.* 2000a), and both embryonic and metamorphic xanthophore populations require *csf1ra* activity (Parichy and Turner 2003b). To investigate whether *csf1ra* mutant guppies entirely lack xanthophores, we thoroughly inspected 7-month-old golden blue and blue fish that shared the same grandparents. In contrast to a previous study (Dzwillo 1959), we found a small number of xanthophores in 19 of 20 *golden blue* mutant individuals and in 5 of 17 *blue* mutants (Figure 3, C and C'). Most of the xanthophores were arranged on scale margins close to the dorsal fin. We could not detect any xanthophores on the lateral or ventral side of adult golden blue or blue fish or in blue embryos and newborns (we here refer to guppies as newborns 1–3 days after birth). A small number of xanthophores can also be found in zebrafish larvae, but not in adults, which are homozygous for *salz*^{tl41a} or *pfeffer*^{tm36b}, two alleles that fail to complement *fms*^{j4blue} (Maderspacher and Nusslein-Volhard 2003).

Expression of *kita*, *csf1ra*, and their ohnologs in female skin

We could detect *kita*, *kitb*, *csf1ra*, and *csf1rb* expression in the skin of adult wild-type, golden, and blue females by Reverse Transcriptase-PCR (data not shown). To assess whether *Kitb* and *Csf1rb* might be upregulated to compensate for the loss of *Kita* and *Csf1ra* function in the *golden* and *blue* mutants, respectively, we investigated the expression levels of these genes and their a-paralogons by real-time quantitative PCR. We found that *csf1ra* expression is downregulated in the skin of *blue* mutant females compared with the wild type, while there was no significant difference in the expression levels of *csf1rb* (Figure S3). In zebrafish, *csf1ra* is expressed in the xanthophore, macrophage, and osteoclast lineages (Parichy *et al.* 2000a). Our data suggest that the guppy ortholog of *csf1ra* is expressed in guppy xanthophores, as the almost complete absence of these cells in blue skin coincides with a low *csf1ra* expression level. Additionally, the blue transcript of *csf1ra* might undergo nonsense-mediated mRNA decay triggered by the premature termination stop codon. In contrast, the expression levels of *kita* and *kitb* were not significantly different in golden skin compared with wild type, respectively (Figure S3), which suggests that the golden *kita* transcripts are not subjected to nonsense-mediated decay. In conclusion, no significantly elevated expression of the *kit* and *csf1r* b-paralogons could be detected by real-time quantitative PCR in the skin of *golden* and *blue* mutants (Figure S3). Yet we cannot

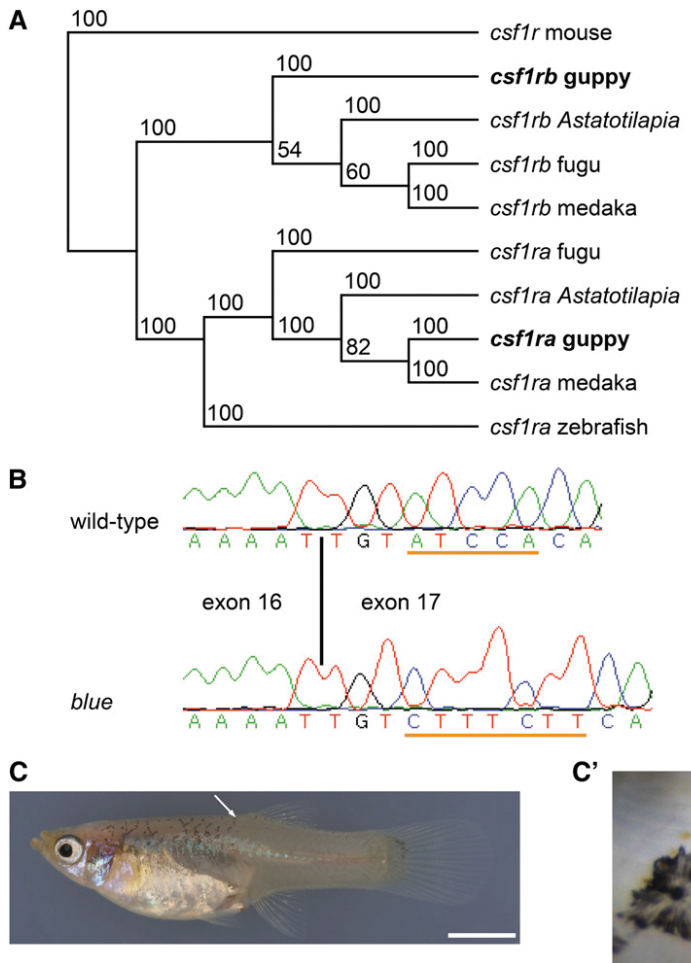


Figure 3 *blue* is an ortholog of *csf1ra*. (A) Maximum-parsimony phylogenetic tree of *csf1ra* and *csf1rb* ORF sequences. Mouse *csf1r* was used as an outgroup. Bootstrap support values from 100 replicates are shown. Accession numbers of sequences are the following: *Astatotilapia burtoni csf1ra*, DQ386648; *A. burtoni csf1rb*, DQ386647; fugu (*Takifugu rubripes*) *csf1ra*, U63926; fugu *csf1rb*, AF411927; guppy *csf1ra*, KC143122; medaka *csf1ra*, ENSORLT00000006111; medaka *csf1rb*, XM_004076731; mouse *csf1r*, NM_001037859; and zebrafish *csf1ra*, AF240639. Guppy *csf1rb* sequence is available upon request. (B) Partial sequence electropherograms of cDNAs from wild-type and *blue* mutant fish, which carry a deletion of 5 nt in exon 17 (underlined in wild-type sequence) that simultaneously contains a 7-nt insertion (underlined in *blue* sequence). The length of the predicted protein produced by *blue* mutants is 794 aa, with the last 12 new. The wild-type protein is 978 aa long. The first nucleotide of exon 17 corresponds to nucleotide 2392 in the 3084-bp wild-type *csf1ra* sequence (GenBank accession numbers of cDNAs: wild-type, KC143122; *blue*, KC143123). (C) *golden blue* mutant female; white arrow points to detail shown in C'. (C') Small patch of xanthophores (X) and melanophore (M) on the back close to the dorsal fin of the female. Variation in the number of xanthophores was high in *blue* and *golden blue* mutant fish. Xanthophores were abundant and evenly distributed in wild-type and *golden* mutant females (Figure 1, E and F). Bars: (C) 5 mm; (C') 50 μ m.

exclude that less efficient salvage pathways mediated by *Kitb* and *Csf1rb* compensate for the loss of *Kita* and *Csf1ra* function in the mutants based on these findings.

Contribution of distinct melanophore populations to the adult reticulate pattern

Kita-dependent and -independent metamorphic melanophores contribute to the adult pigment pattern in zebrafish (Parichy *et al.* 1999; Parichy and Turner 2003b). Additionally, *Kita* activity is required for the dispersal of melanoblasts from the neural crest in zebrafish embryos (Parichy *et al.* 1999). To investigate whether temporally and genetically distinct melanophore populations exist in the guppy, we examined *golden* mutant guppies at different developmental stages.

First, we explanted wild-type and *golden* embryos 12 days after last parturition, which corresponds to the middle-eyed stage, at which the first melanophores differentiate in the skin above the midbrain in wild-type embryos (Martyn *et al.* 2006). *golden* mutant embryos lacked melanophores on the head and the trunk at this stage (Figure 4A). Second, we investigated the development of the pigment pattern between the 1st and the 40th day after birth by taking photographs of the same individuals every 3 days.

Immediately after birth, *golden* mutants had few patches of peritoneal melanophores, as described previously (Goodrich

et al. 1944; Winge and Ditlevsen 1947). Additionally, we found some melanophores in their skin and close to the neural tube (Figure 4B). Four and 7 days after birth, few scattered melanophores were present close to the dorsal midline and on the head of *golden* mutants (Figure 4C and File S1). After 10 days, melanophores had become more abundant on the dorsal part of *golden* mutant fish and formed an incipient reticulate pattern, which became quite prominent after 16 days (Figure 4, D and E). The formation of the reticulate pattern seemed to be completed \sim 22 days after birth in the mutants (Figure 4, F and G), although we detected a few newly arising melanophores even in 40-day-old *golden* individuals (File S1). This suggests that two melanophore populations that are temporally and genetically distinct contribute to the adult reticulate pattern: one that develops early and depends on *Kita* and one that appears late and is independent of *Kita*. In wild-type fish, melanophores were abundant and distributed over the whole body from the day of birth onward (Figure 4, B–G).

Adult *golden* mutant females have about half the number of skin melanophores of wild-type females (Goodrich *et al.* 1944) and lack the pigment spot by the anal fin (Figure 1, D and E). Additionally, the amount of superficial dendritic melanophores associated with the scales is strongly reduced (Haskins and Druzba 1938; Goodrich *et al.* 1944; Winge and

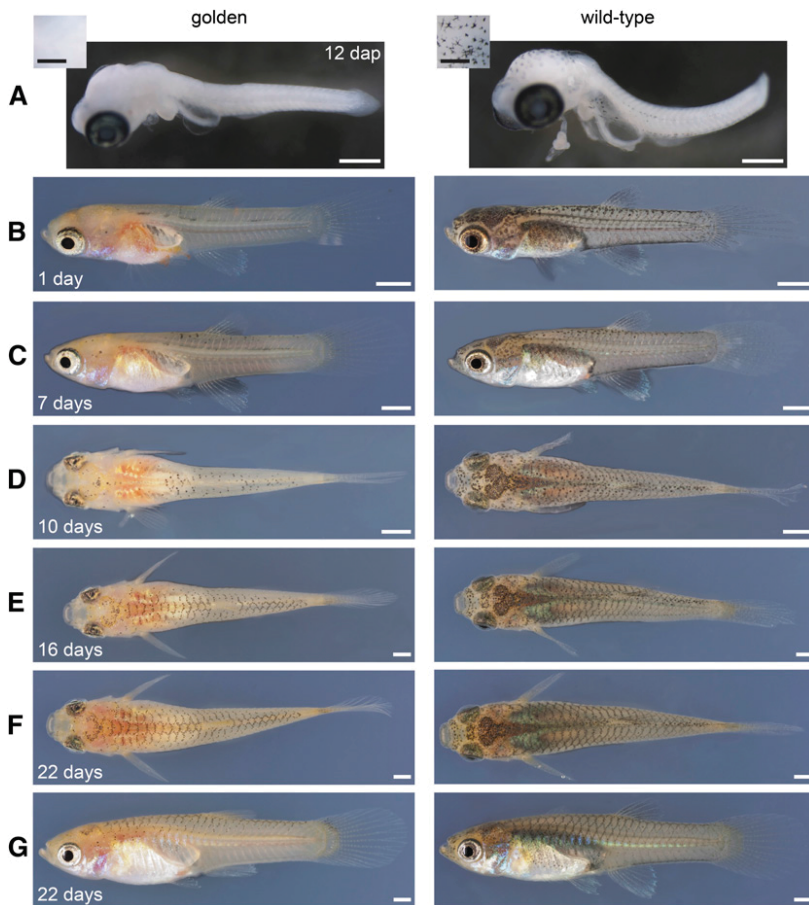


Figure 4 Melanophore pattern development in BDZW1 wild-type and *golden* mutant fish. (A) Embryos explanted 12 days after last parturition (dap). Yolk sacs were removed and embryos were fixed overnight at 5° in 4% paraformaldehyde and 1% dimethyl sulfoxide. Insets: Dorsal aspect of the midbrain region with individual melanophores apparent in wild type. (B, C, and G) Lateral, (D–F) dorsal aspects of the same females over a 3-week time course (days are after birth). All images taken, including the ones of males, can be found in File S1. Bars: (A) 500 μm , (insets) 250 μm ; (B–G) 1 mm.

Ditlevsen 1947), and black pigment is scarce on the choroid of the eyes as well as on the anterior head in golden fish, indicating that these pigmentation traits depend on *Kita* (Figure 1, B–E). The arrangement of the melanophores along the scales seems to be independent of *Kita*, as the size of the reticulate pattern (diameter of rhombi) was similar in golden and wild-type fish (data not shown). Onset of puberty in golden and wild-type males was observed between day 19 and 28 (File S1); the development of the reticulate pattern in golden males was similar to that of golden females (File S1).

***csf1ra*-independent melanophore populations**

In zebrafish, early *kita*-dependent metamorphic melanophores are independent of *Csf1ra*, whereas late-differentiating *kita*-independent melanophores require *Csf1ra* and *Ednrb1a* activity for their differentiation (Parichy *et al.* 2000a,b; Parichy and Turner 2003b). *kita csf1ra* double-mutant zebrafish lack almost all melanophores because of the strong additive effect of mutations in these two genes (Parichy *et al.* 2000a). Since we identified a *kita*-dependent and -independent melanophore population in the guppy, we asked whether any of them requires *csf1ra*.

Inspection of embryos and newborns revealed no major differences between the *blue* mutant and wild-type melanophore patterns (Figure S4A), although we cannot exclude that a small subset of the early appearing melanophores

depends on *Csf1ra* signaling since we could not count these early cells (see Figure S4 legend). To investigate whether the late-differentiating melanophores depend on *csf1ra*, we compared an area below the dorsal fin in golden and golden blue adult females (Figure S4, E and E'). We found that both single- and double-mutant fish have similar numbers of melanophores per area (Figure S4F). Therefore, unlike in zebrafish, mutations in *kita* and *csf1ra* have no additive effect on the reticulate pattern of the guppy, which is further supported by the observation that the reticulate pattern of *blue* mutant guppies develops as in the wild type until at least day 40 after birth (Figure S4, A–D; File S1). Consequently, the late-appearing melanophores of the guppy reticulate pattern are independent of both *Kita* and *Csf1ra* signaling.

Requirement of *Kita* and *Csf1ra* signaling for male-specific ornaments

Guppy male-specific pigmentation patterns vary tremendously within and among populations, yet the within-population variance decreases considerably with inbreeding (personal observation). To investigate the roles of *Kita* and *Csf1ra* in male color pattern formation, we compared the ornamental patterns of related wild-type and mutant males. We crossed *golden blue* mutant BDZW1 females with wild-type males from the inbred wild-derived Cumaná (CUM), Guanapo (GU), Quare6 family II 215-3 (QUII), and Quare6

(QU) strains. The phenotypically wild-type F₁ males were backcrossed to *golden blue* mutant BDZW1 females to produce a N2 generation (Figure 5). As a result of the backcross, the grandfather's Y chromosome was combined with an X chromosome of the BDZW1 strain in all N2 males. Since recombination frequency of sex chromosomes is comparatively low in male meiosis (Tripathi *et al.* 2009a), this experimental design minimized the amount of pattern variation caused by X chromosomes derived from different strains, thereby allowing us to study the influence of the mutant autosomal genes on the pattern directed by a given Y chromosome. The number of male offspring derived from each cross is given in Table 1, and all images of the backcrosses can be found in File S2.

For our analysis, we focused on the most prevalent characteristic traits of each cross, as seen on the grandfather and its wild-type male offspring (Figure 6, Figure 7, Figure 8 and Figure 9; Figure S5). Furthermore, we tried to homologize the male ornaments of the different strains based on their color, shape, and approximate positions. A summary of all traits and generalization of our results is shown in Figure 9, which should facilitate tracking of single traits within the complex male patterns. We are, however, aware of the fact that superficially similar-looking traits need neither be directed by the same developmental pathways nor be derived from the same putative cell precursor pool.

Regardless of the origin of the Y chromosome, *blue* mutant N2 males lacked all orange color traits, indicating that *Csf1ra* activity is also required for the dispersal or differentiation of male-specific xanthophores (Figure 6, Figure 7, and Figure 9). In addition, the location and shape of the black male-specific ornaments were modified in the mutants.

Previous studies of the male-specific color pattern of the Cumaná guppy have shown that the blue iridescent spot on the trunk close to the dorsal fin, the combination of black and orange on the dorsal fin, and the ventral black lining of the caudal peduncle constitute strictly Y-linked traits (Figure 6A and Figure 9) (Tripathi *et al.* 2008, 2009a,b). The male-specific ventral black lining is more pronounced than the ventral black stripe of both sexes described in Figure 1F. Typically, two thicker black horizontal stripes, an anterior and a posterior one, are present on the trunk of Cumaná males (Figure 6A and Figure 9). The orange-black lining of the tail fin, which is often more pronounced on the ventral margin, is another male-specific Cumaná trait (Figure 6A and Figure 9). The prominent ventral black spot on the tail fin of many Cumaná males (Figure 6A and Figure 9; Figure S5) is very likely directed by one or more dominant factors located in the pseudo-autosomal region of the Cumaná sex chromosomes (Tripathi *et al.* 2008).

Most Cumaná male-specific traits were fully developed in the grandfather, in all F₁, and in all wild-type N2 males (Figure 6, A–C; for the ventral black spot on the tail fin, see Figure S5). Of the *golden* mutant N2 males, all but one showed all of these traits as well (Figure 6D and Figure 9; the pattern of the one exceptional individual might be the

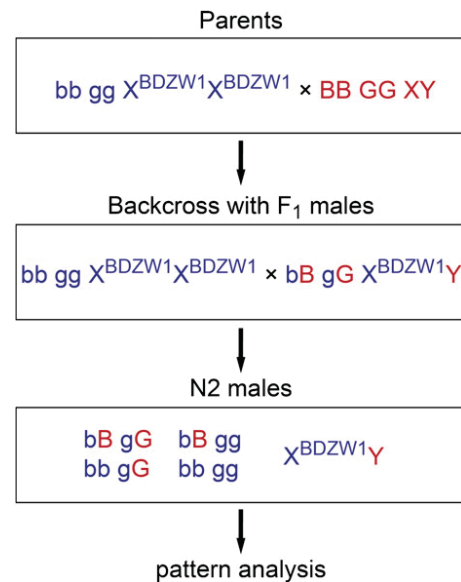


Figure 5 Crossing scheme that was used in the case of the CUM, GU, QUIL, and QU strains. The color patterns of the wild-type, golden, blue, and golden blue N2 males were analyzed. *blue* (b) and *golden* (g) are located on different autosomes and can therefore recombine freely. “B” and “G” indicate wild-type alleles. BDZW1 and MAC males were crossed with females of the same strain (for details see Figure 8).

outcome of a rare recombination event). Comparisons between wild-type and golden males revealed that (i) *golden* mutants had less black on the dorsal fin; (ii) the ventral black lining of the caudal peduncle was shifted upward and was often discontinuous in golden fish; (iii) the posterior black stripe of *golden* mutants was shifted downward and was often discontinuous (Figure 6D and Figure 9). In addition, a concise posterior orange spot on the caudal peduncle was absent in 94% of the *golden* mutants (Figure 6D). The anterior black stripe, the anterior orange spot, the blue iridescent spot, the orange-black lining, and the ventral black spot on the tail fin were not obviously changed by the mutation in *kita* (Figure 6D and Figure 9). The *blue* mutant N2 males not only lacked all orange traits, but also lost the black components of the orange-black lining of the tail fin, whereas the ventral black spot persisted (Figure 6E and Figure 9). Other defects of the *blue* mutant fish were the following: (i) the anterior black stripe was absent or very diffuse; (ii) the posterior black stripe was shifted downward and seemed more diffuse, and small incoherent patches of melanophores were often found on the dorsal trunk; (iii) in only 43% of the blue males a comparatively small blue iridescent spot was visible close to the dorsal fin (Figure 6E and Figure 9). The phenotype of the *golden blue* mutant N2 males resembled the *blue* mutant fish, but they showed fewer melanophores on the dorsal fin and trunk (Figure 6F).

The pattern of the Guanapo grandfather was characterized by several black crescents forming a labyrinthine pattern in proximity to the gonopodium (Figure 6G and Figure 9). The melanophores on the proximal and distal parts of the tail fin were concentrated on the ventral half of the fin, and an

Table 1 Male offspring obtained from each cross

Male parent	F ₁	N ₂			
		Wild type	Golden	Blue	Golden blue
Cumaná (CUM)	55	39	33 ^a	52	53
Guanapo (GU)	30	24	25	18	21
Quare6 family II 215-3 (QUII)	34	16	16	11	10
Quare6 (QU)	43	17	18	25	14
			F ₂		
		Wild type		Golden	
BDZW1	24	56		18	
Maculatus (MAC)	12	30		13	

^a Actual number was 34, but one male had a BDZW1 instead of a CUM-like color pattern (see text).

orange spot was located close by (Figure 6G and Figure 9). The anterior and posterior black horizontal stripes, the ventral black lining of the caudal peduncle, and the anterior and posterior orange spots on the trunk appeared weaker compared with the Cumaná male (Figure 6G). The posterior black stripe approximately demarcated the lateral midline in the Guanapo grandfather.

All of the F₁ and wild-type N₂ males showed the Guanapo traits described above, but only 41% of the wild-type males had an anterior orange spot (Figure 6, H and I). Furthermore, the F₁ and wild-type N₂ males tended to have more complex black labyrinthine ornaments close to the gonopodium than the Guanapo grandfather, suggesting that cofactors derived from the autosomes or X chromosome of the BDZW1 strain modulate this trait (Figure 6, H and I). The black pigment pattern of the *golden* mutant N₂ males was substantially changed in the following ways: (i) black pigment in the dorsal fin was reduced; (ii) the labyrinthine black ornaments close to the gonopodium were mostly lost; (iii) black pigment in the proximal part of the tail fin was concentrated dorsally; (iv) anterior and posterior black stripes were often discontinuous; and (v) the ventral black lining was shifted upward (Figure 6J and Figure 9). The orange ornaments persisted, and an anterior orange spot was found in 32% of the golden N₂ males (Figure 6J and Figure 9). The *blue* mutant N₂ males had an even more severe phenotype: (i) only one to two round black spots were present on the trunk that were in most individuals not located near the gonopodium; (ii) as in golden N₂, the black in the proximal part of the tail fin was located dorsally, and several males had black tail-fin margins; and (iii) the anterior black stripe was absent or diffuse (Figure 6K and Figure 9). The *golden blue* mutant N₂ males had fewer melanophores on the fins and trunk than the *blue* mutants (Figure 6L).

The pigmentation traits of the Quare6 family II 215-3 grandfather are shown in Figure 7A. Compared with the Cumaná grandfather, the black pigment on the dorsal fin and the ventral black lining of the caudal peduncle of the Quare6 family II 215-3 grandfather appeared weak. It had a black spot associated with its anterior black horizontal stripe, which we found in 83% of its wild-type and in 56% of its golden N₂ male offspring (Figure 7, A–D). We found

that *golden* mutant N₂ males of this backcross had (i) less black on the dorsal fin, (ii) a more diffuse posterior black horizontal stripe, (iii) an upwardly shifted or no ventral black lining of the caudal peduncle, and (iv) a slightly upwardly shifted central black spot (Figure 7D and Figure 9). In *blue* mutant N₂ males, black ornaments on the trunk were mostly reduced to a few spots, and in some individuals a spot appeared at an unusual position just behind the operculum (Figure 7E).

Fewer black ornaments on the dorsal fin were also observed in *golden* mutant males of the highly inbred BDZW1 and Maculatus strains (Figure 8). The black spot in the dorsal fin of the Maculatus strain is considered to be a strictly Y-linked trait (Winge 1922), which illustrates that the expression of such traits nevertheless depends on autosomal cofactors. Wild-type males of the BDZW1 strain have a creamy-black margin of the tail fin and a prominent black-and-white eye spot on the caudal peduncle (Figure 8, A–C, and Figure 9). The colors of the creamy-black tail-fin margin were intermingled or switched in *golden* mutant BDZW1 males, and, instead of the eye spot, they had black spots at a more dorsal position on the trunk or ventral position on the tail fin (Figure 8, D–F, and Figure 9; occasionally two spots were present). Hence, the position of the eye spot is more variable in *golden* mutant BDZW1 males compared with the wild type. The posterior black horizontal stripe of golden BDZW1 males was often diffuse (Figure 8, D–F, and Figure 9), while it was curved, absent, or diffuse in golden Maculatus males (Figure 8, G, K, and L, respectively, and Figure 9). The ventral black lining of the caudal peduncle was shifted upward (BDZW1, Figure 8, D–F, and Figure 9) or absent (MAC, Figure 8, G, K, and L, and Figure 9). *golden* mutant Maculatus males showed dorsal or ventral black spots on the tail fin as well, which were only rarely seen in wild-type males (Figure 8, G–L).

Discussion

How the extreme variation in colorful ornaments satisfies the conflicting demands of predator evasion and mate attraction in male guppies has fascinated scientists for almost a century (Winge 1922, 1927; Lindholm and Breden 2002; Magurran 2005). Importantly, despite the extreme interindividual differences, many color traits are highly heritable, and sons greatly resemble their fathers (Winge 1922, 1927; Dzwillo 1959; Lindholm and Breden 2002). A better understanding of these issues requires better knowledge of the ontogeny of guppy pigmentation. This has unfortunately been challenging, due to the intrinsic difficulties of working with a livebearer for which many standard techniques that can be utilized in model organisms are not available. Here, we have exploited the power of forward genetics to advance the understanding of pigmentation in guppies. We have discovered that mutations in the two type III receptor tyrosine kinase genes *kita* and *csf1ra* underlie the guppy *golden* and *blue* phenotype, respectively, and have studied the effects of the mutations on both the reticulate pattern shared by females and males

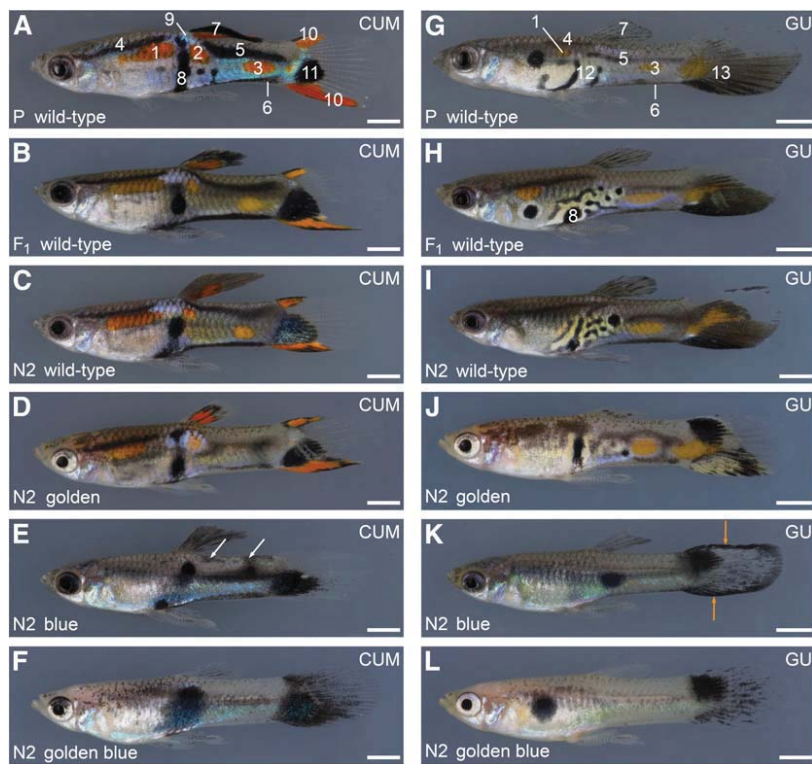


Figure 6 Ornaments in *golden* and *blue* mutant males from the Cumaná and Guanapo backgrounds. (A–F) Cross between a *golden blue* mutant BDZW1 female and a wild-type Cumaná male (A). Representative F₁ (B) and N₂ males with different phenotypes (C–F) are shown. Cumaná traits are highlighted in A. White arrows in E show incoherent patches of melanophores described in the text. (G–L) Cross between a *golden blue* mutant BDZW1 female and a wild-type Guanapo male from a F₅ Guanapo laboratory inbreeding population (G). Representative F₁ (H) and N₂ males with different phenotypes (I–L) are shown. Guanapo traits are highlighted in G and H. I–L lack the anterior orange spot. Orange arrows in K show the black margins of the tail fin described in the text. Traits are labeled with numbers that correspond with numbers used in Figure 9: 1, 2, and 3: anterior, central, and posterior orange spot; 4 and 5: anterior and posterior black horizontal stripes; 6: ventral black lining of caudal peduncle; 7: black pigment on dorsal fin (in CUM in combination with orange); 8: central black spot near gonopodium; 9: blue iridescent spot; 10: orange-black lining of tail fin; 11: ventral black spot on tail fin; 12: black crescents forming a labyrinthine pattern close to the gonopodium; and 13: orange spot and ventrally concentrated melanophores on tail fin. N₂ males shown for each backcross are siblings or cousins. All photos taken from the backcrosses can be found in File S1. Bottom left in each panel: generation (P, grandfather; F₁; N₂) and phenotype. Top right in each panel: Y chromosome origin. Bars: 2 mm.

and the male-specific ornaments. We found that the mutations in *kita* and *csf1ra* have strong effects on the expression of male-specific color patterns. In general, the mutation in *kita* made none or only minor changes in orange ornaments and affected the male melanophore pattern more subtly and in a more reproducible manner than the mutation in *csf1ra*. The salient feature of the *csf1ra* mutant males was the absence of all orange traits, with concomitant severe changes in black ornaments.

In many teleost species, including zebrafish, medaka (*Oryzias latipes*), stickleback (*Gasterosteus aculeatus*), and Japanese flounder (*Paralichthys olivaceus*), larvae and adults differ in their pigmentation patterns (Johnson *et al.* 1995; Parichy and Turner 2003a,b; Lynn Lamoreux *et al.* 2005; Kelsh *et al.* 2009; Yamada *et al.* 2010; Budi *et al.* 2011; Greenwood *et al.* 2012). Our study shows that the camouflage reticulate pattern of newborn guppies is not yet completely developed and that it is fully elaborated only during the first month after birth. Absence of most melanophores in embryonic and newborn *golden* mutants suggests that Kita is essential for the differentiation of an early melanophore population. A second melanophore population arises after birth and remains restricted to the dorsal half of the body in *golden* mutant fish, indicating that Kita signaling is not required for the differentiation of this melanophore subpopulation, yet that it might be essential for its proper migration. Alternatively, the migratory behavior of this subpopulation might be normal in *golden* mutants, with the later-differentiating melanophores enhancing the camouflage in wild-type fish on the dorsal side only. This could be investigated in

the future by selective labeling and tracing of the *kita*-independent population or by finding another mutation that eliminates this population. Independently of these details, we conclude that the guppy has an early-appearing *kita*-dependent and a later-developing partially or fully *kita*-independent melanophore population and that both populations are required to form the non-sex-specific reticulate pattern. Whole-mount *in situ* hybridization experiments turned out to be extremely difficult in guppy embryos due to their size and very low permeability (U. Martyn, and C. Dreyer, unpublished data), but could potentially help to determine the developmental time point at which the first melanophores differentiate in guppy embryos, especially as the melanization of these melanophores might be delayed in a livebearing fish like the guppy. The tracking of putative pigment cell precursors for adult ornaments, however, would require analysis of serial sections of specimens from early embryogenesis to puberty.

Our study suggests that Kita functions have at least partially been conserved across teleosts. The last common ancestor of zebrafish and guppies lived probably >300 million years ago (Kasahara *et al.* 2007); nevertheless, the adult pigment pattern of both species depends on an early *kita*-dependent and a late *kita*-independent melanophore population, and loss-of-function mutations in *kita* decrease the amount of melanophores, including scale melanophores, in both species (Haskins and Druzba 1938; Goodrich *et al.* 1944; Winge and Ditlevsen 1947; Parichy *et al.* 1999; Parichy *et al.* 2000a). Yet the teleost-specific whole-genome duplication likely also facilitated subfunctionalization and

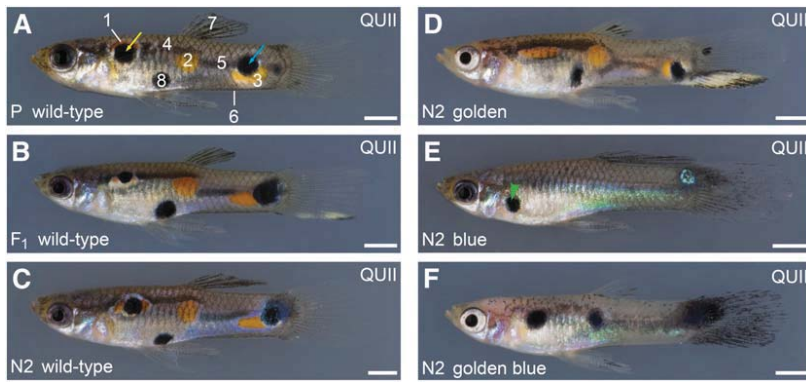


Figure 7 Ornaments in *golden* and *blue* mutant males from the Quare6 family II 215-3 background. Cross between a *golden blue* mutant BDZW1 female and a wild-type Quare6 family II 215-3 male (A). Representative F₁ (B) and N2 males with different phenotypes (C–F) are shown. Quare traits are highlighted in A. Yellow arrow points to black spot associated with anterior black horizontal stripe. Blue arrow points to black spot close to the tail fin that was not included in the analysis as its location was highly variable in wild-type fish. The green arrowhead in E shows a black spot close to the operculum described in the text. Traits are labeled with numbers corresponding with numbers used in Figure 6 and Figure 9. N2 males shown are cousins. All photos from this backcross and from the Quare6 backcross that was very similar regarding the male patterns can be found in File S2. Bottom left: generation (P, grandfather; F₁; N2) and phenotype. Bars: 2 mm.

phenotypic diversification, as revealed in different *Danio* species (Braasch *et al.* 2006; Mills *et al.* 2007).

An early xanthophore population contributes as regularly spaced cells to the reticulate pattern of guppy juveniles and adults (Figure 1, E and F). Our study shows that these non-sex-specific xanthophores depend on *Csf1ra* signaling. The presence of isolated dorsal clusters of xanthophores in *blue* mutant fish suggests that *Csf1ra* activity might not be absolutely required for differentiation, but for proliferation and dispersal of guppy xanthoblasts. We do not know yet when during ontogeny *csf1ra* acts and whether different xanthophore populations exist, but we showed that *Csf1ra* is not required for the formation of the non-sex-specific black reticulate pattern of the guppy. In contrast, *csf1ra* mutant zebrafish cannot form a complete non-sex-specific stripe pattern (Parichy *et al.* 2000a; Parichy and Turner 2003b).

Guppies are conspicuously sexually dimorphic in their pigmentation, and mate-choice experiments have demonstrated that females prefer males with pronounced orange and blue iridescent ornamentation (Endler 1983; Kodric-Brown 1985). Males are also able to intensify their black ornaments while courting (Endler 1983). Crosses between *golden blue* mutant females with male guppies of geographically and genetically diverse origins (Willing *et al.* 2010) gave us the opportunity to study the influence of Kita and *Csf1ra* loss-of-function on the diverse male-specific patterns of the guppy. The males originated from West Trinidad (Guanapo), East Trinidad (Quare), and Venezuela (Cumaná). The latter two strains had previously been used for genetic mapping and QTL analysis (Tripathi *et al.* 2009b). Our study demonstrates that the male-specific xanthophores of the guppy, whose development is induced during puberty like the one of male-specific melanophores and iridophores, also depend on *csf1ra* and that loss of *Csf1ra* and Kita function substantially changes the formation of male ornaments.

Comparison between wild-type and golden males showed that black stripes and spots appeared ectopically in *golden* mutants, although in a manner that varied between populations and individuals; *e.g.*, the ventral melanophores on the Guanapo tail fin were shifted to a more dorsal position, and

golden mutant Maculatus males had novel black spots on their tail fins. In the BDZW1 strain, the arrangement of the creamy-black tail-fin margin, which might involve iridophores (personal observation), appeared reversed. In contrast, loss of Kita function did not change the dorso-ventral arrangement of the orange-black lining of the tail fin of golden N2 from the Cumaná cross. Interestingly, the marginal black components of the Cumaná tail-fin ornaments were lost together with the orange in *blue* mutants, whereas the major black spot on the tail fin persisted. In zebrafish, *kita* is expressed in melanoblasts, while *csf1ra* acts nonautonomously via short- and long-range xanthophore–melanophore interactions to promote melanophore migration and death during adult stripe formation (Parichy *et al.* 1999; Parichy and Turner 2003b; Nakamasu *et al.* 2009; Inaba *et al.* 2012). As transplantation experiments are not yet possible in the guppy, we could not determine whether Kita and *Csf1ra* act cell-autonomously or non-cell-autonomously during male pattern formation. However, as downregulation of *csf1ra* expression coincides with the absence of almost all xanthophores in the skin of blue fish, it is likely that *csf1ra* acts cell-autonomously within guppy xanthophores. Kita is an early melanoblast marker not only in zebrafish, but also in mice, and therefore most likely is expressed in guppy melanophores as well (Kelsh *et al.* 2009). Our observations suggest that some pattern elements in guppy males depend on coordinate expression of different cell types and that the formation of some of these pattern elements requires interactions between, or joint contribution from, different cell types. For example, xanthophore–melanophore interactions might underlie the formation of the orange-black lining of the tail fin of Cumaná males, but not the development of the black spot on the tail fin. Kita might directly affect the migration and/or survival of a subset of male melanophores. Terminal deoxynucleotidyl transferase-dUTP Nick End Labeling (TUNEL) assays could reveal whether cell apoptosis plays a role during male pattern formation in the guppy.

Comparisons between wild-type and blue offspring of the backcrosses suggest that compact black spots can form in absence of *Csf1ra*, most probably without interactions between

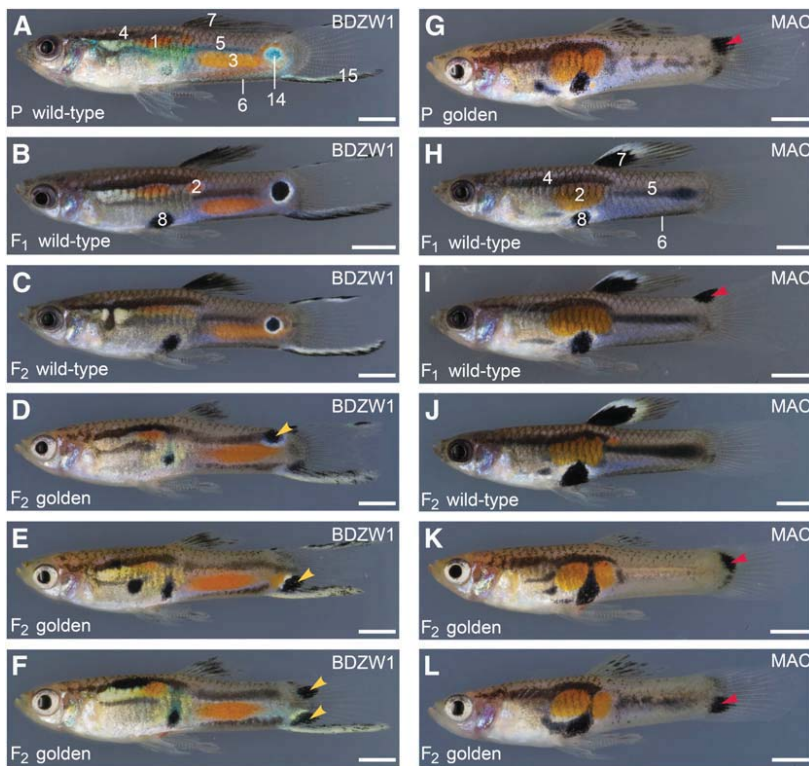


Figure 8 Ornaments in *golden* mutant males from the BDZW1 and Maculatus backgrounds. (A–F) Cross between a *golden* mutant BDZW1 female and a wild-type BDZW1 male (A). F₁ siblings were crossed to produce a F₂ generation. Representative F₁ (B) and F₂ males (C–F) are shown. BDZW1 traits are highlighted in A and B. All wild-type F₂ and 92% of the wild-type F₁ males had a central black-and-white eye spot on the caudal peduncle. Instead of this eye spot, one-half of the *golden* mutant F₂ males had a spot located more dorsally on the trunk, while the other half had a spot at a more ventral position, mostly on the tail fin (yellow arrowheads in D and E). Three males had two spots (yellow arrowheads in F). (G–L) Cross between a wild-type Maculatus female and a *golden* mutant Maculatus male (G). F₁ siblings were crossed to produce a F₂ generation. Representative F₁ (H and I) and F₂ males with different phenotypes (J–L) are shown. Maculatus traits are highlighted in H. Red arrowheads in (G, I, K, and L) indicate untypical black spots on the tail fin. Only one of the F₁ males showed such a black spot (I). It was not seen in any of the wild-type F₂ males, but it was present in 85% of the *golden* mutant F₂ males (K and L). Traits are labeled with numbers corresponding to those shown in Figure 6 and Figure 9. Additional traits to those shown in Figure 6: 14, black-and-white eye spot; 15, creamy-black margin of tail fin. F₂ males shown for each cross are siblings or cousins. Bottom left: generation (P, grandfather; F₁; F₂) and phenotype. Top right: Y chromosome origin. Bars: 2 mm.

xanthophores and melanophores, yet the final positions of these spots appear unpredictable. The labyrinthine ornaments close to the gonopodium in Guanapo males provide an example of interacting genetic cofactors in that backcross and potentially also of interactions between different cell types. Compared with wild type, these ornaments were greatly reduced in complexity in *golden* mutant N2 and lost in *blue* and *golden blue* mutant N2. Since only faint yellow pigment is seen in this area in wild-type fish, the contribution of xanthophores and their interactions is here hard to assess. The loss of the labyrinthine ornaments in *golden* mutant N2 might be explained by a reduced migratory potential of the *kita*-independent melanophores or their precursors in *golden* N2. We can, however, not exclude that a *kita*-dependent subpopulation of late melanophores contributes to this complex trait in wild-type fish.

golden blue double-mutant guppies from four different backcrosses always had less total black than *blue* mutants, but much more than zebrafish *kita csf1ra* double mutants (Parichy 2006). This might reflect different requirements for Kita and Csf1ra signaling: while xanthophores enhance the survival of adult stripe melanophores in zebrafish (Parichy and Turner 2003b), the survival of male hormone-induced melanophores in the guppy might not require xanthophores; yet the ability of these melanophores to form some of the complex traits might depend on interactions with these cells.

Taken together, we conclude that at least three temporally and genetically distinct melanophore populations occur in the guppy: first, a *kita*-dependent population differentiat-

ing during embryogenesis; second, a partially or fully *kita*-independent population mostly differentiating after birth; and third, a male-specific melanophore population whose differentiation, migration, and proliferation might be induced by testosterone during puberty. It remains to be resolved where the precursors of these male-specific pigment cells reside and whether they might be derived from the same pool as the late non-sex-specific *kita*-independent melanophores. Only a few recent publications have addressed the routes and fates of pigment cell precursor pools destined for delayed differentiation in other vertebrates (Watanabe *et al.* 2008; Adameyko *et al.* 2009; Yamada *et al.* 2010; Budi *et al.* 2011). While the embryonic and early larval pigment pattern of zebrafish is formed by melanoblasts that are derived directly from the neural crest, later-appearing metamorphic melanophores of zebrafish develop from post-embryonic extrahypodermal pigment cell precursors, which migrate to the hypodermis during pigment pattern metamorphosis (Budi *et al.* 2011). These precursors are associated with nerves and depend on *ErbB3b* and *Tubulin α 8-like 3a* signaling (Budi *et al.* 2011). Improvement of *in vitro* culture methods of guppy embryos (Martyn *et al.* 2006) may facilitate the ability to treat, and to subsequently raise, explanted guppy embryos with an *ErbB* inhibitor, which might reveal whether *ErbB* signaling is required to establish melanophore stem cells in the guppy as well.

In stickleback, regulatory mutations in *kitla* are associated with the light coloration of gills and ventral skin in several freshwater populations (Miller *et al.* 2007). This indicates that differential distribution of *Kitla* can lead to

	golden	blue
General traits		
Orange traits		
1 Anterior orange spot	present ^a	absent
2 Central orange spot		
3 Posterior orange spot		
Black traits		
Complexity of black ornaments on body		reduced
4 Anterior black horizontal stripe	present ^b	diffuse/absent
5 Posterior black horizontal stripe	shifted/diffuse/absent	shifted/diffuse/absent
6 Ventral black lining of caudal peduncle	shifted/diffuse/absent	present
7 Black pigment on dorsal fin	reduced	present
8 Central black spot near gonopodium	present at same position/slightly shifted	shifted/absent

Presence of traits in wild-type males of crosses								
CUM	1	2	3	4	5	6 ^c	7 ^c	8
GU	(1)		3	4	5	6	7	(8)
QUIII	1	2	3	4 ^d	5	6	7	8
BDZW1	1	(2)	3	4	5	6	7	8
MAC		2 ^c		4	5	6	7 ^c	8 ^c

Figure 9 Summary and generalization of the results regarding the male-specific pattern. Both *Csf1ra* and *Kita* are required for the formation of male ornaments of the guppy. The black pigment on the dorsal fin can be a distinct patch or diffuse. Numbers in parentheses refer to traits that were not present in all wild-type males of the specific strain. Traits that were too variable in wild-type males were not included into the analysis. More details are described in the text and shown in Figure 6, Figure 7, and Figure 8 and in Figure S5. ^aException: a concise posterior orange spot was absent in 94% of the golden N2 males with a Y^{CUM} background. ^bException: often discontinuous in golden N2 males with a Y^{GU} background. ^cY-linked in respective strain. ^dAssociated with a black spot in 83% of the wild-type males with a Y^{QUIII} background.

Additional strain-specific traits

Cumaná			
9 Blue iridescent spot ^c	present	small spot visible in 43% of males	
10 Orange-black lining of tail fin	present	absent	
11 Ventral black spot on tail fin	present	present	
Guanapo			
12 Labyrinthine pattern close to gonopodium	mostly absent	absent	
13 Orange spot and ventrally concentrated melanophores (m) on tail fin	m concentrated dorsally	orange absent; m concentrated dorsally	
BDZW1			
14 Black and white eye spot	shifted	n/a	
15 Creamy-black margin of tail fin	colors intermingled/switched	n/a	

distinct pigmentation patterns in natural populations. In contrast to the receptor *Kita*, the functions of *Csf1ra* seem to be less conserved even among species in the genus *Danio*, as indicated by limited complementation of *csf1ra* loss of function in interspecies hybrids (Quigley *et al.* 2005). Furthermore, a study with haplochromine cichlids has suggested that positive selection has acted on *csf1ra*, which is expressed in the yellow egg spots of these fish (Salzburger *et al.* 2007). QTL mapping with higher marker density may reveal whether or not *Kita* and *Csf1ra*, and/or their ligands, also affect natural variation of guppy ornaments. For this purpose, we are generating a denser genetic map of the guppy based on Restriction-site Associated DNA (RAD) markers. Combined with the ongoing whole-genome sequencing, these

experiments will further enhance our efforts to unravel the network of genetic factors that cooperatively maintain the highly complex male ornaments of the guppy.

Acknowledgments

We thank Harald Auer for the donation of the ARM and BDZW2 guppy strains; Axel Meyer for the BDZW1 guppy strain; David Reznick for guppies from the Quare and Guanapo rivers; Christopher Dooley for general advice on zebrafish pigment pattern mutants; Tobias Langenecker for assistance with real-time quantitative PCR; Gertrud Scheer, Alexandra Schnell, and Philipp Vollmer for guppy images; Richard Neher for help with data analysis; Joffrey Fitz for

technical support; and Bonnie Fraser, Felicity Jones, and Axel Künstner for helpful suggestions on the manuscript. This work was supported by a Gottfried Wilhelm Leibniz Award of the Deutsche Forschungsgemeinschaft and by funds from the Max Planck Society to D.W.

Literature Cited

- Adameyko, I., F. Lallemand, J. B. Aquino, J. A. Pereira, P. Topilko *et al.*, 2009 Schwann cell precursors from nerve innervation are a cellular origin of melanocytes in skin. *Cell* 139: 366–379.
- Alexander, H. J., and F. Breden, 2004 Sexual isolation and extreme morphological divergence in the Cumana guppy: a possible case of incipient speciation. *J. Evol. Biol.* 17: 1238–1254.
- Altschul, S. F., W. Gish, W. Miller, E. W. Myers, and D. J. Lipman, 1990 Basic local alignment search tool. *J. Mol. Biol.* 215: 403–410.
- Braasch, I., W. Salzburger, and A. Meyer, 2006 Asymmetric evolution in two fish-specifically duplicated receptor tyrosine kinase paralogs involved in teleost coloration. *Mol. Biol. Evol.* 23: 1192–1202.
- Budi, E. H., L. B. Patterson, and D. M. Parichy, 2011 Post-embryonic nerve-associated precursors to adult pigment cells: genetic requirements and dynamics of morphogenesis and differentiation. *PLoS Genet.* 7: e1002044.
- Clemens, H. P., C. McDermitt, and T. Inslee, 1966 The effects of feeding methyl testosterone to guppies for sixty days after birth. *Copeia* 1966: 280–284.
- Dzwillo, M., 1959 Genetic investigations of domesticated strains of *Lebistes reticulatus* Peters Mitt. Hamburg. Zool. Mus. Inst. 57: 143–186 (in German).
- Endler, J. A., 1983 Natural and sexual selection on color patterns in poeciliid fishes. *Environ. Biol. Fishes* 9: 173–190.
- Felsenstein, J., 1989 PHYLIP-phylogeny inference package (version 3.2). *Cladistics* 5: 164–166.
- Goodrich, H. B., N. D. Josephson, J. P. Trinkaus, and J. M. Slate, 1944 The cellular expression and genetics of two new genes in *Lebistes reticulatus*. *Genetics* 29: 584–592.
- Goujon, M., H. McWilliam, W. Li, F. Valentin, S. Squizzato *et al.*, 2010 A new bioinformatics analysis tools framework at EMBL–EBI. *Nucleic Acids Res.* 38: W695–W699.
- Greenwood, A. K., J. N. Cech, and C. L. Peichel, 2012 Molecular and developmental contributions to divergent pigment patterns in marine and freshwater sticklebacks. *Evol. Dev.* 14: 351–362.
- Guindon, S., J. F. Dufayard, V. Lefort, M. Anisimova, W. Hordijk *et al.*, 2010 New algorithms and methods to estimate maximum-likelihood phylogenies: assessing the performance of PhyML 3.0. *Syst. Biol.* 59: 307–321.
- Haskins, C. P., and J. P. Druzba, 1938 Note on anomalous inheritance of sex-linked color factors in the Guppy. *Am. Nat.* 72: 571–574.
- Houde, A. E., 1997 *Sex, Color, and Mate Choice in Guppies*. Princeton University Press, Princeton, NJ.
- Hultman, K. A., N. Bahary, L. I. Zon, and S. L. Johnson, 2007 Gene duplication of the zebrafish kit ligand and partitioning of melanocyte development functions to kit ligand a. *PLoS Genet.* 3: e17.
- Huson, D. H., and D. Bryant, 2006 Application of phylogenetic networks in evolutionary studies. *Mol. Biol. Evol.* 23: 254–267.
- Inaba, M., H. Yamanaka, and S. Kondo, 2012 Pigment pattern formation by contact-dependent depolarization. *Science* 335: 677.
- Johnson, S. L., D. Africa, C. Walker, and J. A. Weston, 1995 Genetic control of adult pigment stripe development in zebrafish. *Dev. Biol.* 167: 27–33.
- Kasahara, M., K. Naruse, S. Sasaki, Y. Nakatani, W. Qu *et al.*, 2007 The medaka draft genome and insights into vertebrate genome evolution. *Nature* 447: 714–719.
- Kelsh, R. N., M. L. Harris, S. Colanese, and C. A. Erickson, 2009 Stripes and belly-spots: a review of pigment cell morphogenesis in vertebrates. *Semin. Cell Dev. Biol.* 20: 90–104.
- Kodric-Brown, A., 1985 Female preference and sexual selection for male coloration in the guppy (*Poecilia reticulata*). *Behav. Ecol. Sociobiol.* 17: 199–205.
- Lamason, R. L., M. A. Mohideen, J. R. Mest, A. C. Wong, H. L. Norton *et al.*, 2005 SLC24A5, a putative cation exchanger, affects pigmentation in zebrafish and humans. *Science* 310: 1782–1786.
- Lindholm, A., and F. Breden, 2002 Sex chromosomes and sexual selection in Poeciliid fishes. *Am. Nat.* 160: S214–S224.
- Lynn Lamoreux, M., R. N. Kelsh, Y. Wakamatsu, and K. Ozato, 2005 Pigment pattern formation in the medaka embryo. *Pigment Cell Res.* 18: 64–73.
- Maderspacher, F., and C. Nusslein-Volhard, 2003 Formation of the adult pigment pattern in zebrafish requires leopard and obelix dependent cell interactions. *Development* 130: 3447–3457.
- Magurran, A. E., 2005 *Evolutionary Ecology: The Trinidadian Guppy*. Oxford University Press, Oxford.
- Martyn, U., D. Weigel, and C. Dreyer, 2006 In vitro culture of embryos of the guppy, *Poecilia reticulata*. *Dev. Dyn.* 235: 617–622.
- Mellgren, E. M., and S. L. Johnson, 2005 kitb, a second zebrafish ortholog of mouse Kit. *Dev. Genes Evol.* 215: 470–477.
- Miller, C. T., S. Belez, A. A. Pollen, D. Schluter, R. A. Kittles *et al.*, 2007 cis-regulatory changes in Kit ligand expression and parallel evolution of pigmentation in sticklebacks and humans. *Cell* 131: 1179–1189.
- Mills, M. G., R. J. Nuckels, and D. M. Parichy, 2007 Deconstructing evolution of adult phenotypes: genetic analyses of kit reveal homology and evolutionary novelty during adult pigment pattern development of *Danio* fishes. *Development* 134: 1081–1090.
- Mol, C. D., K. B. Lim, V. Sridhar, H. Zou, E. Y. Chien *et al.*, 2003 Structure of a c-kit product complex reveals the basis for kinase transactivation. *J. Biol. Chem.* 278: 31461–31464.
- Nakamasu, A., G. Takahashi, A. Kanbe, and S. Kondo, 2009 Interactions between zebrafish pigment cells responsible for the generation of Turing patterns. *Proc. Natl. Acad. Sci. USA* 106: 8429–8434.
- Nusslein-Volhard, C., and R. Dahm, 2002 *Zebrafish: A Practical Approach*. Oxford University Press, Oxford.
- Parichy, D. M., 2006 Evolution of danio pigment pattern development. *Heredity (Edinb)* 97: 200–210.
- Parichy, D. M., and J. M. Turner, 2003a Zebrafish *puma* mutant decouples pigment pattern and somatic metamorphosis. *Dev. Biol.* 256: 242–257.
- Parichy, D. M., and J. M. Turner, 2003b Temporal and cellular requirements for Fms signaling during zebrafish adult pigment pattern development. *Development* 130: 817–833.
- Parichy, D. M., J. F. Rawls, S. J. Pratt, T. T. Whitfield, and S. L. Johnson, 1999 Zebrafish *sparse* corresponds to an orthologue of *c-kit* and is required for the morphogenesis of a subpopulation of melanocytes, but is not essential for hematopoiesis or primordial germ cell development. *Development* 126: 3425–3436.
- Parichy, D. M., D. G. Ransom, B. Paw, L. I. Zon, and S. L. Johnson, 2000a An orthologue of the *kit*-related gene *fms* is required for development of neural crest-derived xanthophores and a subpopulation of adult melanocytes in the zebrafish, *Danio rerio*. *Development* 127: 3031–3044.
- Parichy, D. M., E. M. Mellgren, J. F. Rawls, S. S. Lopes, R. N. Kelsh *et al.*, 2000b Mutational analysis of *endothelin receptor b1* (*rose*) during neural crest and pigment pattern development in the zebrafish *Danio rerio*. *Dev. Biol.* 227: 294–306.
- Parichy, D. M., M. R. Elizondo, M. G. Mills, T. N. Gordon, and R. E. Engeszer, 2009 Normal table of postembryonic zebrafish

- development: staging by externally visible anatomy of the living fish. *Dev. Dyn.* 238: 2975–3015.
- Pfaffl, M. W., 2001 A new mathematical model for relative quantification in real-time RT-PCR. *Nucleic Acids Res.* 29: e45.
- Quigley, I. K., J. L. Manuel, R. A. Roberts, R. J. Nuckels, E. R. Herrington *et al.*, 2005 Evolutionary diversification of pigment pattern in *Danio* fishes: differential fins dependence and stripe loss in *D. albolineatus*. *Development* 132: 89–104.
- Reznick, D., and J. A. Endler, 1982 The impact of predation on life history evolution in Trinidadian guppies (*Poecilia reticulata*). *Evolution* 36: 160–177.
- Salzburger, W., I. Braasch, and A. Meyer, 2007 Adaptive sequence evolution in a color gene involved in the formation of the characteristic egg-dummies of male haplochromine cichlid fishes. *BMC Biol.* 5: 51.
- Sievers, F., A. Wilm, D. Dineen, T. J. Gibson, K. Karplus *et al.*, 2011 Fast, scalable generation of high-quality protein multiple sequence alignments using Clustal Omega. *Mol. Syst. Biol.* 7: 539.
- Takeuchi, I. K., 1976 Electron microscopy of two types of reflecting chromatophores (iridophores and leucophores) in the guppy, *Lebistes reticulatus* Peters. *Cell Tissue Res.* 173: 17–27.
- Traut, W., and H. Winking, 2001 Meiotic chromosomes and stages of sex chromosome evolution in fish: zebrafish, platyfish and guppy. *Chromosome Res.* 9: 659–672.
- Tripathi, N., M. Hoffmann, and C. Dreyer, 2008 Natural variation of male ornamental traits of the guppy, *Poecilia reticulata*. *Zebrafish* 5: 265–278.
- Tripathi, N., M. Hoffmann, D. Weigel, and C. Dreyer, 2009a Linkage analysis reveals the independent origin of Poeciliid sex chromosomes and a case of atypical sex inheritance in the guppy (*Poecilia reticulata*). *Genetics* 182: 365–374.
- Tripathi, N., M. Hoffmann, E. M. Willing, C. Lanz, D. Weigel *et al.*, 2009b Genetic linkage map of the guppy, *Poecilia reticulata*, and quantitative trait loci analysis of male size and colour variation. *Proc. Biol. Sci.* 276: 2195–2208.
- Vandesompele, J., K. De Preter, F. Pattyn, B. Poppe, N. Van Roy *et al.*, 2002 Accurate normalization of real-time quantitative RT-PCR data by geometric averaging of multiple internal control genes. *Genome Biol* 3: RESEARCH0034.
- Watanabe, K., Y. Washio, Y. Fujinami, M. Aritaki, S. Uji *et al.*, 2008 Adult-type pigment cells, which color the ocular sides of flounders at metamorphosis, localize as precursor cells at the proximal parts of the dorsal and anal fins in early larvae. *Dev. Growth Differ.* 50: 731–741.
- Willing, E. M., P. Bentzen, C. van Oosterhout, M. Hoffmann, J. Cable *et al.*, 2010 Genome-wide single nucleotide polymorphisms reveal population history and adaptive divergence in wild guppies. *Mol. Ecol.* 19: 968–984.
- Winge, Ö., 1922 One-sided masculine and sex-linked inheritance in *Lebistes reticulatus*. *J. Genet.* 12: 145–162.
- Winge, Ö., 1927 The location of eighteen genes in *Lebistes reticulatus*. *J. Genet.* 18: 1–43.
- Winge, Ö., and E. Ditlevsen, 1947 Colour inheritance and sex determination in *Lebistes*. *Heredity* 1: 65–83.
- Yamada, T., M. Okauchi, and K. Araki, 2010 Origin of adult-type pigment cells forming the asymmetric pigment pattern, in Japanese flounder (*Paralichthys olivaceus*). *Dev. Dyn.* 239: 3147–3162.
- Yarden, Y., and A. Ullrich, 1988 Growth factor receptor tyrosine kinases. *Annu. Rev. Biochem.* 57: 443–478.

Communicating editor: D. Parichy

Concluding remarks

The mechanistic basis of pigment pattern formation is the key problem in the field of pigment cell research, which is only partially resolved. In the presented studies we provide new insights into the control of pigment cell behaviour during pattern formation. We show that the scaffold protein Tight Junction Protein 1a regulates iridophore cell shape transition from the dense to the loose shape during stripe formation in zebrafish. Truncation of *Tjp1a* leads to a delayed transition in an iridophore-autonomous manner and, consequently, interruptions in the dark stripes. These results support the important role of iridophores in pigment pattern formation. *Tjp1a* is the first intracellular protein implicated in the rearrangements of pigment cells during pigment pattern formation. It is expressed in iridophores, but seems to regulate their response to other pigment cell types. This provides the basis for identification of the upstream transmembrane proteins responsible for iridophore communication with melanophores and xanthophores, as well as the downstream signalling cascade responsible for iridophore cell shape change.

Iridophores clones distribute along the dorso-ventral axis, but also disperse along the antero-posterior axis. This results in the mixing of iridophores, originating from stem cells that are located in adjacent segments. We demonstrate the novel roles for an established iridophore specification factor – Leukocyte Tyrosine Kinase. Although our data confirm that *Ltk* is required for iridophore establishment, we also show that *Ltk* plays a role in the survival of iridophores as well as their homotypic interactions, which restrict the expansion of iridophores along the anterior-posterior axis. Future research should identify the *Ltk* ligand and determine whether iridophore homotypic interactions depend on this ligand.

An important question in the pigment cell patterning field is whether the mechanisms described in zebrafish are at play in other fish species. We demonstrate that *kita* and *csfr1a* receptor tyrosine kinases in guppies serve functions in control of pigment cell specification similar to the functions of their zebrafish orthologs. Development of gene-editing techniques in guppy will allow addressing the functions of other guppy orthologs of zebrafish genes, implicated in pattern formation.

Bibliography

- Amores A, Force A, Yan Y-L, Joly L, Amemiya C, Fritz A, Ho RK, Langeland J, Prince V, Wang Y-L, Westerfield M, Ekker M & Postlethwait JH (1998) Zebrafish hox Clusters and Vertebrate Genome Evolution. *Sci.* **282** : 1711–1714 Available at: <http://www.sciencemag.org/cgi/doi/10.1126/science.282.5394.1711> [Accessed September 6, 2014]
- Amsterdam A, Burgess S, Golling G, Chen W, Sun Z, Townsend K, Farrington S, Haldi M & Hopkins N (1999) A large-scale insertional mutagenesis screen in zebrafish. *Genes Dev.* **13** : 2713–2724
- Anderson JM & Itallie CM Van (1995) Tight junctions and the molecular basis for regulation of paracellular permeability. *Am. J. Physiol. Liver Physiol.* **32**: 467–475
- Anelli V, Santoriello C, Distel M, Köster RW, Ciccarelli FD & Mione M (2009) Global repression of cancer gene expression in a zebrafish model of melanoma is linked to epigenetic regulation. *Zebrafish* **6**: 417–24 Available at: <http://www.ncbi.nlm.nih.gov/pubmed/20047469>
- Balda MS & Matter K (2009) Tight junctions and the regulation of gene expression. *Biochim. Biophys. Acta* **1788**: 761–7 Available at: <http://www.ncbi.nlm.nih.gov/pubmed/19121284> [Accessed September 9, 2014]
- Bard JBL (1981) A model for generating aspects of zebra and other mammalian coat patterns. *J. Theor. Biol.* **93**: 363–385 Available at: <http://www.sciencedirect.com/science/article/pii/0022519381901090>
- Bauer H, Zweimueller-Mayer J, Steinbacher P, Lametschwandtner A & Bauer HC (2010) The dual role of zonula occludens (ZO) proteins. *J. Biomed. Biotechnol.* **2010**: 402593 Available at: <http://www.pubmedcentral.nih.gov/articlerender.fcgi?artid=2836178&tool=pmcentrez&rendertype=abstract> [Accessed March 27, 2012]
- Blum Y, Belting H-G, Ellertsdottir E, Herwig L, Lüders F & Affolter M (2008) Complex cell rearrangements during intersegmental vessel sprouting and vessel fusion in the zebrafish embryo. *Dev. Biol.* **316**: 312–22 Available at: <http://www.ncbi.nlm.nih.gov/pubmed/18342303> [Accessed September 2, 2014]
- Braasch I, Brunet F, Volff J-N & Schartl M (2009) Pigmentation pathway evolution after whole genome duplication in fish. *Genome Biol. Evol.*: evp050
- Brand M, Heisenberg CP, Jiang YJ, Beuchle D, Lun K, Furutani-Seiki M, Granato M,

- Haffter P, Hammerschmidt M, Kane DA, Kelsh RN, Mullins MC, Odenthal J, van Eeden FJ & Nusslein-Volhard C (1996) Mutations in zebrafish genes affecting the formation of the boundary between midbrain and hindbrain. *Development* **123**: 179–190
- De Brouwer S, De Preter K, Kumps C, Zabrocki P, Porcu M, Westerhout EM, Lakeman A, Vandesompele J, Hoebeeck J & Van Maerken T (2010) Meta-analysis of neuroblastomas reveals a skewed ALK mutation spectrum in tumors with MYCN amplification. *Clin. Cancer Res.* **16**: 4353–4362
- Budi EH, Patterson LB & Parichy DM (2008) Embryonic requirements for ErbB signaling in neural crest development and adult pigment pattern formation. *Development* **135**: 2603–2614 Available at: <http://www.pubmedcentral.nih.gov/articlerender.fcgi?artid=2704560&tool=pmcentrez&rendertype=abstract>
- Carén H, Abel F, Kogner P & Martinsson T (2008) High incidence of DNA mutations and gene amplifications of the ALK gene in advanced sporadic neuroblastoma tumours. *Biochem. J* **416**: 153–159
- Chand D, Yamazaki Y, Ruuth K, Schönherr C, Martinsson T, Kogner P, Attiyeh EF, Maris J, Morozova O, Marra M a, Ohira M, Nakagawara A, Sandström P-E, Palmer RH & Hallberg B (2013) Cell culture and Drosophila model systems define three classes of anaplastic lymphoma kinase mutations in neuroblastoma. *Dis. Model. Mech.* **6**: 373–82 Available at: <http://www.pubmedcentral.nih.gov/articlerender.fcgi?artid=3597019&tool=pmcentrez&rendertype=abstract> [Accessed October 17, 2014]
- Chen Y, Takita J, Choi YL, Kato M, Ohira M, Sanada M, Wang L, Soda M, Kikuchi A & Igarashi T (2008) Oncogenic mutations of ALK kinase in neuroblastoma. *Nature* **455**: 971–974
- Cismasiu VB, Denes SA, Reiländer H, Michel H & Szedlacsek SE (2004) The MAM (Meprin/A5-protein/PTPmu) Domain Is a Homophilic Binding Site Promoting the Lateral Dimerization of Receptor-like Protein-tyrosine Phosphatase μ . *J. Biol. Chem.* **279** : 26922–26931 Available at: <http://www.jbc.org/content/279/26/26922.abstract>
- Cooper WE & Greenberg N (1992) Reptilian coloration and behavior. *Biol. Reptil.* **18**: 298–422
- Darwin C (1871) The descent of man, and selection in relation to sex. *London: Murray*
- Denefle J-P & Lechaire J-P (1990) Localization of pigment cells in cultured frog skin. *Am. J. Anat.* **188**: 212–220

- Dooley CM, Mongera A, Walderich B & Nüsslein-Volhard C (2013) On the embryonic origin of adult melanophores: the role of ErbB and Kit signalling in establishing melanophore stem cells in zebrafish. *Development* **140**: 1003–13 Available at: <http://www.ncbi.nlm.nih.gov/pubmed/23364329> [Accessed September 4, 2014]
- Le Douarin N & Kalcheim C (1999) *The neural crest* Cambridge University Press
- Driever W, Solnica-Krezel L, Schier a F, Neuhauss SC, Malicki J, Stemple DL, Stainier DY, Zwartkruis F, Abdelilah S, Rangini Z, Belak J & Boggs C (1996) A genetic screen for mutations affecting embryogenesis in zebrafish. *Development* **123**: 37–46 Available at: <http://www.ncbi.nlm.nih.gov/pubmed/9007227>
- Dutton K a, Pauliny a, Lopes SS, Elworthy S, Carney TJ, Rauch J, Geisler R, Haffter P & Kelsh RN (2001) Zebrafish colourless encodes sox10 and specifies non-ectomesenchymal neural crest fates. *Development* **128**: 4113–25 Available at: <http://www.ncbi.nlm.nih.gov/pubmed/11684650>
- Dzwillo M (1959) Genetische Untersuchungen an domestizierten Stämmen von *Lebistes reticulatus* Peters. *Mitt Hambg. Zool Mus Inst* **57**: 143–186
- van Eeden FJ, Granato M, Schach U, Brand M, Furutani-Seiki M, Haffter P, Hammerschmidt M, Heisenberg CP, Jiang YJ, Kane DA, Kelsh RN, Mullins MC, Odenthal J, Warga RM & Nusslein-Volhard C (1996) Genetic analysis of fin formation in the zebrafish, *Danio rerio*. *Development* **123**: 255–262
- Endler JA (1984) Natural and sexual selection on color patterns in poeciliid fishes. In *Evolutionary ecology of neotropical freshwater fishes* pp 95–111. Springer
- Eom DS, Inoue S, Patterson LB, Gordon TN, Slingwine R, Kondo S, Watanabe M & Parichy DM (2012) Melanophore migration and survival during zebrafish adult pigment stripe development require the immunoglobulin superfamily adhesion molecule Igsf11. *PLoS Genet.* **8**: e1002899 Available at: <http://www.pubmedcentral.nih.gov/articlerender.fcgi?artid=3420941&tool=pmcentrez&rendertype=abstract> [Accessed July 10, 2014]
- Fanning AS, Jameson BJ, Jesaitis LA & Anderson JM (1998) The tight junction protein ZO-1 establishes a link between the transmembrane protein occludin and the actin cytoskeleton. *J. Biol. Chem.* **273**: 29745–29753 Available at: <http://www.ncbi.nlm.nih.gov/pubmed/9792688>
- Fass D, Blacklow S, Kim PS & Berger JM (1997) Molecular basis of familial hypercholesterolaemia from structure of LDL receptor module. *Nature* **388**: 691–693
- Forbes SA, Beare D, Gunasekaran P, Leung K, Bindal N, Boutselakis H, Ding M, Bamford S, Cole C, Ward S, Kok CY, Jia M, De T, Teague JW, Stratton MR,

- McDermott U & Campbell PJ (2015) COSMIC: exploring the world's knowledge of somatic mutations in human cancer. *Nucleic Acids Res.* **43** : D805–D811 Available at: <http://nar.oxfordjournals.org/content/43/D1/D805.abstract>
- Frohnhofer HG, Krauss J, Maischein H-M & Nüsslein-Volhard C (2013) Iridophores and their interactions with other chromatophores are required for stripe formation in zebrafish. *Development* **140**: 2997–3007 Available at: <http://www.pubmedcentral.nih.gov/articlerender.fcgi?artid=3912879&tool=pmcentrez&rendertype=abstract> [Accessed September 1, 2014]
- Galeotti P, Rubolini D, Dunn PO & Fasola M (2003) Colour polymorphism in birds: causes and functions. *J. Evol. Biol.* **16**: 635–646
- Geissler EN, Ryan MA & Housman DE (1988) The dominant-white spotting (W) locus of the mouse encodes the c-kit proto-oncogene. *Cell* **55**: 185–192
- George RE, Sanda T, Hanna M, Fröhling S, Luther II W, Zhang J, Ahn Y, Zhou W, London WB & McGrady P (2008) Activating mutations in ALK provide a therapeutic target in neuroblastoma. *Nature* **455**: 975–978
- Godfrey D, Lythgoe JN & Rumball DA (1987) Zebra stripes and tiger stripes: the spatial frequency distribution of the pattern compared to that of the background is significant in display and crypsis. *Biol. J. Linn. Soc.* **32**: 427–433 Available at: <http://dx.doi.org/10.1111/j.1095-8312.1987.tb00442.x>
- Goodrich HB, Josephson ND, Trinkaus JP & Slate JM (1944) The cellular expression and genetics of two new genes in *Lebistes reticulatus*. *Genetics* **29**: 584
- Gunnarsson U, Kerje S, Bed'hom B, Sahlqvist A, Ekwall O, Tixier-Boichard M, Kämpe O & Andersson L (2011) The Dark brown plumage color in chickens is caused by an 8.3-kb deletion upstream of SOX10. *Pigment Cell Melanoma Res.* **24**: 268–274
- Haffter J, Odenthal M, Shuo L, J FM, Elisabeth V, Fabian H, Michael B, Michael G, Matthias H, A KD, N KR, Nancy H & Christiane N-V (1996) Mutations affecting pigmentation and shape of the adult zebrafish. *Dev. Genes Evol.*: 260–276
- Haffter P & Nüsslein-Volhard C (1996) Large scale genetics in a small vertebrate, the zebrafish. *Int. J. Dev. Biol.* **40**: 221–7 Available at: <http://www.ncbi.nlm.nih.gov/pubmed/8735932>
- Hairston NC (1976) Photoprotection by carotenoid pigments in the copepod *Diaptomus nevadensis*. *Proc. Natl. Acad. Sci.* **73**: 971–974
- Haskins CP & Druzba JP (1938) Note on anomalous inheritance of sex-linked color factors in the Guppy. *Am. Nat.*: 571–574
- Hawkes JW (1974) The structure of fish skin. *Cell Tissue Res.* **149**: 159–172

- Hirata M, Nakamura K, Kanemaru T, Shibata Y & Kondo S (2003) Pigment cell organization in the hypodermis of zebrafish. *Dev. Dyn.* **227**: 497–503 Available at: <http://www.ncbi.nlm.nih.gov/pubmed/12889058>
- Hirata M, Nakamura K-I & Kondo S (2005) Pigment cell distributions in different tissues of the zebrafish, with special reference to the striped pigment pattern. *Dev. Dyn.* **234**: 293–300 Available at: <http://www.ncbi.nlm.nih.gov/pubmed/16110504> [Accessed October 12, 2010]
- Houde AE (1997) Sex, color, and mate choice in guppies Princeton University Press
- Huang P, Xiao A, Zhou M, Zhu Z, Lin S & Zhang B (2011) Heritable gene targeting in zebrafish using customized TALENs. *Nat. Biotechnol.* **29**: 699–700
- Hung AY & Sheng M (2002) PDZ domains: structural modules for protein complex assembly. *J. Biol. Chem.* **277**: 5699–702 Available at: <http://www.ncbi.nlm.nih.gov/pubmed/11741967> [Accessed September 1, 2014]
- Huo L, Wen W, Wang R, Kam C, Xia J, Feng W & Zhang M (2011) Cdc42-dependent formation of the ZO-1/MRCK β complex at the leading edge controls cell migration. *EMBO J.* **30**: 665–78 Available at: <http://www.pubmedcentral.nih.gov/articlerender.fcgi?artid=3041950&tool=pmcentrez&rendertype=abstract> [Accessed August 20, 2014]
- Hwang WY, Fu Y, Reyon D, Maeder ML, Tsai SQ, Sander JD, Peterson RT, Yeh JRJ & Joung JK (2013) Efficient genome editing in zebrafish using a CRISPR-Cas system. *Nat. Biotechnol.* **31**: 227–229
- Ikenouchi J, Umeda K, Tsukita S, Furuse M & Tsukita S (2007) Requirement of ZO-1 for the formation of belt-like adherens junctions during epithelial cell polarization. *J. Cell Biol.* **176**: 779–86 Available at: <http://www.pubmedcentral.nih.gov/articlerender.fcgi?artid=2064052&tool=pmcentrez&rendertype=abstract> [Accessed September 4, 2014]
- Inaba M, Yamanaka H & Kondo S (2012) Pigment pattern formation by contact-dependent depolarization. *Science (80-.).* **335**: 677
- Inoue S, Kondo S, Parichy DM & Watanabe M (2014) Tetraspanin 3c requirement for pigment cell interactions and boundary formation in zebrafish adult pigment stripes. *Pigment Cell Melanoma Res.* **27**: 190–200 Available at: <http://doi.wiley.com/10.1111/pcmr.12192> [Accessed September 4, 2014]
- Irion U, Frohnhöfer HG, Krauss J, Çolak Champollion T, Maischein H-M, Geiger-Rudolph S, Weiler C, Nüsslein-Volhard C & Bronner ME (2014) Gap junctions composed of connexins 41.8 and 39.4 are essential for colour pattern formation in zebrafish. *Elife* **3**: Available at: <http://elifesciences.org/content/3/e05125.abstract>

- Iwashita M, Watanabe M, Ishii M, Chen T, Johnson SL, Kurachi Y, Okada N & Kondo S (2006) Pigment pattern in jaguar/obelix zebrafish is caused by a Kir7.1 mutation: implications for the regulation of melanosome movement. *PLoS Genet.* **2**: e197 Available at: <http://www.pubmedcentral.nih.gov/articlerender.fcgi?artid=1657052&tool=pmcentrez&rendertype=abstract> [Accessed September 17, 2014]
- Janoueix-Lerosey I, Lequin D, Brugieres L, Ribeiro A, de Pontual L, Combaret V, Raynal V, Puisieux A, Schleiermacher G & Pierron G (2008) Somatic and germline activating mutations of the ALK kinase receptor in neuroblastoma. *Nature* **455**: 967–970
- Johnson SL, Africa D, Walker C & Weston JA (1995) Genetic control of adult pigment stripe development in zebrafish. *Dev. Biol.* **167**: 27–33 Available at: <http://www.sciencedirect.com/science/article/pii/S0012160685710044> [Accessed August 31, 2014]
- Katsuno T, Umeda K, Matsui T, Hata M, Tamura A, Itoh M, Takeuchi K, Fujimori T, Nabeshima Y, Noda T, Tsukita S & Tsukita S (2008) Deficiency of Zonula Occludens-1 Causes Embryonic Lethal Phenotype Associated with Defected Yolk Sac Angiogenesis and Apoptosis of Embryonic Cells. **19**: 2465–2475
- Kausalya PJ, Reichert M & Hunziker W (2001) Connexin45 directly binds to ZO-1 and localizes to the tight junction region in epithelial MDCK cells. *FEBS Lett.* **505**: 92–96 Available at: <http://www.ncbi.nlm.nih.gov/pubmed/11557048>
- Kelsh RN, Brand M, Jiang YJ, Heisenberg CP, Lin S, Haffter P, Odenthal J, Mullins MC, van Eeden FJ, Furutani-Seiki M, Granato M, Hammerschmidt M, Kane D a, Warga RM, Beuchle D, Vogelsang L & Nüsslein-Volhard C (1996) Zebrafish pigmentation mutations and the processes of neural crest development. *Development* **123**: 369–389 Available at: <http://www.ncbi.nlm.nih.gov/pubmed/9007256>
- Kelsh RN, Harris ML, Colanesi S & Erickson CA (2009) Stripes and belly-spots -- a review of pigment cell morphogenesis in vertebrates. *Semin. Cell Dev. Biol.* **20**: 90–104 Available at: <http://www.pubmedcentral.nih.gov/articlerender.fcgi?artid=2744437&tool=pmcentrez&rendertype=abstract> [Accessed May 16, 2011]
- Kiener TK, Sleptsova-Friedrich I & Hunziker W (2007) Identification, tissue distribution and developmental expression of tjp1/zo-1, tjp2/zo-2 and tjp3/zo-3 in the zebrafish, *Danio rerio*. *Gene Expr. Patterns* **7**: 767–76 Available at: <http://www.ncbi.nlm.nih.gov/pubmed/17632043> [Accessed February 7, 2011]
- Kobelt F & Linsenmair KE (1986) Adaptations of the reed frog *Hyperolius viridiflavus* (Amphibia, Anura, Hyperoliidae) to its arid environment. *Oecologia* **68**: 533–541

- Krauss J, Astrinidis P, Astrinides P, Frohnhöfer HG, Walderich B & Nüsslein-Volhard C (2013) transparent, a gene affecting stripe formation in Zebrafish, encodes the mitochondrial protein Mpv17 that is required for iridophore survival. *Biol. Open* **2**: 703–10 Available at: <http://www.pubmedcentral.nih.gov/articlerender.fcgi?artid=3711038&tool=pmcentrez&rendertype=abstract> [Accessed September 3, 2014]
- Krauss J, Frohnhöfer HG, Walderich B, Maischein H-M, Weiler C, Irion U & Nüsslein-Volhard C (2014) Endothelin signalling in iridophore development and stripe pattern formation of zebrafish. *Biol. Open* **3**: 503–9 Available at: <http://www.pubmedcentral.nih.gov/articlerender.fcgi?artid=4058085&tool=pmcentrez&rendertype=abstract> [Accessed September 3, 2014]
- Levesque MP, Krauss J, Koehler C, Boden C & Harris MP (2013) New tools for the identification of developmentally regulated enhancer regions in embryonic and adult zebrafish. *Zebrafish* **10**: 21–9 Available at: <http://www.pubmedcentral.nih.gov/articlerender.fcgi?artid=3670562&tool=pmcentrez&rendertype=abstract> [Accessed August 31, 2014]
- Lister JA, Robertson CP, Lepage T, Johnson SL & Raible DW (1999) Nacre Encodes a Zebrafish Microphthalmia-Related Protein That Regulates Neural-Crest-Derived Pigment Cell Fate. *Development* **126**: 3757–3767 Available at: <http://www.ncbi.nlm.nih.gov/pubmed/10433906>
- Liu JH, Wen S, Luo C, Zhang YQ, Tao M, Wang DW, Deng SM & Xiao YM (2015) Involvement of the mitfa gene in the development of pigment cell in Japanese ornamental (Koi) carp (*Cyprinus carpio* L.). *Genet. Mol. Res. GMR* **14**: 2775
- Lopes SS, Yang X, Müller J, Carney TJ, McAdow AR, Rauch G-J, Jacoby AS, Hurst LD, Delfino-Machín M, Haffter P, Geisler R, Johnson SL, Ward A & Kelsh RN (2008) Leukocyte Tyrosine Kinase Functions in Pigment Cell Development. *PLoS Genet.* **4**: e1000026 Available at: <http://dx.plos.org/10.1371/journal.pgen.1000026>
- Maderspacher F & Nüsslein-Volhard C (2003) Formation of the adult pigment pattern in zebrafish requires leopard and obelix dependent cell interactions. *Development* **130**: 3447–3457 Available at: <http://dev.biologists.org/cgi/doi/10.1242/dev.00519> [Accessed July 12, 2011]
- Mahalwar P, Walderich B, Singh AP & Nüsslein-Volhard C (2014) Local reorganization of xanthophores fine-tunes and colors the striped pattern of zebrafish. *Sci.* Available at: <http://www.sciencemag.org/content/early/2014/08/27/science.1254837.abstract>
- Martinsson T, Eriksson T, Abrahamsson J, Caren H, Hansson M, Kogner P, Kamaraj S, Schönherr C, Weinmar J & Ruuth K (2011) Appearance of the novel activating

- F1174S ALK mutation in neuroblastoma correlates with aggressive tumor progression and unresponsiveness to therapy. *Cancer Res.* **71**: 98–105
- McClure M (1999) Development and evolution of melanophore patterns in fishes of the genus *Danio* (Teleostei: Cyprinidae). *J. Morphol.* **241**: 83–105
- McMenamin SK, Bain EJ, McCann AE, Patterson LB, Eom DS, Waller ZP, Hamill JC, Kuhlman JA, Eisen JS & Parichy DM (2014) Thyroid hormone–dependent adult pigment cell lineage and pattern in zebrafish. *Science* (80-.). **345**: 1358–1361
- Miwa M, Inoue-Murayama M, Aoki H, Kunisada T, Hiragaki T, Mizutani M & Ito S (2007) Endothelin receptor B2 (EDNRB2) is associated with the panda plumage colour mutation in Japanese quail. *Anim. Genet.* **38**: 103–108
- Mongera A, Singh AP, Levesque MP, Chen Y-Y, Konstantinidis P & Nüsslein-Volhard C (2013) Genetic lineage labeling in zebrafish uncovers novel neural crest contributions to the head, including gill pillar cells. *Development* **140**: 916–925
- Monteiro A, Glaser G, Stockslager S, Glansdorp N & Ramos D (2006) Comparative insights into questions of lepidopteran wing pattern homology. *BMC Dev. Biol.* **6**: 52
- Mosse I, Kostrova L, Subbot S, Maksimenya I & Molophei V (2000) Melanin decreases clastogenic effects of ionizing radiation in human and mouse somatic cells and modifies the radioadaptive response. *Radiat. Environ. Biophys.* **39**: 47–52
- Mossé YP, Laudenslager M, Longo L, Cole KA, Wood A, Attiyeh EF, Laquaglia MJ, Sennett R, Lynch JE & Perri P (2008) Identification of ALK as a major familial neuroblastoma predisposition gene. *Nature* **455**: 930–935
- Mullins MC, Hammerschmidt M, Haffter P & Nüsslein-Volhard C (1994) Large-scale mutagenesis in the zebrafish: in search of genes controlling development in a vertebrate. *Curr. Biol.* **4**: 189–202 Available at: <http://www.ncbi.nlm.nih.gov/pubmed/7922324>
- Murray JD (1981) On Pattern Formation Mechanisms for Lepidopteran Wing Patterns and Mammalian Coat Markings. *Philos. Trans. R. Soc. London B Biol. Sci.* **295**: 473–496 Available at: <http://rstb.royalsocietypublishing.org/content/295/1078/473.abstract>
- Nakamasu A, Takahashi G, Kanbe A & Kondo S (2009) Interactions between zebrafish pigment cells. **106**:
- Nasevicius A & Ekker SC (2000) Effective targeted gene ‘knockdown’ in zebrafish. *Nat. Genet.* **26**: 216–220
- Odenthal J, Rossnagel K, Haffter P, Kelsh RN, Vogelsang E, Brand M, van Eeden FJ,

Furutani-Seiki M, Granato M, Hammerschmidt M, Heisenberg CP, Jiang YJ, Kane D a, Mullins MC & Nüsslein-Volhard C (1996) Mutations affecting xanthophore pigmentation in the zebrafish, *Danio rerio*. *Development* **123**: 391–398 Available at: <http://www.ncbi.nlm.nih.gov/pubmed/9007257>

Otaki JM (2011) Color-pattern analysis of eyespots in butterfly wings: a critical examination of morphogen gradient models. *Zoolog. Sci.* **28**: 403–413

Palmer RH & Hallberg B (2015) Receptor Tyrosine Kinases: Family and Subfamilies Available at: <http://link.springer.com/10.1007/978-3-319-11888-8>

Parichy D & Johnson S (2001) Zebrafish hybrids suggest genetic mechanisms for pigment pattern diversification in *Danio*. *Dev. Genes Evol.* **211**: 319–328 Available at: <http://www.springerlink.com/openurl.asp?genre=article&id=doi:10.1007/s004270100155> [Accessed June 7, 2011]

Parichy DM, Mellgren EM, Rawls JF, Lopes SS, Kelsh RN & Johnson SL (2000a) Mutational analysis of endothelin receptor b1 (rose) during neural crest and pigment pattern development in the zebrafish *Danio rerio*. *Dev. Biol.* **227**: 294–306 Available at: <http://www.ncbi.nlm.nih.gov/pubmed/11071756> [Accessed June 28, 2011]

Parichy DM, Ransom DG, Paw B, Zon LI & Johnson SL (2000b) An orthologue of the kit-related gene *fms* is required for development of neural crest-derived xanthophores and a subpopulation of adult melanocytes in the zebrafish, *Danio rerio*. *Development* **127**: 3031–3044 Available at: <http://www.ncbi.nlm.nih.gov/pubmed/10862741>

Parichy DM, Rawls JF, Pratt SJ, Whitfield TT & Johnson SL (1999) Zebrafish sparse corresponds to an orthologue of *c-kit* and is required for the morphogenesis of a subpopulation of melanocytes, but is not essential for hematopoiesis or primordial germ cell development. *Development* **126**: 3425–3436 Available at: <http://www.ncbi.nlm.nih.gov/pubmed/10393121>

Parichy DM & Turner JM (2003) Zebrafish *puma* mutant decouples pigment pattern and somatic metamorphosis. *Dev. Biol.* **256**: 242–257 Available at: <http://linkinghub.elsevier.com/retrieve/pii/S0012160603000150> [Accessed July 17, 2011]

Patterson LB & Parichy DM (2013) Interactions with iridophores and the tissue environment required for patterning melanophores and xanthophores during zebrafish adult pigment stripe formation. *PLoS Genet.* **9**: e1003561 Available at: <http://www.pubmedcentral.nih.gov/articlerender.fcgi?artid=3667786&tool=pmcentrez&rendertype=abstract> [Accessed September 4, 2014]

- Rawles ME (1948) Origin of melanophores and their role in development of color patterns in vertebrates. *Physiol. Rev* **28**: 383–408
- Rodrigues FSLM, Yang X, Nikaido M, Liu Q & Kelsh RN (2012) A Simple, Highly Visual in Vivo Screen for Anaplastic Lymphoma Kinase Inhibitors.
- Roll JD & Reuther GW (2012) ALK-activating homologous mutations in LTK induce cellular transformation. *PLoS One* **7**: e31733 Available at:
<http://www.pubmedcentral.nih.gov/articlerender.fcgi?artid=3276580&tool=pmcentrez&rendertype=abstract>
- Ryeom SW, Paul D & Goodenough DA (2000) Truncation mutants of the tight junction protein ZO-1 disrupt corneal epithelial cell morphology. *Mol. Biol. Cell* **11**: 1687–96 Available at:
<http://www.pubmedcentral.nih.gov/articlerender.fcgi?artid=14876&tool=pmcentrez&rendertype=abstract>
- Sander JD, Cade L, Khayter C, Reyon D, Peterson RT, Joung JK & Yeh J-RJ (2011) Targeted gene disruption in somatic zebrafish cells using engineered TALENs. *Nat. Biotechnol.* **29**: 697–698
- Santos ME, Braasch I, Boileau N, Meyer BS, Sauteur L, Böhne A, Belting H-G, Affolter M & Salzburger W (2014) The evolution of cichlid fish egg-spots is linked with a cis-regulatory change. *Nat. Commun.* **5**:
- Serfas MS & Carroll SB (2005) Pharmacologic approaches to butterfly wing patterning: Sulfated polysaccharides mimic or antagonize cold shock and alter the interpretation of gradients of positional information. *Dev. Biol.* **287**: 416–424 Available at:
<http://www.sciencedirect.com/science/article/pii/S0012160605006214>
- Singh AP & Nüsslein-Volhard C (2015) Zebrafish stripes as a model for vertebrate colour pattern formation. *Curr. Biol.*
- Singh AP, Schach U & Nüsslein-Volhard C (2014) Proliferation, dispersal and patterned aggregation of iridophores in the skin prefigure striped colouration of zebrafish. *Nat. Cell Biol.* **16**: 607–14 Available at:
<http://www.ncbi.nlm.nih.gov/pubmed/24776884> [Accessed July 10, 2014]
- Spence R & Smith C (2007) The role of early learning in determining shoaling preferences based on visual cues in the zebrafish, *Danio rerio*. *Ethology* **113**: 62–67
- Stemple DL, Solnica-Krezel L, Zwartkruis F, Neuhauss SC, Schier AF, Malicki J, Stainier DY, Abdelilah S, Rangini Z, Mountcastle-Shah E & Driever W (1996) Mutations affecting development of the notochord in zebrafish. *Development* **123**: 117–128
- Stevens M & Merilaita S (2009) Animal camouflage: current issues and new

perspectives. *Philos. Trans. R. Soc. B Biol. Sci.* **364**: 423–427

- Suzu S, Hayashi Y, Harumi T, Nomaguchi K, Yamada M, Hayasawa H & Motoyoshi K (2002) Molecular cloning of a novel immunoglobulin superfamily gene preferentially expressed by brain and testis. *Biochem. Biophys. Res. Commun.* **296**: 1215–1221 Available at: <http://www.ncbi.nlm.nih.gov/pubmed/12207903>
- Toyoshima H, Kozutsumi H, Maru Y, Hagiwara K, Furuya A, Mioh H, Hanai N, Takaku F, Yazaki Y & Hirai H (1993) Differently spliced cDNAs of human leukocyte tyrosine kinase receptor tyrosine kinase predict receptor proteins with and without a tyrosine kinase domain and a soluble receptor protein. *Proc. Natl. Acad. Sci.* **90** : 5404–5408 Available at: <http://www.pnas.org/content/90/12/5404.abstract>
- Umeda K, Ikenouchi J, Katahira-Tayama S, Furuse K, Sasaki H, Nakayama M, Matsui T, Tsukita SS & Furuse M (2006) ZO-1 and ZO-2 independently determine where claudins are polymerized in tight-junction strand formation. *Cell* **126**: 741–754 Available at: <http://www.ncbi.nlm.nih.gov/pubmed/16923393> [Accessed July 12, 2010]
- Umeda K, Matsui T, Nakayama M, Furuse K, Sasaki H, Furuse M & Tsukita S (2004) Establishment and characterization of cultured epithelial cells lacking expression of ZO-1. *J. Biol. Chem.* **279**: 44785–94 Available at: <http://www.ncbi.nlm.nih.gov/pubmed/15292177> [Accessed September 4, 2014]
- Unbekandt M & Olson MF (2014) The actin-myosin regulatory MRCK kinases: regulation, biological functions and associations with human cancer. *J. Mol. Med. (Berl)*. **92**: 217–25 Available at: <http://www.pubmedcentral.nih.gov/articlerender.fcgi?artid=3940853&tool=pmcentrez&rendertype=abstract> [Accessed September 3, 2014]
- Watanabe M, Iwashita M, Ishii M, Kurachi Y, Kawakami A, Kondo S & Okada N (2006) Spot pattern of leopard Danio is caused by mutation in the zebrafish connexin41.8 gene. *EMBO Rep.* **7**: 893–7 Available at: <http://www.pubmedcentral.nih.gov/articlerender.fcgi?artid=1559663&tool=pmcentrez&rendertype=abstract> [Accessed March 19, 2012]
- Willott E, Balda MS, Heintzelman M, Jameson B & Anderson JM (1992) Localization and differential expression of two isoforms of the tight junction protein ZO-1. *Am. J. Physiol.* **262**: C1119–C1124
- Winge Ö (1922) One-sided masculine and sex-linked inheritance in *Lebistes reticulatus*. *J. Genet.* **12**: 145–162
- Winge Ö (1927) The location of eighteen genes in *Lebistes reticulatus*. *J. Genet.* **18**: 1–43
- Winge O & Ditlevsen E (1947) Colour inheritance and sex determination in *Lebistes*.

Heredity (Edinb). **1**: 65–83

Xu J, Lim SBH, Ng MY, Ali SM, Kausalya JP, Limvipuvadh V, Maurer-Stroh S, Hunziker W, Rippon H & Bishop A (2012) ZO-1 Regulates Erk, Smad1/5/8, Smad2, and RhoA Activities to Modulate Self-Renewal and Differentiation of Mouse Embryonic Stem Cells. *Stem Cells* **30**: 1885–1900 Available at: <http://onlinelibrary.wiley.com/doi/10.1111/j.1365-2184.2004.00298.x/full> [Accessed September 4, 2014]

Yamanaka H & Kondo S (2014) In vitro analysis suggests that difference in cell movement during direct interaction can generate various pigment patterns in vivo. *Proc. Natl. Acad. Sci. U. S. A.* **111**: 1867–72 Available at: <http://www.pubmedcentral.nih.gov/articlerender.fcgi?artid=3918784&tool=pmcentrez&rendertype=abstract> [Accessed September 4, 2014]

Contributions

Publication 1

Fadeev, A., Krauss, J., Frohnhöfer, H.G., Irion, U., Nüsslein-Volhard, C.* (2015) Tight Junction Protein 1a regulates pigment cell organisation during zebrafish colour patterning. *eLife*. doi: /10.7554/eLife.06545

The project was conceived by C. Nüsslein-Volhard and J. Krauss with help of A. Fadeev. Most of the experiments have been carried out by A. Fadeev, H.G. Frohnhöfer and J. Krauss identifying 4 alleles and U. Irion performed the yeast two-hybrid experiment and crosses with *luc* and *leo*. The analysis of the data was performed A. Fadeev under the supervision of J. Krauss. The manuscript was written by A. Fadeev, followed by editing by C. Nüsslein-Volhard and review by other authors.

Publication 2

Fadeev, A., Krauss, J., Singh, A.P., Nüsslein-Volhard, C.* (2016) Zebrafish Leucocyte tyrosine kinase controls iridophore establishment, proliferation and survival. *Pigment Cell and Melanoma Research*. doi: /10.1111/pcmr.12454

The project was conceived by C. Nüsslein-Volhard, A. Fadeev and J. Krauss. J. Krauss identified the mutant. The experiments were carried out by A. Fadeev. A. P. Singh helped by performing a part of confocal microscopy repeated imaging. Analysis of data was carried out by A. Fadeev, supervised by C. Nüsslein-Volhard, and A. P. Singh. The manuscript was written by C. Nüsslein-Volhard and A. Fadeev.

Publication 3

Kottler, V.A.*, **Fadeev, A.**, Weigel, D., and Dreyer, C. (2013) Pigment pattern formation in the guppy, *Poecilia reticulata*, involves the Kita and Csf1ra receptor tyrosine kinases. *Genetics* 194.3 (2013): 631-646

A. Fadeev acquired part of the images of *golden*, *blue* and wild type fish, assisted in epinephrine treatment and melanophore counts, participated in discussion and analysis of results.

Curriculum Vitae

Fadeev Andrey

Born on 20th of October, 1987, in Almetyevsk, Russia

<i>01/2010 - present</i>	PhD thesis Tight Junction Protein 1a regulates pigment cell organisation during Zebrafish colour patterning	Supervisor: Prof. Dr. Christiane Nüsslein-Volhard Max Planck Institute for Developmental Biology, Tübingen, Germany
<i>06/2009</i>	A degree with distinction of a specialist in bioinformatics with specialization in bioengineering.	Lomonosov Moscow State University, Russia
<i>05/2008 – 06/2009</i>	Master thesis Evolution of substrates and substrate specificity of 3C and 3C-like proteases of +RNA viruses	Supervisors: Prof. Dr. Alexander Gorbalenya, Dr. Kalina Zlateva, Dr. Andrey Leontovich MoBiLE (Moscow Bioinformatics Leiden) group in A.N. Belozersky Institute of Physico-Chemical Biology, Moscow, Russia and Section of Molecular Virology, Department of Medical Microbiology, Leiden University Medical Center - LUMC, The Netherlands
<i>08/2007 – 04/2008</i>	Bachelor Project Investigation of cell localization of Phloem Protein 2 in epidermal cells	Supervisor: Dr. Andrey Soloviev Laboratory of gene engineering of viruses, Department of biochemistry of plant viruses, A.N. Belozersky Institute of Physico-Chemical Biology, Moscow, Russia
<i>07/2007</i>	Internship Improving effectiveness of GSEA	Supervisor: Dr. Jelle J. Goeman Section of Medical Statistics, Leiden University Medical Center, Leiden, The Netherlands.
<i>04/2006 – 04/2007</i>	Rotation projects Purification of tankyrase 2 complex of human kidney cell line 293	Supervisor: Dr. Alexander Kuimov Laboratory of animal cell cultures, Department of chemistry and biochemistry of nucleoproteins, A.N. Belozersky Institute of Physico-Chemical Biology, Moscow, Russia.
<i>04/2005 – 04/2006</i>	Reconstruction of evolution of TERF family proteins	
<i>09/1994 – 06/2004</i>	Gymnasium 4, Elabuga, Tatarstan, Russia	

Full publications list

1. **Fadeev, A.**, Krauss, J., Singh, A.P., Nüsslein-Volhard, C.* (2016) Zebrafish Leucocyte tyrosine kinase controls iridophore establishment, proliferation and survival. *Pigment Cell and Melanoma Research*. doi: /10.1111/pcmr.12454
2. **Fadeev, A.**, Krauss, J., Frohnhöfer, H.G., Irion, U., Nüsslein-Volhard, C.* (2015) Tight Junction Protein 1a regulates pigment cell organisation during zebrafish colour patterning. *eLife*. doi: /10.7554/eLife.06545
3. Kottler, V.A., **Fadeev, A.**, Weigel, D., Dreyer, C.* (2013) Pigment pattern formation in the guppy, *Poecilia reticulata*, involves the Kita and Csf1ra receptor tyrosine kinases. *Genetics* 194.3 (2013): 631-646
4. Sidorova, N. N., **Fadeev A. O.**, and Kuimov A. N.* (2008) Isolation and physicochemical properties of tankyrase of human embryonic kidney cells of line 293. *Biochemistry (Moscow)* 73.3 (2008): 289-295.

Acknowledgements

I would like to thank Janni for providing me with an opportunity to work on these exciting projects in the fruitful environment of her lab, as well as guidance, support, motivation and sharing her experience. Without her, this work would not be possible.

I would like to thank Jana for introducing me to the world of zebrafish research and Rolf for supervising this work. I thank Uwe, Hans-Georg, Richard, Adrian, Mahendra, Christian, Hans and Matthias for sharing their vast expertise with me. I thank April for proofreading this thesis.

I thank Ajeet for all the advice, help and motivation he provided.

I thank Verena, Christine and Detlef for allowing me to bring my humble expertise into the guppy project.

I thank Brigitte and Christian for all the answers to the dumb questions and all the caretakers for their labours in keeping the fish. I would like to thank Heike for all the help with the bureaucracy. I express sincere gratitude to all my co-workers who helped me along the way and allowed me to do research in a great working atmosphere. Chris, Ale, Paolo, Simon, Martina, Xuefan, Soeren, Ines, Alessandra, Yi-Yen, Daniela – thanks for everything. I would like to thank Anastasia for being a passionate opera lover. I am grateful for the fun times we had with Cindy, Pandi and Matthias while elbowing each other over the mapping plates. I would like to thank Hans-Martin for being a great help as well as a passionate Warcraft player. I am grateful to Iris and Chris for all the help.

I would like to express gratitude to Robert for sharing his expertise and encouraging the *ltk* project. I would like to thank him, Jose and Josep for the spotlight they provided for *sbr* project. I would like to say big thanks to all PhD students who joined the institute with me and allowed me to appreciate cultural diversity. And especially to Allana, Anna-Lena, Anna, and Andre (go A-team!). I would like to say thanks to Ole for all the immense support and listening capabilities in tough times. And of course my thanks go to Olga and Vahan for all the scientific expertise and board games. Chloe, Pavel, Fabio, Dmitry and Stephi thanks for being such a great friends.

I would like to express everlasting gratitude to Vera, Felix, Sarah, Stefan, Raffaele, Irina, Leo, Lena, Oliver, Jack, Thekla, Silvester, Janet, Diane, Konrad, Eva, Steffy, Anja, Moritz, Burkhardt and so many others for allowing me to feel more at home in Tübingen than I ever did anywhere else and all the fun and histrionics we shared in BrechtBau. Break a leg guys!

Last but not least, I want to say thank you to my Mom, Grandma and Grandad. I would never get anywhere without your support and care.